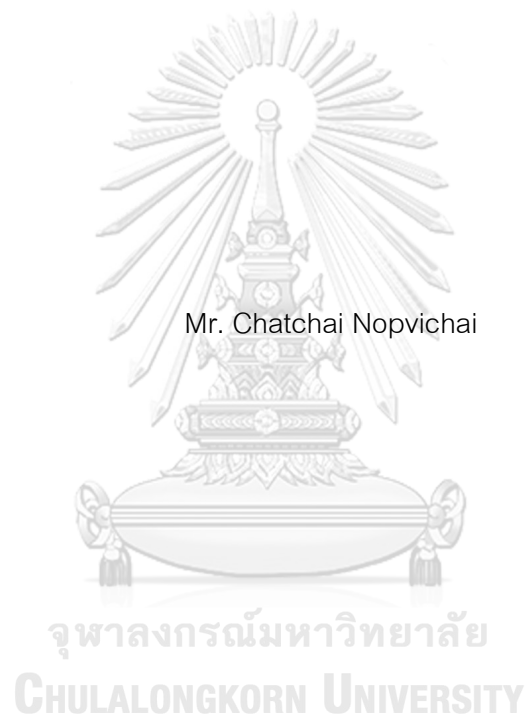


PRODUCTION AND PURIFICATION OF MANNAN OLIGOSACCHARIDE AND ITS ROLE  
IN TIGHT JUNCTION ASSEMBLY IN EPITHELIAL CELLS



A Dissertation Submitted in Partial Fulfillment of the Requirements  
for the Degree of Doctor of Philosophy in Biochemistry and Molecular Biology

Department of Biochemistry

Faculty of Science

Chulalongkorn University

Academic Year 2018

Copyright of Chulalongkorn University

การผลิตและทำบริสุทธิ์ของแมนแนนโพลิโกแซคคาไรด์และบทบาทในการกระตุ้นการยึดเกาะ  
ระหว่างเซลล์เยื่อ



วิทยานิพนธ์นี้เป็นส่วนหนึ่งของการศึกษาตามหลักสูตรปริญญาวิทยาศาสตรดุษฎีบัณฑิต

สาขาวิชาชีวเคมีและชีววิทยาโมเลกุล ภาควิชาชีวเคมี

คณะวิทยาศาสตร์ จุฬาลงกรณ์มหาวิทยาลัย

ปีการศึกษา 2561

ลิขสิทธิ์ของจุฬาลงกรณ์มหาวิทยาลัย



ฉัตรชัย นพวิชัย : การผลิตและทำบริสุทธิ์ของแมนแนนโอลิโกแซคคาไรด์และบทบาทในการกระตุ้นการยึดเกาะระหว่างเซลล์เยื่อ. ( PRODUCTION AND PURIFICATION OF MANNAN OLIGOSACCHARIDE AND ITS ROLE IN TIGHT JUNCTION ASSEMBLY IN EPITHELIAL CELLS) อ.ที่ปรึกษาหลัก : ผศ. ดร.รัฐ พิชญางกูร, อ.ที่ปรึกษาร่วม : รศ. นพ.ดร.ฉัตรชัย เหมือนประสาธา

แมนแนน โอลิโกแซคคาไรด์ (MOS) นั้นเป็นที่รู้จักอย่างกว้างขวางในฐานะของอาหารเสริมสำหรับจุลชีพในระบบทางเดินอาหารซึ่ง สามารถเพิ่มคุณภาพของปศุสัตว์ได้เป็นอย่างดี มีหลายรายงานแสดงว่า MOS นั้นสามารถปรับปรุงลักษณะทางกายภาพของลำไส้และเพิ่มการเจริญเติบโต น้ำหนัก รวมถึงสามารถกระตุ้นระบบเผาผลาญและการตอบสนองต่อความเครียดได้ การให้ MOS เป็นอาหารยังมีผลในการกระตุ้นการทำงานของระบบต่างๆ และรวมถึงสามารถกระตุ้นการแสดงออกของยีนที่เกี่ยวข้องกับระบบภูมิคุ้มกันในเซลล์เม็ดเลือดขาวชนิดนิวเคลียสเดี่ยว ซึ่งสามารถปกป้องและลดการอักเสบที่เกิดจากการติดเชื้อไวรัสได้ในสุกร แต่อย่างไรก็ตามกลไกการทำงานและขนาดที่มีฤทธิ์ทางชีวภาพของ MOS นั้นยังไม่มีการรายงานออกมาชัดเจน รวมถึงการผลิตและการทำบริสุทธิ์นั้นยังต้องการการพัฒนาต่อไปในอนาคต ในการทดลองนี้ ผู้ทดลองได้พัฒนาเทคนิคในการผลิต MOS โดยใช้รีคอมบิแนนท์แมนแนนเนส ซึ่งพบว่าวิธีการผลิตดังที่ได้รายงานนี้สามารถในผลผลิตของ MOS ในสัดส่วนที่สูงภายใต้ภาวะกรดต่างและอุณหภูมิที่กว้างตั้งแต่ 4-80 องศาเซลเซียสและพีเอช 2.5-10.0 ตามลำดับ และเป็นที่น่าสนใจว่าหากใช้เอนไซม์ร่วมกับซับสเตรทในอัตราส่วนที่ต่ำกว่า 1 ยูนิตต่อกรัมของน้ำหนักแห้งของกากมะพร้าวจะสามารถให้ผลผลิต MOS ในสัดส่วนที่ดีกว่าการใช้อัตราส่วนที่สูงการบ่มปฏิกริยาที่นานกว่า 18 ชั่วโมงก็ยังไม่ให้ผลผลิตเป็นโอลิโกแซคคาไรด์ขนาดเล็กมากขึ้นเช่นกัน โดย MOS ขนาดต่างๆได้ถูกแยกผ่านคอลัมน์ Biogel P2 โดยแยกขนาดได้ถึง 2 ถึง 9 เมอร์ในส่วนของฤทธิ์ทางชีวภาพ ผู้ทดลองยังได้ศึกษาผลของ MOS ในการกระตุ้นการยึดติดกันของเซลล์เนื้อเยื่อผ่านเทคนิคการวัดความต้านทานไฟฟ้าระหว่างเนื้อเยื่อ (TEER) โดยใช้เซลล์ T84 เป็นตัวอย่าง โดยผลการทดลองที่ได้พบว่า MOS นั้นมีฤทธิ์ในการเพิ่มการยึดเกาะระหว่างเซลล์โดย MOS เพนตาเมอร์ (MOS5) นั้นให้ผลที่ดีที่สุดที่ความเข้มข้น 10 ไมโครโมลาร์ และให้ผลการกระตุ้นที่ดีที่สุดที่ 24 ชั่วโมง การศึกษาผลของ MOS ต่อกลไกการฟื้นฟูสภาพเชื่อมต่อของเซลล์พบว่า MOS5 นั้นสามารถฟื้นฟูสภาพเชื่อมต่อของเซลล์ที่ถูกทำลายได้อย่างมีนัยสำคัญ และ MOS5 อาจทำการเพิ่มการยึดเกาะของเซลล์ผิวผ่านกลไกการเกิดฟอสโฟไรเลชันของ AMPK ซึ่งสมมติฐานนี้ได้ถูกสนับสนุนด้วยผลการทดลองที่ศึกษาการกระตุ้นด้วย MOS5 ควบคู่กับการยับยั้งวิถีของ AMPK โดยใช้ Dorsomorphine นอกจากนี้ ผลการวิเคราะห์การแสดงออกของ AMPK ด้วยวิธี western blot พบว่า MOS5 สามารถเพิ่มอัตราการเกิดฟอสโฟไรเลชันของ AMPK ได้อย่างมีนัยสำคัญ การศึกษาโครงสร้างของ MOS5 ด้วยการใชการย่อยด้วยเอนไซม์ร่วมกับเทคนิค Nuclear magnetic resonance และ Mass spectrometry พบว่า MOS5 ประกอบไปด้วยโครงสร้างหลักคือแมนโนสเทโทรสที่ยึดกันด้วยพันธะเบต้า-1,4-ไกลโคซิดิก และมีกาแลกโตสหนึ่งหมู่ เกาะที่บริเวณแมนโนสหมู่ที่สองจากด้าน non-reducing ด้วยพันธะอัลฟา-1,6 ไกลโคซิดิก

สาขาวิชา ชีวเคมีและชีววิทยาโมเลกุล

ปีการศึกษา 2561

ลายมือชื่อนิสิต .....

ลายมือชื่อ อ.ที่ปรึกษาหลัก .....

ลายมือชื่อ อ.ที่ปรึกษาร่วม .....

## 5672806323 : MAJOR BIOCHEMISTRY AND MOLECULAR BIOLOGY

KEYWORD: Mannan oligosaccharide; Tight junction integration; epithelial tissues

Chatchai Nopvichai : PRODUCTION AND PURIFICATION OF MANNAN OLIGOSACCHARIDE AND ITS ROLE IN TIGHT JUNCTION ASSEMBLY IN EPITHELIAL CELLS. Advisor: Asst. Prof. Rath Pichyangkura, Ph.D. Co-advisor: Assoc. Prof. Chatchai Muanprasat, MD.Ph.D.

Mannan Oligosaccharide (MOS) is well-known as prebiotic supplement that help increasing life quality of livestock and animals. Many reports revealed that MOS supplement can help improve intestinal morphology, enhancing growth performance, raising body weight, and increasing metabolic and stress response. MOS feeding also affected several biological processes in peripheral blood mononuclear cells in pigs and modulates expression of many immune-related genes that helps to prevent and reduce the severity of viral infection. However, the mechanism of action of MOS is remained unclear and the production, purification, identification of bioactive MOS molecular type is needed. In this study, we developed a method for mannan oligosaccharide (MOS) production by using a recombinant mannanase. We found that the reaction can be performed in the wide range of temperature and pH, from 4 to 80 degree celcius and 2.5 to 10.0, respectively. Interestingly, low manannase concentration at below 1Unit per 1 gram of coconut meal dried weight yielded a higher amount of MOS rather than using a higher enzyme/ substrate ratio. Longer incubation time exceed 18hr also gave smaller oligosaccharides. MOS products were seperated through Biogel P2 column yielding purified MOS from 2 to 9 mers. We have also investigated the biological effects of MOS on prevention and a treatment of an epithelium inflammation models by using Transepithelial electrical resistant (TEER) assay on T84 cells. The results obtained showed that MOS enhanced cells integrity and MOS pentamer (MOS-5) showed the highest activity and the optimum dose was 10 uM with an activating time of 24 hours. The study on tight junction integration recovery with calcium ions switching shown that MOS5 have the ability to reassemble the cells tight junction. A strudy on MOS5 and Dorsomorphine, an AMPK inhibitor, also shown that MOS5 may activate cellular integration through AMPK signaling pathway. The mechanism of action of MOS5 to an integration of cellular tight junction through AMPK was confirmed with western blot analysis. A structure determination of MOS5 was performed by enzyme hydrolytic assay together with mass spectrometry and nuclear magnetic resonance. The results shown that MOS5 is a galactomannan polymer composed of mannantetrasaccharide with beta-1,4-glycosidic linkage with one galactose unit attached on the second mannose unit from non-reducing end with alpha-1,6-glycosidic linkage.

Field of Study:	Biochemistry and Molecular Biology	Student's Signature .....
Academic Year:	2018	Advisor's Signature .....
		Co-advisor's Signature .....

## ACKNOWLEDGEMENTS

First of all, this work cannot be initiated and done without a grateful help from my advisor, Asst.Prof. Rath Pichyangura, Ph.D. I would like to express my deepest appreciation to him for his kindly support, ideas, suggestion and everything though years of working.

My gratitude also extends to my co-advisor, Prof. Chatchai Muanprasat, MD, Ph.D. from department of physiology, faculty of science, Mahidol university and Assoc.Prof. Kazuo Ito, Ph.D. from Osaka City University for an opportunity that he gave to me for this work and also his collaboration, suggestions and ideas that were very important to this work.

I am also extremely grateful to my committee, Asst.Prof. Kanoktip Packdibamrung, Ph.D., Asst.Prof. Kunlaya Sombonwivat, Ph.D., Asst.Prof. Suchart Chanama, Ph.D., and Wannop Vissessanguan, Ph.D.

This work cannot be completed without a great help from all my co-researchers, Karan Wangpaiboon, Ph.D., Mr. Thanapon Charoenwongpaiboon, Pawin Pongkorsakol, Ph.D., and Ms.Preedajit Wongkrasant from 709 lab and TDED lab. Thank you for all your collaboration and suggestions.

I would like to extend my sincere thanks to all my families. I cannot be at this point without my parents, Mr.Weerasakdi Nopvichai and Mrs.Nisarath Boonlert. Also, Mr.Paul Zahra and Ms.Peeraya Boonsiriseth for their unconditionally helps and support.

I also want to give my sincere thanks to Mr.Nopadol Suanprasert and Mr.Aunyawut Phoopanthapuk for their kindly support for my overseas research in Japan.

I would like to thanks all staffs in department of pathology, faculty of medicine, Chulalongkorn university, and academic staffs in department of anatomical pathology, faculty of medicine Vajira hospital, Navamindradhiraj university for all their support in my scientific career.

I cannot leave Chulalongkorn university without mentioning my kendo team, judo team, and also CK and ScCUCL family. A life would be much harder without them.

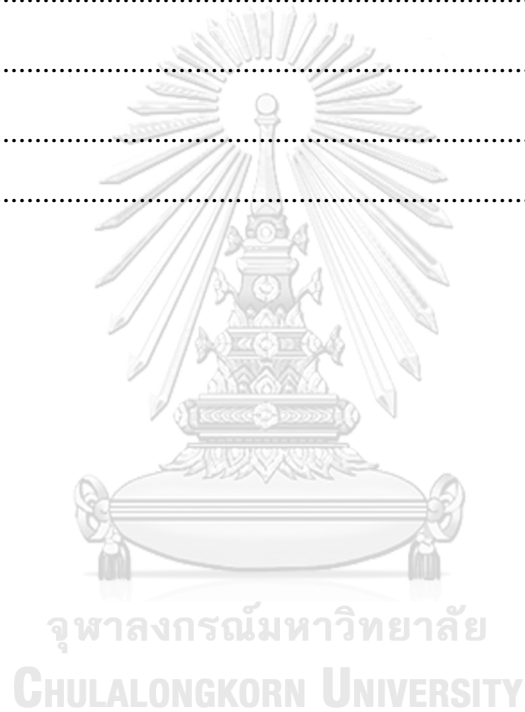
Lastly, I would like to give a special thanks to Ms.Wannit Charusirisawad, who was always helped and supported me all the time. All help, efforts, and kindness will always be recognized and appreciated.

The thesis is supported by 100th Chulalongkorn university scholarship, the office of graduate school, Chulalongkorn university.

Chatchai Nopvichai

## TABLE OF CONTENTS

	Page
ABSTRACT (THAI) .....	iii
ABSTRACT (ENGLISH).....	iv
ACKNOWLEDGEMENTS.....	v
TABLE OF CONTENTS.....	vi
LIST OF TABLES.....	vii
LIST OF FIGURES .....	viii
REFERENCES .....	10
VITA.....	140



## LIST OF TABLES

	Page
Table 1. Percentage yield of MOS production compared between S-GalMan and G-GalMan. ....	78





## LIST OF FIGURES

	Page
Figure 1. Structure of glucomannan.....	22
Figure 2. Structure of galactomannan.....	22
Figure 3. The optimum pH of RMase24 in various buffer and pH.....	27
Figure 4. Optimum temperature of RMase24.....	28
Figure 5. Relative activity of RMase24 under a various storage buffer and pH conditions.....	29
Figure 6. Relative activity of RMase24 under a various temperature at pH6.0.....	30
Figure 7. Relative activity of RMase24 with a presence of various chemicals and ions.....	31
Figure 8. Cross section of epithelial tissue shown a compartment of cell junctions including tight junction, adherens junction (adhesive belt), and gap junction. ....	35
Figure 9. Cross section of epithelium cell shown a compartment of cell junctions with scanning electron microscope image. ....	36
Figure 10. Activators, substrates, and downstream regulations schema of AMPK pathway related to adherens junctions and tight junction of the cell. ....	39
Figure 11. Sequence of Bs24Man (accession number KY951415).....	64
Figure 12. Amino acid alignment sequence of Bs24Man.....	65
Figure 13. Three-dimensional structure comparison between Bs24Man and exported mannan endo-1, 4- $\beta$ -mannosidase from Bacillus subtilis BEST7613.....	67
Figure 14. Cloning result of pvRM24-A, analyzed on 0.8% (w/v) agarose gel. ....	69
Figure 15. Surface structure of S-GalMan and G-GalMan imaged by scanning electron microscope. ....	71
Figure 16. Evaluation of the incubation period at different incubation time, compared between S-GalMan (A) and G-GalMan (B).....	75
Figure 17. The pattern of MOS production from RMase24 with a different concentration of RMase24.....	77
Figure 18. A separation of each MOS, from MOS4 to MOS7 demonstrated in thin layer chromatography under butan-1-ol: acetic acid: water, 3:3:2 system. ....	81
Figure 19. Mass spectrometry analysis of purified MOS. ....	83

Figure 20. Relative percentage of TEER changed of T84 cells after 24 hours treatment with purified MOS4 to MOS7 compared to control group (DMEM).....	86
Figure 21. Relative percentage TEER change of T84 cells after a treatment of various concentration of MOS5.....	87
Figure 22. Determination of tight junction reassembly of M5 compared to control. ..	89
Figure 23. Determination of AMPK activation of MOS5 through a challenging of Compound C. ....	91
Figure 24. Western blot analysis of p-AMPK, AMPK- $\alpha$ , and $\beta$ -actin protein collected at various time point of MOS5 treated group and vehicle (non-treated) group.....	93
Figure 25. Relative percentage of expression level of p-AMPK over AMPK- $\alpha$ . ....	94
Figure 26. High performance anion exchange chromatography (HPAEC-PAD) chromatogram of the purified MOS5.....	96
Figure 27. Thin layer chromatography of digestion products of MOS5 with a fraction of purified $\alpha$ -galactosidase from <i>A. fulica</i> (Amano, Japan) in butyl acetate system (A) and acetonitrile system (B). ....	99
Figure 28. A digestion of MOS5 with AfMAN and RMase24. ....	102
Figure 29. Thin layer chromatography analysis of a digestion of MOS5 with various amount of P-AMAN-AfGLA-f35. ....	105
Figure 30. MALDI imaging mass spectrometer analysis of m-2 and m-3 .....	108
Figure 31. NMR structural analysis of m-2. ....	111
Figure 32. $^1\text{H}$ NMR spectra of m-2, analyzed at 600MHz. ....	112
Figure 33. $^{13}\text{C}$ NMR spectra of m-2, analyzed at 150MHz. ....	113
Figure 34. NMR structural analysis of m-3. ....	114
Figure 35. $^1\text{H}$ NMR spectra of m-3, analyzed at 600MHz. ....	115
Figure 36. $^{13}\text{C}$ NMR spectra of m-2, analyzed at 150MHz. ....	116
Figure 37. Structure of MOS5 .....	125

## REFERENCES

- Additives, E. P. o. F., Food, N. S. a. t., Mortensen, A., Aguilar, F., Crebelli, R., Di Domenico, A., . . . Lambré, C. (2017). Re-evaluation of konjac gum (E 425 i) and konjac glucomannan (E 425 ii) as food additives. *EFSA Journal*, 15(6), e04864.
- Ai, Q., Xu, H., Mai, K., Xu, W., Wang, J., & Zhang, W. (2011). Effects of dietary supplementation of *Bacillus subtilis* and fructooligosaccharide on growth performance, survival, non-specific immune response and disease resistance of juvenile large yellow croaker, *Larimichthys crocea*. *Aquaculture*, 317(1-4), 155-161.
- Boven, L., Middel, J., Verhoef, J., De Groot, C., & Nottet, H. (2000). Monocyte infiltration is highly associated with loss of the tight junction protein zonula occludens in HIV-1-associated dementia. *Neuropathology and applied neurobiology*, 26(4), 356-360.
- Cescutti, P., Campa, C., Delben, F., & Rizzo, R. (2002). Structure of the oligomers obtained by enzymatic hydrolysis of the glucomannan produced by the plant *Amorphophallus konjac*. *Carbohydrate Research*, 337(24), 2505-2511.
- Chauhan, P. S., Puri, N., Sharma, P., & Gupta, N. (2012). Mannanases: microbial sources, production, properties and potential biotechnological applications. *Applied microbiology and biotechnology*, 93(5), 1817-1830.
- Che, T., Johnson, R., Kelley, K., Dawson, K., Moran, C., & Pettigrew, J. (2012). Effects of mannan oligosaccharide on cytokine secretions by porcine alveolar macrophages and serum cytokine concentrations in nursery pigs. *Journal of Animal Science*, 90(2), 657-668.
- Che, T., Johnson, R., Kelley, K., Van Alstine, W., Dawson, K., Moran, C., & Pettigrew, J. (2011). Mannan oligosaccharide modulates gene expression profile in pigs experimentally infected with porcine reproductive and respiratory syndrome virus. *Journal of animal science*, 89(10), 3016-3029.

- Che, T., Song, M., Liu, Y., Johnson, R., Kelley, K., Van Alstine, W., . . . Pettigrew, J. (2012). Mannan oligosaccharide increases serum concentrations of antibodies and inflammatory mediators in weanling pigs experimentally infected with porcine reproductive and respiratory syndrome virus. *Journal of Animal Science*, 90(8), 2784-2793.
- Cheled-Shoval, S., Amit-Romach, E., Barbakov, M., & Uni, Z. (2011). The effect of in ovo administration of mannan oligosaccharide on small intestine development during the pre-and posthatch periods in chickens. *Poultry science*, 90(10), 2301-2310.
- Cheled-Shoval, S., Gamage, N. W., Amit-Romach, E., Forder, R., Marshal, J., Van Kessel, A., & Uni, Z. (2014). Differences in intestinal mucin dynamics between germ-free and conventionally reared chickens after mannan-oligosaccharide supplementation. *Poultry science*, 93(3), 636-644.
- Corrigan, A., Horgan, K., Clipson, N., & Murphy, R. (2012). Effect of dietary prebiotic (mannan oligosaccharide) supplementation on the caecal bacterial community structure of turkeys. *Microbial ecology*, 64(3), 826-836.
- Dimitroglou, A., Merrifield, D. L., Spring, P., Sweetman, J., Moate, R., & Davies, S. J. (2010). Effects of mannan oligosaccharide (MOS) supplementation on growth performance, feed utilisation, intestinal histology and gut microbiota of gilthead sea bream (*Sparus aurata*). *Aquaculture*, 300(1-4), 182-188.
- Edelblum, K. L., & Turner, J. R. (2009). The tight junction in inflammatory disease: communication breakdown. *Current opinion in pharmacology*, 9(6), 715-720.
- Ganter, J. L. M., Heyraud, A., Petkowicz, C. L., Rinaudo, M., & Reicher, F. (1995). Galactomannans from Brazilian seeds: characterization of the oligosaccharides produced by mild acid hydrolysis. *International journal of biological macromolecules*, 17(1), 13-19.

- Genc, M., Aktas, M., Genc, E., & Yilmaz, E. (2007). Effects of dietary mannan oligosaccharide on growth, body composition and hepatopancreas histology of *Penaeus semisulcatus* (de Haan 1844). *Aquaculture Nutrition*, 13(2), 156-161.
- Ghosh, A., Verma, A. K., Tingirikari, J. R., Shukla, R., & Goyal, A. (2015). Recovery and purification of oligosaccharides from copra meal by recombinant endo- $\beta$ -mannanase and deciphering molecular mechanism involved and its role as potent therapeutic agent. *Molecular biotechnology*, 57(2), 111-127.
- Gridale-Helland, B., Helland, S. J., & Gatlin III, D. M. (2008). The effects of dietary supplementation with mannanoligosaccharide, fructooligosaccharide or galactooligosaccharide on the growth and feed utilization of Atlantic salmon (*Salmo salar*). *Aquaculture*, 283(1-4), 163-167.
- Gupta, V. K., & Tuohy, K. (2016). *Microbial enzymes in bioconversions of biomass*: Springer.
- Homann, A., Timm, M., & Seibel, J. (2012). Chemo-enzymatic synthesis and in vitro cytokine profiling of tailor-made oligofructosides. *BMC biotechnology*, 12(1), 90.
- Johnson, R. J., Segal, M. S., Sautin, Y., Nakagawa, T., Feig, D. I., Kang, D.-H., . . . Sánchez-Lozada, L. G. (2007). Potential role of sugar (fructose) in the epidemic of hypertension, obesity and the metabolic syndrome, diabetes, kidney disease, and cardiovascular disease—. *The American journal of clinical nutrition*, 86(4), 899-906.
- Laplante, M., & Sabatini, D. M. (2012). mTOR signaling in growth control and disease. *Cell*, 149(2), 274-293.
- Lee, J. H., Koh, H., Kim, M., Kim, Y., Lee, S. Y., Karess, R. E., . . . Kim, J. (2007). Energy-dependent regulation of cell structure by AMP-activated protein kinase. *Nature*, 447(7147), 1017.
- Lin, S. J., Hu, Y., Zhu, J., Woodruff, T. K., & Jardetzky, T. S.

- (2011). Structure of betaglycan zona pellucida (ZP)-C domain provides insights into ZP-mediated protein polymerization and TGF- $\beta$  binding. *Proceedings of the National Academy of Sciences*, 108(13), 5232-5236.
- Maeda, M., Shimahara, H., & Sugiyama, N. (1980). Detailed examination of the branched structure of konjac glucomannan. *Agricultural and Biological Chemistry*, 44(2), 245-252.
- Mansour, M. R., Akrami, R., Ghobadi, S., Denji, K. A., Ezatrahimi, N., & Gharaei, A. (2012). Effect of dietary mannan oligosaccharide (MOS) on growth performance, survival, body composition, and some hematological parameters in giant sturgeon juvenile (*Huso huso* Linnaeus, 1754). *Fish physiology and biochemistry*, 38(3), 829-835.
- Mattaveewong, T., Wongkrasant, P., Chanchai, S., Pichyangkura, R., Chatsudthipong, V., & Muanprasat, C. (2016). Chitosan oligosaccharide suppresses tumor progression in a mouse model of colitis-associated colorectal cancer through AMPK activation and suppression of NF- $\kappa$ B and mTOR signaling. *Carbohydrate polymers*, 145, 30-36.
- Matter, K., & Balda, M. S. (2003). Signalling to and from tight junctions. *Nat Rev Mol Cell Biol*, 4(3), 225-236.
- Mihaylova, M. M., & Shaw, R. J. (2011). The AMPK signalling pathway coordinates cell growth, autophagy and metabolism. *Nature cell biology*, 13(9), 1016.
- Mirouse, V., Swick, L. L., Kazgan, N., St Johnston, D., & Brenman, J. E. (2007). LKB1 and AMPK maintain epithelial cell polarity under energetic stress. *J Cell Biol*, 177(3), 387-392.
- Miyazawa, T., & Funazukuri, T. (2006). Noncatalytic hydrolysis of guar gum under hydrothermal conditions. *Carbohydrate Research*, 341(7), 870-877.
- Mourão, J. L., Pinheiro, V., Alves, A., Guedes, C., Pinto, L., Saavedra, M. J., . . . Kocher, A. (2006). Effect of mannan oligosaccharides on the performance, intestinal morphology

- and cecal fermentation of fattening rabbits. *Animal Feed Science and Technology*, 126(1-2), 107-120.
- Muanprasat, C., & Chatsudthipong, V. (2017). Chitosan oligosaccharide: Biological activities and potential therapeutic applications. *Pharmacology & therapeutics*, 170, 80-97.
- Muanprasat, C., Wongkrasant, P., Satitsri, S., Moonwiriyaakit, A., Pongkorpsakol, P., Mattaveewong, T., . . . Chatsudthipong, V. (2015). Activation of AMPK by chitosan oligosaccharide in intestinal epithelial cells: Mechanism of action and potential applications in intestinal disorders. *Biochemical pharmacology*, 96(3), 225-236.
- Orci, L., & Perrelet, A. (2012). *Freeze-etch histology: a comparison between thin sections and freeze-etch replicas*: Springer Science & Business Media.
- Ozaki, K., Fujii, S., & Hayashi, M. (2007). Effect of dietary manooligosaccharides on the immune system of ovalbumin-sensitized mice. *Journal of health science*, 53(6), 766-770.
- Rosengren, A., Reddy, S. K., Sjöberg, J. S., Aurelius, O., Logan, D. T., Kolenová, K., & Stålbrand, H. (2014). An *Aspergillus nidulans*  $\beta$ -mannanase with high transglycosylation capacity revealed through comparative studies within glycosidase family 5. *Applied microbiology and biotechnology*, 98(24), 10091-10104.
- Rowart, P., Wu, J., Caplan, M., & Jouret, F. (2018). Implications of AMPK in the Formation of Epithelial Tight Junctions. *International journal of molecular sciences*, 19(7), 2040.
- Rungrassamee, W., Kingcha, Y., Srimarut, Y., Maibunkaew, S., Karoonuthaisiri, N., & Visessanguan, W. (2014). Mannooligosaccharides from copra meal improves survival of the Pacific white shrimp (*Litopenaeus vannamei*) after exposure to *Vibrio harveyi*. *Aquaculture*, 434, 403-410.
- Shen, L., Su, L., & Turner, J. R. (2009). Mechanisms and functional implications of intestinal barrier defects.

- Digestive diseases*, 27(4), 443-449.
- Sittikijyothin, W., Torres, D., & Gonçalves, M. (2005). Modelling the rheological behaviour of galactomannan aqueous solutions. *Carbohydrate Polymers*, 59(3), 339-350.
- Staykov, Y., Spring, P., Denev, S., & Sweetman, J. (2007). Effect of a mannan oligosaccharide on the growth performance and immune status of rainbow trout (*Oncorhynchus mykiss*). *Aquaculture International*, 15(2), 153-161.
- Yousef, M., Pichyangkura, R., Soodvilai, S., Chatsudthipong, V., & Muanprasat, C. (2012). Chitosan oligosaccharide as potential therapy of inflammatory bowel disease: therapeutic efficacy and possible mechanisms of action. *Pharmacological research*, 66(1), 66-79.
- Yu, L. C.-H., Wang, J.-T., Wei, S.-C., & Ni, Y.-H. (2012). Host-microbial interactions and regulation of intestinal epithelial barrier function: From physiology to pathology. *World journal of gastrointestinal pathophysiology*, 3(1), 27.
- Zhang, L., Li, J., Young, L. H., & Caplan, M. J. (2006). AMP-activated protein kinase regulates the assembly of epithelial tight junctions. *Proceedings of the National Academy of Sciences*, 103(46), 17272-17277.
- Zheng, B., & Cantley, L. C. (2007). Regulation of epithelial tight junction assembly and disassembly by AMP-activated protein kinase. *Proceedings of the National Academy of Sciences*, 104(3), 819-822.
- Zhou, G., Myers, R., Li, Y., Chen, Y., Shen, X., Fenyk-Melody, J., . . . Fujii, N. (2001). Role of AMP-activated protein kinase in mechanism of metformin action. *The Journal of clinical investigation*, 108(8), 1167-1174.
- Zihni, C., Balda, M. S., & Matter, K. (2014). Signalling at tight junctions during epithelial differentiation and microbial pathogenesis. *J Cell Sci*, 127(16), 3401-3413.
- Zihni, C., Mills, C., Matter, K., & Balda, M. S. (2016). Tight junctions: from simple barriers to multifunctional molecular gates. *Nature reviews Molecular cell biology*, 17(9), 564.





จุฬาลงกรณ์มหาวิทยาลัย  
**CHULALONGKORN UNIVERSITY**

# CHAPTER I

## INTRODUCTION

Carbohydrates is well-known as one of the main energy sources for living organisms for decades. Human known how to grow crops for food and manage its leftover products as. Interestingly, some carbohydrate leftover materials from food manufacturing that had been used to feed livestock as it supplement found to have an unexpected ability health beneficial property that can raise up health status (Muanprasat et al., 2015).The trend of food supplement is recently turned in and focused on these materials and a searching for bioactive carbohydrate compounds is become a great challenge.

### 1.1 Mannan Oligosaccharide

Mannan Oligosaccharide (MOS) is an indigestible short chain polymer and a well-known supplement for increasing the life quality of pets and livestock. Several reports revealed that MOS supplement could improve growth performance and body weight in various animals. It can enhance the immunity and metabolic and stress response of aquamarine cultures including shrimp, seabream, sturgeon and rainbow trout (Ai et al., 2011; Cheled-Shoval et al., 2014; Corrigan, Horgan, Clipson, &

Murphy, 2012; Dimitroglou et al., 2010; Mansour et al., 2012; Shen, Su, & Turner, 2009). In addition, the beneficial effects of MOS are observed in terrestrial animals like poultry and mammals as it raises nutrient digestibility, cecal fermentation, and improves the intestinal morphology. Many studies reported that feeding MOS to rabbits could increase length, density and improve the organization of the ileac villi (Cheled-Shoval, Amit-Romach, Barbakov, & Uni, 2011; Cheled-Shoval et al., 2014; Mourão et al., 2006; Yu, Wang, Wei, & Ni, 2012). This suggests a higher rate of intestinal nutrient uptake; thus, improved growth performance (Mourão et al., 2006). Research conducted in chickens, turkeys, pigs, and calves also demonstrated similar results (Genc, Aktas, Genc, & Yilmaz, 2007; Grisdale-Helland, Helland, & Gatlin III, 2008; Johnson et al., 2007; Mansour et al., 2012; Staykov, Spring, Denev, & Sweetman, 2007). Moreover, MOS supplement have been shown positive effects on immune response in several species. There were several reports that MOS can modulated genes that involving in an innate and adaptive immune response, which can help reduced the severity of porcine respiratory syndrome virus (PRSV) infection. Peripheral blood mononuclear cells of infected pigs were found to have a lower expression of proinflammatory cytokines and chemokines as compared with control group (Che, Johnson, et al., 2012; Che et al., 2011; Che, Song, et al., 2012). The

reduction in these proinflammatory cytokines may resulting in less severity and help improve the survival rate of infected pigs. Similar results were also observed in an experiment with ovalbumin-sensitized mice. Ozaki, et al. reported that MOS treatment strongly suppressed TH-2 type cytokine, IL-10 production (but not TH-1 type cytokine), IL-2 and IFN- $\gamma$  production at the time of ovalbumin sensitization(Ozaki, Fujii, & Hayashi, 2007). Interestingly, Homann, et al. reported that Mannose-capped oligofructosides evoke the highest increase in chemokine (C-C motif) ligand 2 (CCL2) and interleukin-8 (CXCL8) release in Caco2 cells when compare with the other oligofructosides (Homann, Timm, & Seibel, 2012). These findings indicate that MOS or MOS-featured oligosaccharides might possess the anti-inflammation properties. Although the identification and the mechanism of action of MOS remained unclear, existing evidence strongly suggests that MOS may exert biological effects on the intestinal tissue in terms of compact and increased in size and activities.

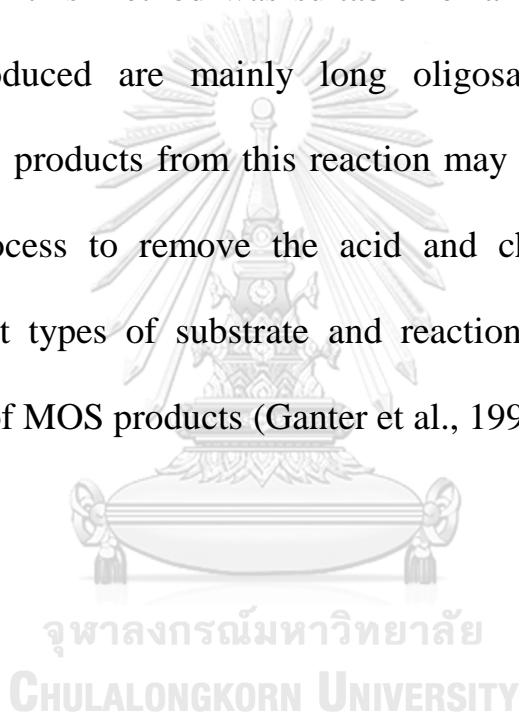
## 1.2 Production of Mannan oligosaccharide from biomaterial resources

MOS is often prepared by hydrolysis reaction of a mannose-contained glucan polymer, mainly glucomannan and galactomannan. Glucomannan, a soluble dietary fiber, is a heteropolymer chain of  $\beta$ -D-glucose and  $\beta$ -D-

mannose which is partially attached with acetyl groups in a molar ratio of 1: 1.6 with  $\beta$ -1–4 linkages (Figure1). Glucomannan is widely distributed in the tuber or root of the konjac (*Amorphophallus konjac* or *Amorphophallus rivieri*) (Maeda, Shimahara, & Sugiyama, 1980). Unfortunately, a recent study revealed that the oligosaccharides obtained from the digestion of glucomannan is composed of several random sequences of glucose and mannose residues which hinders the characterization of the oligosaccharides produced (Cescutti, Campa, Delben, & Rizzo, 2002).

In contrast, galactomannan, which is an insoluble fiber found in the endosperm of many plant species, such as fruits of coconut trees (*Cocos nucifera*) or coconut meal (copra meal), guar gum or guaran from cluster beans (*Cyamopsis tetragonoloba*), and tara gum from Peruvian carobs (*Caesalpinia spinosa*). The other source of galactomannan is yeast cell wall (*Saccharomyces cerevisiae*), commercially available as Bio-Mos® (Alltech, Inc., Nicholasville, KY). These types of polymannan consist of (1-4)- $\beta$ -D-mannose repeating units with (1-6)- $\alpha$ -D-galactose units attached to the mannose backbone (Ganter, Heyraud, Petkowicz, Rinaudo, & Reicher, 1995; Ghosh, Verma, Tingirikari, Shukla, & Goyal, 2015) (Figure2).

The production of MOS from galactomannan can be performed either by acid or enzymatic hydrolysis. Acid hydrolysis is the conventional method for an industrial scale guar gum production from cluster bean. The oligosaccharide products were composed of mannose and galactose with the degree of polymerization up to 20 (Miyazawa & Funazukuri, 2006). Although this method was suitable for a large-scale production, the MOSs produced are mainly long oligosaccharides and barely predicted. MOS products from this reaction may also require additional purification process to remove the acid and chemical contaminants. Hence, different types of substrate and reaction condition effects the characteristics of MOS products (Ganter et al., 1995).



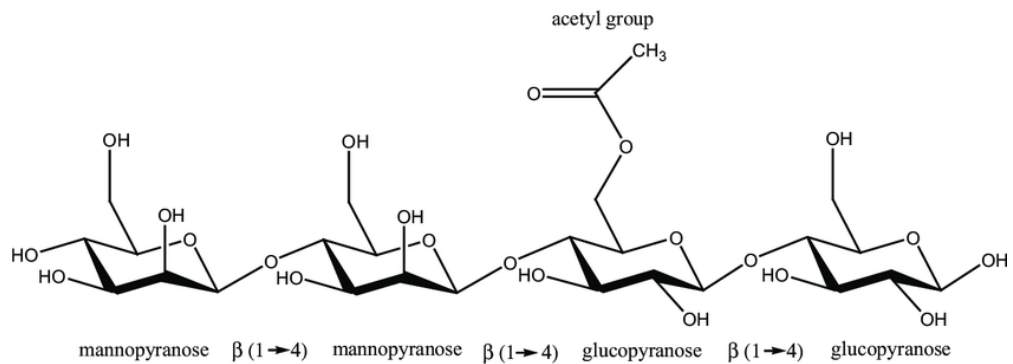


Figure 1. Structure of glucomannan.

(Figure from Mortensen, A. et al. 2017)(Additives et al., 2017).

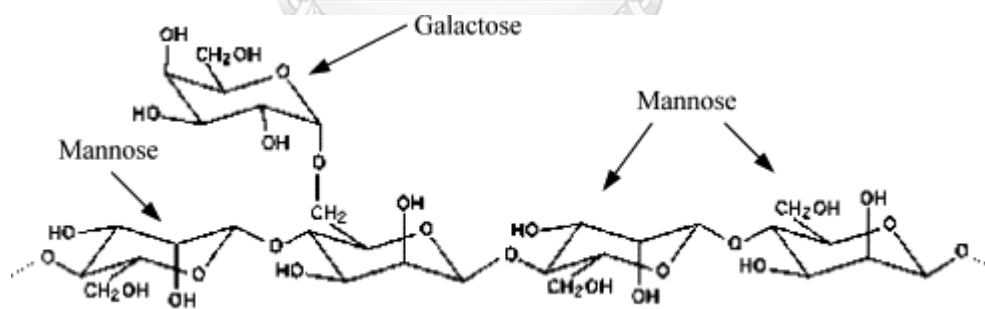


Figure 2. Structure of galactomannan

(Figure modified from Sittikijyothin, W. et al 2005) (Sittikijyothin, Torres, & Gonçalves, 2005).

Recently, production of MOS by enzymatic hydrolysis is of great interested. The enzyme that is mainly uses for this method is  $\beta$ -mannosidase which is a member of glycoside hydrolase family, which can be either obtained from a fungus, bacteria, or engineered recombinant enzyme. Several studies reported that enzymatic production can yield MOS with the degree of polymerization from 2-6, which can be related to those bioactive oligosaccharides that mostly have a low molecular weight or contained a low to moderate degree of polymerization (Mattaveewong et al., 2016; Muanprasat & Chatsudthipong, 2017; Muanprasat et al., 2015; Yousef, Pichyangkura, Soodvilai, Chatsudthipong, & Muanprasat, 2012). However, many recent studies still have a problem in MOS production from leftover biomaterials especially galactomannan from copra meal. Ghosh, *et al.* reported the production of MOS using enzymatic method that can yield MOS from monomer to hexamer, but there was a very low production of the moderate oligosaccharide (Ghosh et al., 2015). Other MOS production from copra meal was reported by Rungrassamee, *et al.* The results shown the larger oligosaccharide was produced but also with a low percentage yield (Rungrassamee et al., 2014). Hence, enzymatic hydrolysis production of MOS with a higher yield is currently a great challenge.



### 1.3 Mannanase

Mannanase or endo-1,4- $\beta$ -D-mannosidase is an endotype hydrolase that can catalyse the random hydrolysis of  $\beta$ -1,4-d-mannopyranosyl linkage of various mannan-based betaglucan polysaccharides to yield MOS. Mannanase have been isolated and characterized from a different source in both prokaryotes and eukaryotes such as bacteria, fungi, or snail (Gupta & Tuohy, 2016). However, a different mannanase from a different source seems to have a different property and might yield a different type of products or require a different condition to perform its reaction. For example,  $\beta$ -mannanase isolated from eukaryote such as *Aspergillus nidulans* also possess a transglycosylation activity but  $\beta$ -mannanase isolated from prokaryote like *Bacillus subtilis* don't possessed this activity (Rosengren et al., 2014). Mannanase is now wildy used in many industries such as food manufacturing, paper industry, and detergent manufacturing. Mannanase also had been used to digest a mannan polymer to produce MOS for animal food supplement (Chauhan, Puri, Sharma, & Gupta, 2012; Gupta & Tuohy, 2016).

Purification and determination of recombinant mannanase, RMase24, optimum condition was performed in a study from Nopvichai, C. *et al.* 2018. (manuscript submitted). The RMase24 was purified through DEAE Toyopearl 650M and Toyopearl phenyl 650M column chromatography,

respectively. The specific activity of RMase24 increased a 3.1fold, 1800 unit per milligrams. This result showed the high endurance of RMase24 through the purification process. RMase24 also possess an ability to work under a wide pH range and seems to work properly under a various buffer. The optimum pH of RMase24 was in citrate buffer pH 6.0 and RMase24 had over 80% of the maximum activity at the pH ranging from 5.0 to 8.0 (Figure 3). The optimum temperature of RMase24 was at 70 °C (Figure 4). Thus, the broad spectrum of pH and temperature of RMase24 made it possible to set up the reaction under various desirable reaction conditions. Interestingly, purified RMase24 was stable, retaining most of its activity, when stored under alkali condition at 4°C for 24 hours. The activity of RMase24 significantly dropped when the pH of the storage buffer became more acidic (Figure 5).

RMase24 showed stability on a wide range of temperature at its optimum pH. The enzyme retains over 75% at temperatures ranging from 40 to 60 °C up to 360 minutes. RMase24 lose 50% of its activity after 120 minutes at 70 °C and dramatically lose its activity down to 10% at 360 minutes. This can be suggested that reaction temperature should be settled at the range of 40-60 °C (Figure 6).

The effects of metal ions had been investigated also. The ion that shown the highest enhancing effects to RMase24 were  $\text{Co}^{2+}$  and  $\text{Zn}^{2+}$  ions which increased its activity to about 136 and 137 percent, respectively. Moreover, the results shown that surfactants and chelating agents also affected the activity of RMase24. Reaction contained SDS or EDTA would decreased RMase24's activity to 25% and 44%, respectively. Whilst Triton X-100 has no effects to RMase24 activity (Figure 7).



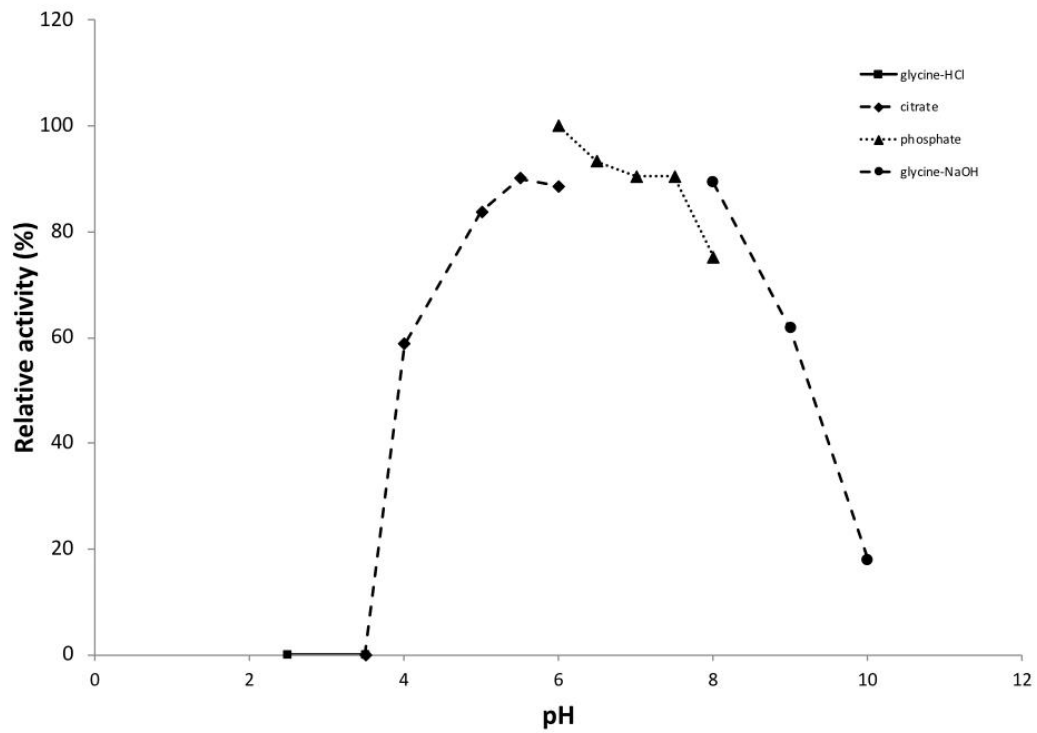


Figure 3. The optimum pH of RMase24 in various buffer and pH

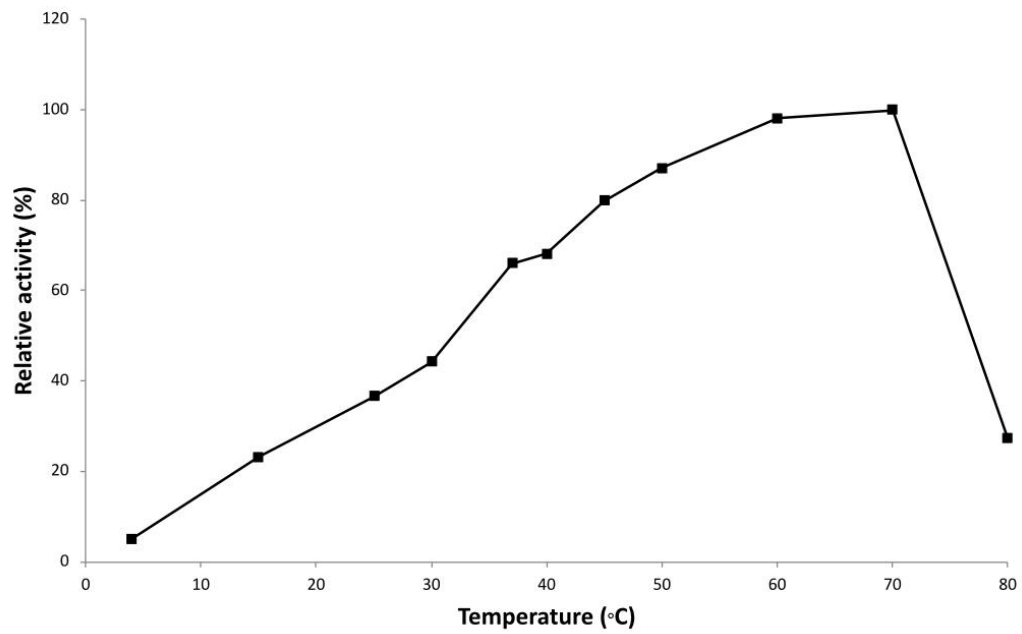


Figure 4. Optimum temperature of RMase24.



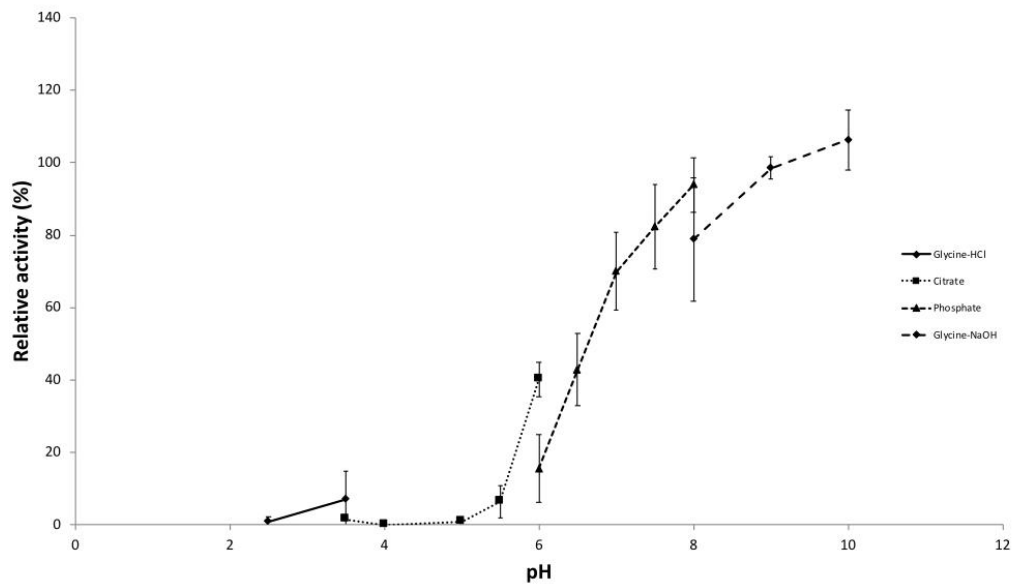


Figure 5. Relative activity of RMase24 under a various storage buffer and pH conditions.



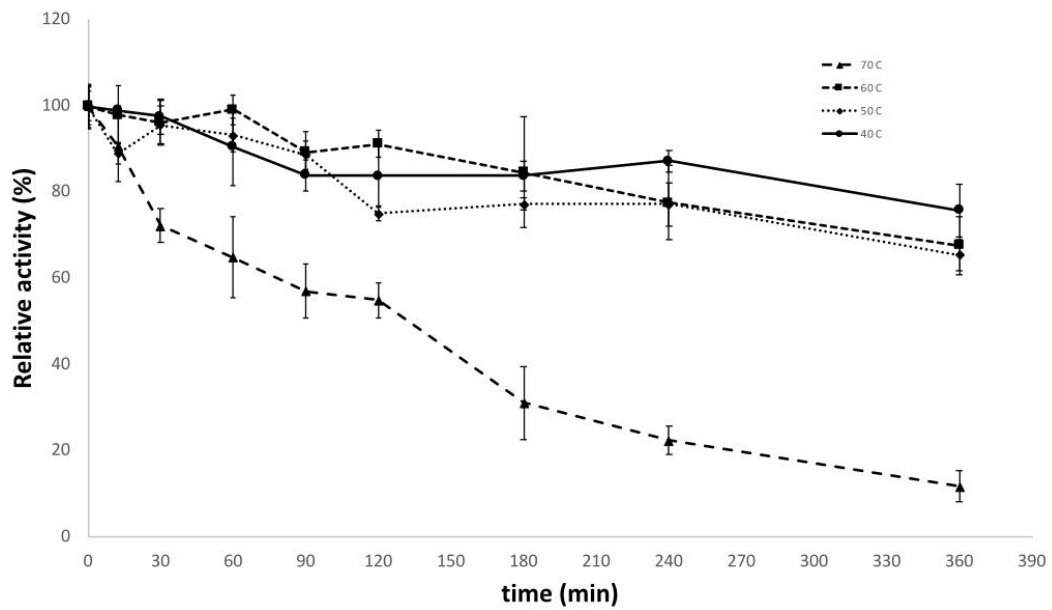


Figure 6. Relative activity of RMase24 under a various temperature at pH6.0.

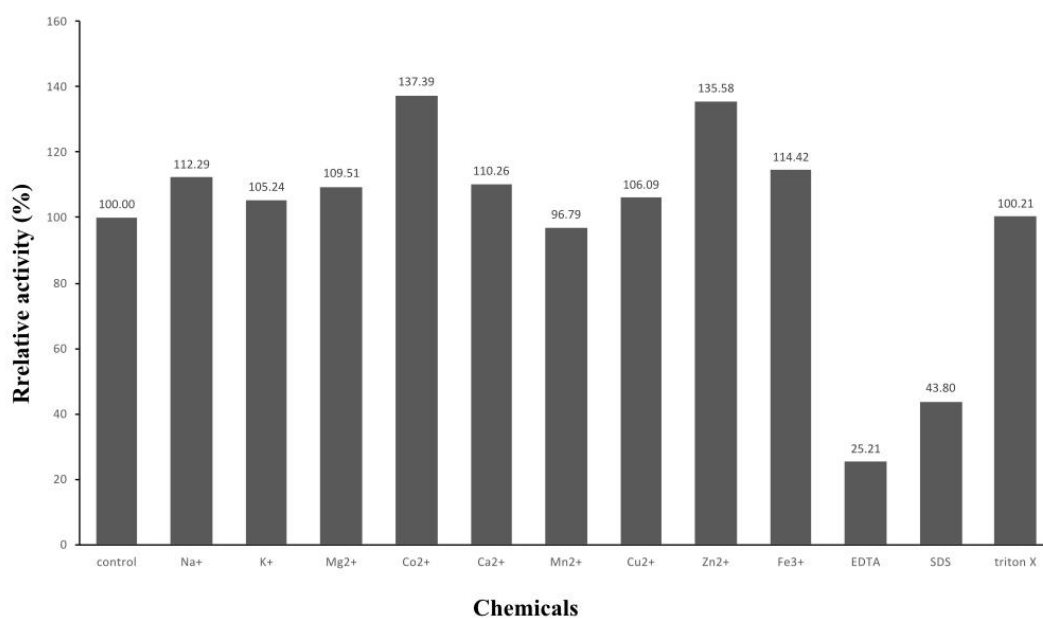
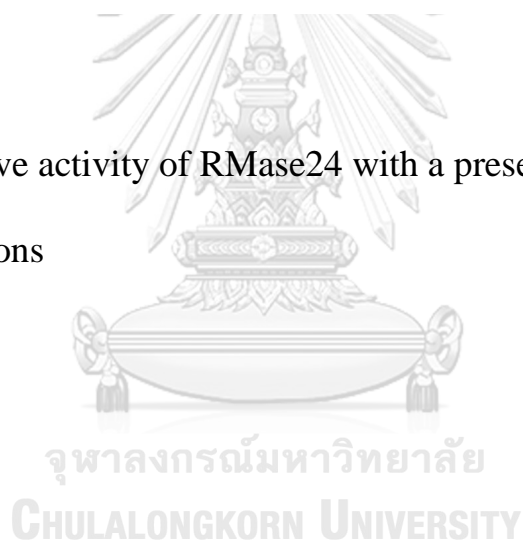


Figure 7. Relative activity of RMase24 with a presence of various chemicals and ions





#### 1.4 Tight junction of epithelial tissues

Tight junction is a continuous, circumferential, belt-like structure at the boundary between the apical and the basolateral membrane domains in epithelia and endothelia that control paracellular permeability (Figure 8, 9). Tight junctions form bidirectional signaling platforms that receive signals from the cell interior, which regulate their assembly and function, and that transduce signals to the cell interior to control cell proliferation, migration, differentiation and survival (Zihni, Mills, Matter, & Balda, 2016). There are a classes of integral membrane proteins that play an important role of tight junction assembly, occludin, members of claudin protein family, and junction adhesion molecule-1 (JAM-1) (Boven, Middel, Verhoef, De Groot, & Nottet, 2000). Tight junction formation can be activated through many pathways including Rho GTPase signaling and the mechanistic target of rapamycin (mTOR) signaling pathways (Laplante & Sabatini, 2012; Matter & Balda, 2003; Zihni, Balda, & Matter, 2014). One of the main pathways that control the assembly of tight junction is an activation of adenosine monophosphate-activated protein kinase (AMPK) pathway by 5-aminoimidazole-4-carboxamide ribonucleoside facilitates tight junction assembly under conditions of normal extracellular  $\text{Ca}^{2+}$  concentrations and initiates tight junction assembly in the absence of  $\text{Ca}^{2+}$  led by the relocation of *zonula occludens*

1, the establishment of transepithelial electrical resistance, and the paracellular flux assay. Expression of a dominant negative AMPK construct inhibits tight junction assembly in MDCK cells, and this defect in tight junction assembly can be partially ameliorated by rapamycin. These results suggest that AMPK plays a role in the regulation of tight junction assembly (Zhang, Li, Young, & Caplan, 2006).

Tight junction is also one of the crucial compartments of a barrier function of an epithelial tissue which is a part of anatomical barriers of an innate immunity in complex and higher organism. A loss of tight junction is a common pathologic feature in many inflammatory disease (Edelblum & Turner, 2009). In several diseases that possess an inflammation especially one with an epithelial inflammation such as inflammatory bowel disease (IBD) or Crohn's disease or even a chronic diarrhea in HIV-infected patient, or a side-effect of some drugs such as Gefitinib or other drugs in EGFR-inhibitor family. Loss of tight junction may lead to many symptoms such as leaking of intra- and intercellular fluid to the gut, leading to diarrhea and others related symptoms. The loss of tight junction might also lead to a dysfunction of a villi that might resulting in an abnormality in nutrient absorption.

Interestingly, many recent studies had reported that a  $\beta$ glycan polymer have an effect to increase tight junction formation through AMPK signaling pathway which is a part of the mTOR signaling pathway (Lin, Hu, Zhu, Woodruff, & Jardetzky, 2011; Mattaveewong et al., 2016; Muanprasat et al., 2015). The hypothesis of this study is that a MOS, which is also a  $\beta$  glycan polymer may have an ability to enhance cellular tight junction assembly.



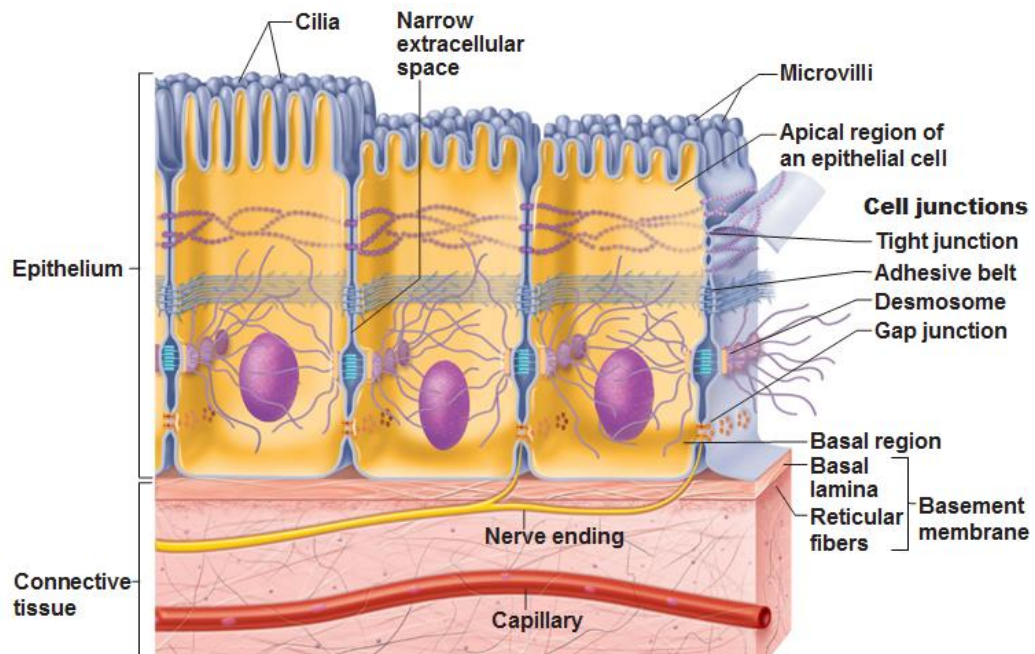


Figure 8. Cross section of epithelial tissue shown a compartment of cell junctions including tight junction, adherens junction (adhesive belt), and gap junction.

(Figure modified from <https://antranik.org/detailed-features-of-epithelia/>)

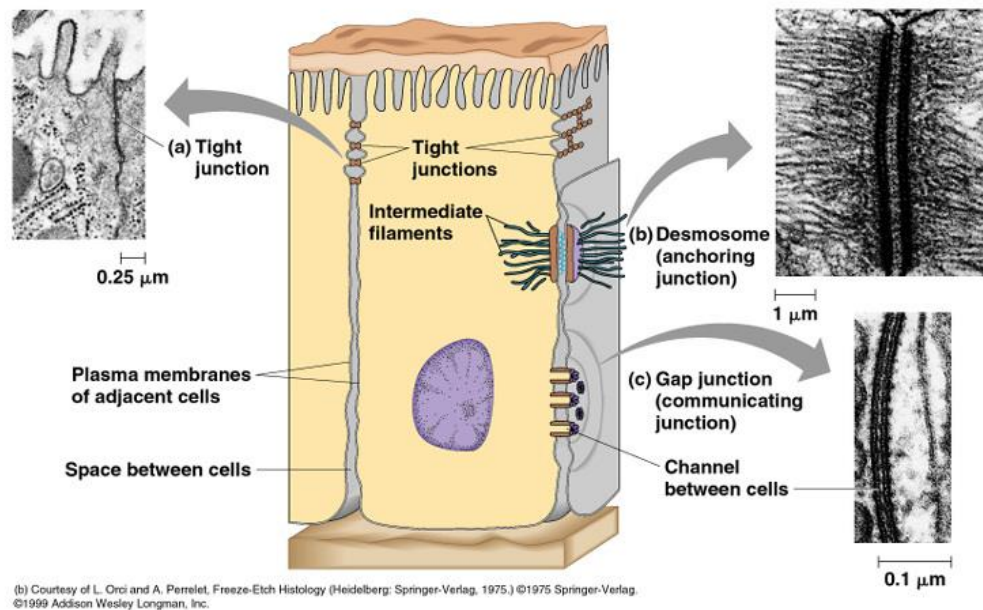


Figure 9. Cross section of epithelium cell shown a compartment of cell junctions with scanning electron microscope image.

(A figure from Orci, L.& Perrelet, A. Freeze-Etch Histology: A Comparison between Thin Sections and Freeze-Etch Replicas. Springer publishing) (Orci & Perrelet, 2012).

### 1.5 Adenosine monophosphate-activated protein kinase (AMPK) pathway

Adenosine monophosphate-activated protein kinase (AMPK) is a highly conserved sensor of intracellular adenosine nucleotide levels that is activated to promote catabolic pathway to generate ATP and inhibits anabolic pathway. AMPK functions had been conserved as an energy sensing in many species and also involved in several cellular activities such as cell growth, cell differentiation, or even a specific role in cellular metabolism especially in eukaryotic cells (Mihaylova & Shaw, 2011).

Several studies also revealed that AMPK also involved in cell polarity and tight junction formation (Mihaylova & Shaw, 2011). In *Drosophila*, loss of AMPK results in altered cell polarity (Lee et al., 2007; Mirouse, Swick, Kazgan, St Johnston, & Brenman, 2007). A study in mammalian Madin-Darby canine kidney (MDCK) cells also shown that AMPK was activated and needed for proper re-polarization and tight junction formation following calcium switch (Mihaylova & Shaw, 2011; Zhang et al., 2006; Zheng & Cantley, 2007).

Moreover, AMPK is also believed that it might involved in tight junction formation. Activated AMPK also phosphorylates afadin and induces its association with ZO-1 (Mihaylova & Shaw, 2011). AMPK also phosphorylates G-alpha interacting vesicle associated protein (GIV), which regulates cell polarity and morphogenesis, as well as cell-cell

junction formation through its ability to bind Par3 and the Cadherin-catenin complex (Figure10) (Rowart, Wu, Caplan, & Jouret, 2018).

A study from Zheng, *et al.* (2007) also revealed that hyperactivation of AMPK can enhance the stability of tight junctions under conditions of calcium depletion. These results raise the interesting possibility that during conditions of mild energy stress leading to elevation of AMP, activation of AMPK stabilizes contacts between epithelial cells. These findings also raise the possibility that drugs that activate AMPK, for example, metformin, could provide a beneficial effect in diseases during which tight junctions are disrupted (Zheng & Cantley, 2007; Zhou et al., 2001).

In this work, an investigation was focused on 1) a high efficiency of MOS production protocol using a recombinant mannanase, 2) a determination of bioactive MOS that can increase a tight junction of epithelial cells, and 3) an investigation on a regulation of AMPK that might be activated through a treatment of those bioactive MOS.

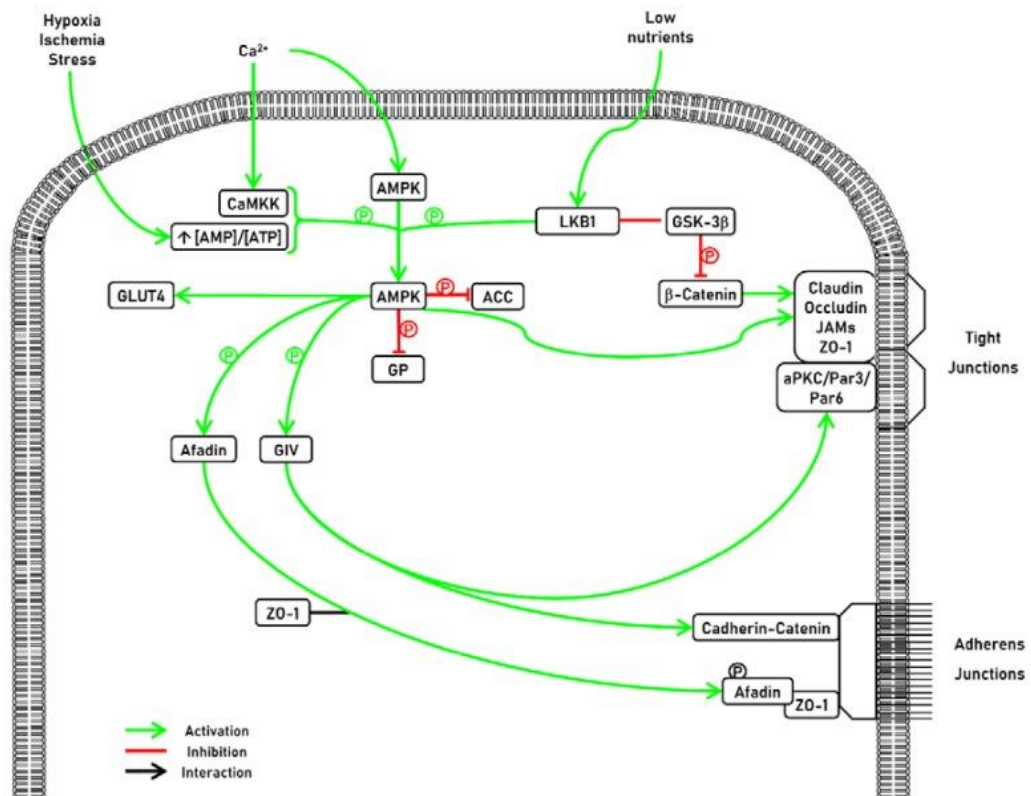


Figure 10. Activators, substrates, and downstream regulations schema of AMPK pathway related to adherens junctions and tight junction of the cell.

A figure from Rowart P, et al. (2018) (Rowart et al., 2018).



## CHAPTER II

### MATERIALS AND METHODS

#### 2.1 Equipments

Autoclave: Model 29MLS-2400. Sanyo, Japan

Autoflex maX MALDI-TOF and TOF/TOF: Bruker, Germany

Autopipette: Pipetteman Gilson, France

Centrifuge, refrigerated centrifuge: Model J2-21, Beckman Instrument, Inc., U.S.A. and Sorvall Legend XTR, ThermoFisher Scientific, Inc., Germany

Centrifuge, microcentrifuge: Model 5430, Eppendorf Co., Ltd., Germany

Electrophoresis unit:

- Mini protein, Bio-Rad, U.S.A.
- Mini Horizontal Gel Electrophoresis System, Major Science, U.S.A.
- Submarine agarose gel electrophoresis unit, Bio-Rad, U.S.A.

Eppendorf Biospectrometer® basic: Eppendorf, Germany

EVOM2 volt-ohm meter, World Precision Instruments, Inc., Sarasota, FL, USA

Filter: Whatman no.1 filter paper, Whatman cellulose filter paper grade 4, and 0.45 micrometers cellulose acetate membrane filter, Sigma Aldrich,

USA

Fraction collector: Frac-920, GE Healthcare Bio-Sciences AB, Sweden

FT-NMR 600MHz: Bruker, Germany

Gel Document: SYNGEND, England

High performance anion exchange chromatography (HPAEC-PAD),

Dionex, USA

High-power blender Moulinex, France

Humidified carbon dioxide incubator

Incubator, shaker: Innova™ 4000 and 4080, New Brunswick Scientific,

U.S.A.

Incubator, waterbath: Model M20S, Lauda, Germany and Biochiller

2000, FOTODYNE Inc., U.S.A. and ISOTEMP 210, Fisher Scientific,

U.S.A.

Laminar flow: HT123, ISSCO, U.S.A. and Streamline® Vertical Laminar

Flow Cabinet Model SCV-4A1, Gibthai Co., Ltd., Singapore

Luminata Crescendo Western HRP Substrate (Merck Milli- pore,

Billerica, MA, USA)

Magnetic stirrer: Model Fisherbrand, Fisher Scientific, U.S.A.

Magnetic spinbar: Teflon® PTFE, Scienceware®, Capitol Scientific, Inc.,

U.S.A. Microplate reader: Synergy™ H1,

MicroPulser™ electroporator: Bio-Rad, U.S.A.

MALDI-TOF mass spectrometer (Solari X, FT mass spectrometry, Bruker, United states).

pH meter: Model MP220, Mettler-Toledo International, Inc., U.S.A.

Spectrophotometer: Model G10S UV-Vis,

SEM-EDS: Jeol JSM-6400 scanning electron microscope, Jeol Ltd.

Japan.

ThermoFisher Scientific, Inc., U.S.A. Thermal Cycler Block: Type 5020,

ThermoFisher Scientific, Inc., Finland

Transwell® insert (Corning Glass Works, Corning, NY, USA)

Vortex: Model G560E, Scientific Industries, Inc., U.S.A.

Water bath: Charles Hearson Co. Ltd., England

$1 \times 10^6$  cells/ well (Corning Life Sciences, Tewksbury, MA, USA)

## 2.2 Chemicals

Absolute ethanol (Merck)

Acrylamide (AppliChem PanReac)

Agarose (Invitrogen)

Ammonium hydroxide (Sigma-Aldrich)

Ammonium persulfate (AppliChem)

Ampicillin (Affymetrix)

Antibodies:

Rabbit antibodies to phospho-AMPK (Thr-172) (Cell Signaling Technology)

AMPK- $\alpha$  (Cell Signaling Technology)

$\beta$ -actin (Cell Signaling Technology)

$\beta$ -mercaptoethanol (Bio Basic)

Biogel P2 resin (Biorad)

Biogel P4 resin (Biorad)

Citric acid (Univar)

Cobalt (II) chloride (Merck)

Copper (II) sulphate (Sigma-Aldrich)

Dipotassium phosphate (Univar)

Ethylenediaminetetraacetic acid (EDTA) (AppliChem)

Glacial acetic acid (Merck)

Glucose (Univar)

Glycerol (Univar)

Glycine (Norgen Biotek)

Calcium (II) chloride (Univar)

Chloroform (Carlo Erba)

Dinitrosalicylic acid (Sigma-Aldrich)

Dulbecco's Modification of Eagle's Medium (DMEM) /Ham's F-12  
(Corning)

Horseradish peroxidase-conjugated goat antibody to rabbit  
immunoglobulin G (Cell Signaling Technology)

Hydrochloric acid (Labscan)

Iron (III) chloride (Univar)

Isopropyl  $\beta$ -D-1-thiogalactopyranoside (IPTG) (ThermoFisher Scientific)

Magnesium (II) chloride (Univar)

Methanol (Honeywell)

Minimum Essential Medium Eagle, Spinner Modification (SMEM)  
(Corning)

Potassium chloride (Univar)

Potassium dihydrogen phosphate (Univar)

Phenol (Merck)

Sodium chloride (Univar)

Sodium citrate (Univar)

Sodium azide (Univar)

Sodium dodecyl sulfate (Univar)

Sodium hydroxide (Lab-Scan)

Tris-Buffered Saline Tween-20 (TBST)

Tetramethylethylenediamine (TEMED) (ThermoFisher Scientific)

Toyopearl DEAE 650m resin (Sigma-Aldrich)

Toyopearl phenyl 650m resin (Sigma-Aldrich)

TriColor Broad Protein Ladder (Biotechrabbit)

Trifluoroacetic acid (ThermoFisher Scientific)

Tris (Vivantis)

Triton X-100 (Schalau)

Tryptone type-I (Biobasic)

Tween-20 (Sigma)

Yeast extract (Biobasic)

Zinc (II) sulfate (Univar)

5% non-fat dried milk (BioRad)

### 2.3 Enzymes and restriction enzymes

$\alpha$ -galactosidase from *Achantina fulica* (Amano) (labeled as AMAN-AfGLA)

Exo- $\beta$ -mannosidase from *Achantina fulica* (Seigaku) (labeled as AfMAN)

T4 DNA Ligase (NEB)

*Nde*I (NEB)

*Xho*I (NEB)

PrimeSTAR® DNA polymerase (Takara)

### 2.4 Bacterial strains, Cell line and plasmids

*Bacillus subtilis* CAe24 screened from previous study, was used for genomic DNA template for mannase gene amplification.

*Escherichia coli* TOP10 (Invitrogen™, Thermo Scientific), genotype:

F- mcrA  $\Delta$ (mrr- hsdRMS-mcrBC)  $\phi$ 80lacZ $\Delta$ M15  $\Delta$ lacX74 recA1

araD139  $\Delta$ (araleu)7697 galU galK rpsL (StrR) endA1 nupG, was used as a host for plasmid propagation.

*Escherichia coli* BL21 (DE3) (Novagen), genotype: F- ompT gal dcm

lon hsdSB(rB- mB-)  $\lambda$ (DE3 [lacI lacUV5-T7p07 ind1 sam7 nin5])

[malB+]K-12( $\lambda$ S), was used as an expression host for protein production.

pGEM-t-easy (Promega) was used as recombination vector

pET21b (Novagen) was used as expression vector

**T84 human cell line** (American Type Culture Collection), was used as a represent of human epithelial cells.





## **2.5 General technique for molecular cloning, gene expression and protein expression.**

### **2.5.1 Genome extraction**

The 1 mL of overnight culture was harvested by centrifugation at 8,000xg for 5 minutes. Cells supernatant were then removed and the cell pellets were resuspended with 0.5 mL SET buffer. Collected cells were lysed by adding 30  $\mu$ L of 10% SDS and gently mixed by inverting the tube. Then, 50  $\mu$ L of 5 M sodium acetate was added and gently mixed. Cells lysate were centrifuged at 10,000xg for 10 min and the supernatant was collected. The protein contaminant was gently extracted by phenol: chloroform: isoamylalcohol and then centrifuged at 10,000xg for 10 min, twice. The upper phase of the reaction was transferred into nuclease-free microcentrifuge tube. Genomic DNA was precipitated by adding of 2.5 volumes of absolute ethanol and pellet by centrifugation at 10,000xg for 5 min. The DNA pellet was washed by 70 % (v/v) ethanol and dried to remove the residual ethanol at 60 °C for 10 min. The genomic DNA was dissolved in sterile nuclease-free ultrapure (UP) water and stored at 4 °C.

### 2.5.2 Plasmid preparation

Cells harbouring plasmid were cultured in 4 mL of LB broth containing appropriate antibiotics at 37 °C with shaking at 250 rpm for overnight. Cells were then harvested by centrifugation at 10,000xg for 30 sec and applied to Presto™ Mini Plasmid Kit (Geneaid).

### 2.5.3 Electrocompetent cell preparation

The method was modified based on Sambrook et al. Overnight *E. coli* culture was diluted in fresh LB medium with ratio of 1:100. The culture was then grown in at 37 °C shaking 250 rpm. The bacterial growth was monitored until OD600 reached ~0.3-0.35. Cells were immediately kept on ice for 10 min. Thereafter, cells were collected by centrifugation at 2,000 xg, 4 °C for 10 min. The cell pellets were gently washed by cold sterile UP-water and collected by centrifugation at 2,000 xg, 4 °C for 10 min (repeat this step twice). Then, cells were washed by cold 10 % (v/v) glycerol and collected by centrifugation at 2,000xg, 4 °C for 12 min. Cell pellets were suspended with ratio of 500 µL of cold 10 % (v/v) glycerol:1 L of cell culture. Forty microliters of cell suspension were then aliquoted into microcentrifuge tube and immediately stored at -80 °C freezer.

#### **2.5.4 Transformation of recombinant plasmid into *E. coli* host cell**

The 3  $\mu\text{L}$  of plasmid solution or purified ligation mixture was gently mixed with the competent cells on ice. Then, cells mixture was transferred to a 0.1 or 0.2 cm-gap cold sterile electroporation cuvette and electroporated by using 25  $\mu\text{F}$ , 200  $\Omega$  of the pulse controller unit with 18 kV. Then, 0.5 mL of LB medium was added to the cells mixture for recovery and cells were culture at 37 °C with shaking at 250 rpm for 45 min. The recovered culture was thoroughly plated on LB agar containing appropriate antibiotic and incubated at 37 °C for overnight.

#### **2.5.5 Agarose gel electrophoresis**

The 8 % (w/v) agarose gel was prepared. 8 g. of agarose was dissolved in 100 mL of 1xTAE buffer and heated until completely dissolved. The gel was then cast. After gel was set completely, the DNA samples were mixed well with 6x loading dye and subsequently loaded into the wells. Electrophoresis was constantly run at 100 Volts for 30-45 min. The gel was stained with 50 mg/L ethidium bromide solution and visualised under UV light by Gel Document device.

### 2.5.6 Construction of recombinant mannannase

In our previous study, we have isolated a bacterial strain that can produce mannannase. The selected candidate was *Bacillus subtilis* strain CAe24 and its identity was confirmed with 16sRNA characterization as *Bacillus subtilis* CAe24. The amplification of target mannannase gene was designed using an information from the genome database il433616933:611507-613595 from *Bacillus subtilis* stain BEST7613. Polymerase chain reaction was performed using 5'-GGGGAGTTGCA TATGTTTAAGA-3' and 5'-GCGGAACGTCTGATTAGAGC-3' as a forward primer and reverse primer, respectively.

The gene product encoding mannannase was sequenced and submitted to NCBI, accession number KY951415. The PCR product was recombined to the pGEM-t-easy vector and then transformed to TOP10 *E.coli* using electroporation technique. Collected recombination plasmid was cut and the gene was subcloned into pET21b expression vector using *XhoI* and *NdeI* as a restriction-recombination enzyme. The final recombinant plasmid, pvRM24-A, was transformed into BL21 expression host using the same method as mentioned above. This mannannase-containing bacterial strain is entitled as RM24.

### 2.5.7 Western blot analysis

T84 Cells were grown on 6-well plates at a density of  $1 \times 10^6$  cells/ well (Corning Life Sciences, Tewksbury, MA, USA). After treatments for subjected timepoint, cell lysates were harvested using lysis buffer. Thirty-microgram proteins were separated using sodium dodecyl sulfate polyacrylamide gel electrophoresis (SDS-PAGE) before transferring to nitrocellulose membrane. The membrane was incubated for 1 h with 5% non-fat dried milk (BioRad, Hercules, CA, USA), and incubated overnight with rabbit antibodies to phospho-AMPK (Thr-172), AMPK- $\alpha$  and  $\beta$ -actin (Cell Signaling Technology, Boston, MA, USA). The membrane was then washed for 4 times with Tris-Buffered Saline Tween-20 (TBST) and incubated for 1 hour at room temperature with horseradish peroxidase-conjugated goat antibody to rabbit immunoglobulin G (Cell Signaling Technology, Boston, MA, USA). The signals were detected using Luminata Crescendo Western HRP Substrate (Merck Millipore, Billerica, MA, USA). Band density was analyzed using Image J software (version 1.51s, National Institute of Health, Bethesda, MD, USA) following the manufacturer's protocol available at <http://www.yorku.ca/yisheng/Internal/Protocols/ImageJ.pdf> . Expression of pAMPK over AMPK- $\alpha$  was calculated with the formula following by:

(pAMPK/pAMPK's  $\beta$ -actin)/ (AMPK- $\alpha$ / AMPK- $\alpha$ 's  $\beta$  actin). pAMPK expression level was neutralized over control group to translate to percentage relative value.

## **2.6 Preparation and characterization of galactomannan substrate**

### **2.6.1 Pretreatment of galactomannan substrate**

Galactomannan substrate was received as a dried, rough copra meal which is a leftover waste from a coconut milk and oil extraction process. Forty grams of copra meal was ground using a high-power blender (Moulinex, France). A Fine grain of copra meal powder then subjected solvent extraction to remove the remaining oil by dissolving in 200 mL of n-hexane, and then sonicated for 10 minutes. The suspension was filtered with a cellulose filter paper (Whatman no.1, Sigma Aldrich, USA.). The oil removing process was repeated 3 times before left to dry in an incubator chamber at 60 °C overnight. The dried substrate then dissolved in 400 mL of deionized water and then homogenized before autoclaved at 110 °C and 15psi for 20 minutes. The product of this step is labelled as G-GalMan.

Thereafter, the G-GalMan was sonicated using a probe-type sonicator at 40% power, 2seconds/1second pulse, for 300 minutes. The

sonicated products then spun down at 10,000xg and wash with deionized water twice before resuspending in 100 mL of 0.05M citrate buffer pH 6.5. The final pretreated product is labelled as S-GalMan. Wet weight and dry weight of S-GalMan was measured.

### **2.6.2 Characterization pretreated galactomannan substrate**

Galactomannan substrates were washed with ultrapure water and store at 4 °C before subjected to perform a surface imaging at Scientific and Technological Research Equipment Center (STREC), Chulalongkorn University. Substrate samples including deoiled, G-GalMan, S-GalMan and digested substrates were analyzed with SEM-EDS (Jeol JSM-6400 scanning electron microscope, Jeol Ltd. Japan).

## **2.7 Mannan oligosaccharide (MOS) production and purification**

### **2.7.1 Production of MOS from pretreated galactomannan substrate**

The digestion of S-GalMan and G-GalMan with RMase24 was performed. After the digestion reactions were completed, digestion mixtures were centrifuged at 10,000g to remove the undigested debris. The hydrolysate was filtered using filter paper (Whatman cellulose filter paper grade 4, Sigma Aldrich, USA) and 0.45 micrometers cellulose acetate membrane filter (Whatman cellulose acetate membrane, Sigma Aldrich, USA). Crude MOS produced from each substrate were collected at 24 hours and then measured their dried weight and calculated the percentage yield.

### **2.7.2 Separation and purification of MOS**

Crude MOS was purified using biogel p2 size exclusion column chromatography. The collected MOS fractions were then lyophilized and analyzed using thin layer chromatography (TLC) in system A (as mentioned below at section 2.9.1.1.) at 35-40 °C. Each separated MOS on TLC was visualized by orcinol-sulfuric acid staining solution [21]. Thereafter, each purified MOS was lyophilized and measured the weight and kept at -4°C.



## **2.8 Technique for cell experiment**

### **2.8.1 Cell line preparation**

T84 were grown in a mixture of Dulbecco's Modification of Eagle's Medium (DMEM) /Ham's F-12, supplemented with 10% fetal bovine serum (FBS) and 100U/ml penicillin/streptomycin and cultured at 37°C in a humidified CO<sub>2</sub> incubator. To form polarized monolayers, T84 cells were seeded in the 6-wells transwell<sup>®</sup> insert at a density of approximately  $5 \times 10^5$  cells/insert and cultured for 14 days or until transepithelial electrical resistance (TEER) reached 1000 Ohm/cm<sup>2</sup>. The culture media were replaced every 20 to 24 hours.

### **2.8.2 Transepithelial electrical resistance (TEER) measurement**

TEER measurement was performed using EVOM2 volt-ohm meter following by the manufacturer's protocol which is available at [https://www.wpiinc.com/pub/media/wysiwyg/pdf/EVOM2\\_IM.pdf](https://www.wpiinc.com/pub/media/wysiwyg/pdf/EVOM2_IM.pdf). The resistance values were collected in a unit of millivolts

### **2.8.3 Determination of a change in TEER induced with MOS**

Each purified MOS4, MOS5, MOS6, and MOS7 were dissolved separately in ultrapure water to make a 50  $\mu\text{M}$  to 100  $\mu\text{M}$  stock concentration then filtered through 0.2 micrometer filter membrane before mixed with DMEM/Ham's F-12 without 10% FBS up to desire concentration (20  $\mu\text{M}$ , 10  $\mu\text{M}$ , 5  $\mu\text{M}$ , 1  $\mu\text{M}$ , and 0.1  $\mu\text{M}$ ). After the cell were grown and the polarized monolayer was formed, each prepared MOS in DMEM was treated to the cells and the change in TEER was monitored before and at 24 hours after a treatment.

### **2.8.4 Calcium switch assay**

T84 cells were cultured in DMEM in a transwell<sup>®</sup> insert until cells were formed the monolayer and the population of the cells reached 80% or until the TEER of the cells were steady. After that, DMEM medium was substituted with the Minimum Essential Medium Eagle, Spinner Modification (SMEM) ( $\text{Ca}^{2+}$ -free culture media) to disrupt tight junctions. Twenty-four hours later, SMEM medium was replaced with regular DMEM/Ham's F-12 (containing  $\text{Ca}^{2+}$ ) supplemented with vehicle, MOS5 (10  $\mu\text{M}$ ), MOS5 (10  $\mu\text{M}$ ) plus compound C (80 mM), or

compound C (80 mM) alone. TEER was measured before and every 15 minutes after  $\text{Ca}^{2+}$  switch up to 12 hours.

## **2.9 Technique for characterization**

### **2.9.1 Product characterization techniques**

#### **2.9.1.1 Thin layer chromatography**

The mobile phase system A comprises 2-butanol: acetic acid: water (3:3:2). The system A was equilibrated at 30-37 °C at least 72 hr. On the other hand, the mobile phase system B consists of Acetonitrile:Ethyl acetate:1- propanol: water (85:20:50:60). The system B was equilibrated at room temperature for 48 hours before used. The samples were spotted on TLC aluminium plate or glass plate and run in saturated tanks until the mobile phase reached the top mark before left to dry. The procedure was repeated for 3 times for 10 cm in length plate and 4 times for full 20 cm plate. The products were visualised by spraying with orcinol-sulfuric solution and burning at 110 °C or baked in 120 °C oven for 8-10 minutes.

### **2.9.1.2 High Performance Anion Exchange Chromatography-Pulse Amperometric Detection (HPAEC-PAD) analysis**

MOS 5 was diluted to 1  $\mu\text{M}$  before it was filtered through 0.45  $\mu\text{m}$  syringe filter prior to injection. MOS5 was analyzed by CarboPac PA100 (2 or 4 mm. in diameter x 250 mm. in length) and eluted with linear gradient of 0-150 mM of sodium acetate in 150 mM NaOH.

### **2.9.1.3 Mass spectrometry analysis**

Lyophilized samples of MOS4, MOS5, MOS6, and MOS7 were dissolved to make 20  $\mu\text{M}$  solution. The molecular mass determination of each purified MOS was performed using MALDI-TOF mass spectrometer at Osaka city university (Solari X, FT mass spectrometry, Bruker, United states).

### **2.9.1.4 Nuclear Magnetic Resonance (NMR) analysis**

Purified samples in ultrapure water were lyophilized and then dissolved in D<sub>2</sub>O at the highest concentration as possible before subjected to NMR analysis using FT-NMR 600MHz (Bruker). NMR was performed and the result was analyzed by NMR specialist at Osaka City University.

## 2.9.2 Enzymatic hydrolysis analysis

### 2.9.3.1 Purification of $\alpha$ -galactosidase from *A. fulica* (Amano, Japan)

One hundred milligrams of  $\alpha$ -galactosidase from *A. fulica* (Amano, Japan) (AMAN-AfGLA) was dissolved in 20 mL of 10 mM sodium acetate buffer. The solution was centrifuged at 10,000 xg for 10 minutes. The supernatant was collected and purified through ammonium sulfate precipitation technique. The solution was set up to 30% w/v of ammonium sulfate and left to precipitate overnight at 4 °C before centrifuged to collect precipitant. The collected precipitant was re-suspended in 10mM sodium acetate buffer again before repeating the precipitation with 70% w/v of ammonium sulfate. The supernatant was collected and performed a further precipitation with 90% ammonium sulfate for 48 hours at 4 °C. The solution was centrifuged at 12,000 xg for 10 minutes. The precipitated enzyme was labeled as P-AMAN-AfGLA and dialyzed against 5mM sodium potassium phosphate buffer for overnight at 4 °C. The dialysis was repeated twice with buffer renewal. The collected enzyme was tested its activities with 10 mM mannobiose and 10 mM melibiose before performed a further purification through Sephadex G150 gel filtration column chromatography (3.0 cm. in diameter and 45.0 cm. in length) with 400 mL of 10 mM sodium potassium phosphate buffer

and 0.15 M NaCl pH 6.5 as running buffer. Each fraction was collected with 5 mL volume.

### **2.9.3.2 Enzymatic digestion of MOS5**

#### **2.9.3.2.1 MOS5 digestion with *exo*- $\beta$ mannosidase (*A. fulica*) (Seigaku), (AfMAN)**

One microliter of 1  $\mu$ M MOS5 was digested with 1 uL of 10U/mL AfMAN before incubated at 37 °C. The reaction product was analyzed on TLC under system A.

#### **2.9.3.2.2 MOS5 digestion with $\alpha$ -galactosidase (*A.fulica*) (Amano) (AMAN-AfGLA)**

One microliter of 1  $\mu$ M MOS5 was digested with 0.25uL, 0.5uL, and 1uL of 5mg/mL AMAN-AfGLA before incubated at 37 °C. The reaction was analysed on TLC under system A.

### **2.9.3.2.3 MOS5 digestion with purified $\alpha$ -galactosidase (*A.fulica*) (Amano) fraction number 35 (P-AMAN-AfGLA-f35)**

One microliter of 1  $\mu$ M MOS5 was digested with 0.0625uL, 0.125uL, 0.25uL, 0.5uL, 1uL, 2uL, 4.5uL, and 9uL of P-AMAN-AfGLA-f35. The reaction was analyzed on TLC under system A.

### **2.9.3.2.3 Preparation of digested products of MOS5 with P-AMAN-AfGLA-f35 for NMR analysis**

The reaction of MOS5 with excess amount of P-AMAN-AfGLA-f35 was performed using 400 uL of 1  $\mu$ M MOS5 with 3.6 mL P-AMAN-AfGLA-f35. The reaction was incubated at 37°C for 30 hours to allow the reaction went to complete. One microliter of digested reaction was spotted on TLC and visualized under system A to confirm the digestion. The remaining reaction was separated through Biogel P2 column chromatography. The collected fractions then lyophilized and dissolved in D<sub>2</sub>O before submitted to NMR analysis.

## CHAPTER III RESULTS

### 3.1 Cloning and expression of recombinant mannanase gene from *Bacillus subtilis* CAE24

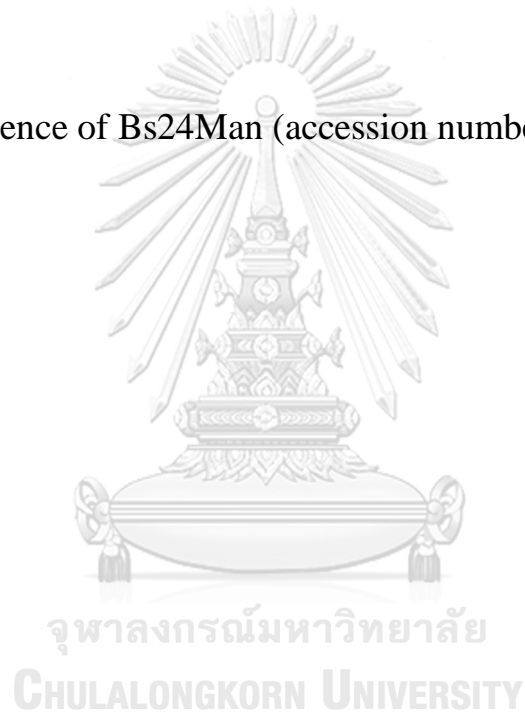
#### 3.1.1 Cloning and characterization of mannanase gene

The mannanase gene was amplified by using a genomic DNA of *Bacillus subtilis* CAe24 as a template. The amplification of target mannanase gene was designed as previously described. The gene product was entitled as *Bs24Man*. *Bs24Man* is 1090 bp in size and encoding 362 residues of deduced amino acids. The sequence is shown below in Figure 11. The theoretical molecular weight and pI is 40,918.08 Da and 5.80, respectively. The amino acid sequence was blasted with NCBI database and aligned with various mannanase sequence of various *Bacillus subtilis* strain as shown in Figure 12. The alignment result showed 99% identity with only two different amino acid residues highlight in yellow was present outside of catalytic domain. Three-dimensional structure of *Bs24Man* was constructed using Swiss-PdbViewer, DeepView version 4.1, compared with mannan endo-1,4- $\beta$  mannosidase from *Bacillus subtilis* BEST7613 (Figure 13).



ATGTTTAAGAAACATACGATCTCTTTGCTCATTATATTTTTACTTGCGTCTGCTGTTTTAGCAAAACCAA  
 TTGAAGCGCATACTGTGTGCGCTGTGAATCCTAATGCCAGCAGACAACAAAAACAGTGATGAACTGGCT  
 TGCGCACCTGCCGAACCGAACGGAAAACAGAGTCCTTTCCGGAGCGTTCCGGAGGTTACAGTCATGACACA  
 TTTTCTATGGCTGAGGCTGATAGAATCCGAAGCGCCACCGGGCAATCGCCTGCTATTTATGGCTGCGATT  
 ATGCCAGAGGATGGCTTGAAACAGCAAATATTGAAGATTCAATAGATGTAAGCTGCAACGGCGATTAAAT  
 GTCGTATTGGAAAAATGGCGGAATTCGGCAAATCAGTTTGACCTGGCGAACCCCTGCTTTTCAGTCAGGG  
 CATTTTAAAACACCGATTACAAATGATCAGTATAAAAAAATACTAGATTCTTCAACAGTAGAAGGAAAGC  
 GGCTAAATGCCATGCTCAGCAAATTTGCTGACGGACTTCAAGAGTTGGAGAACCAAGGTGTGCCTGTTCT  
 GTTCAGCCGCTGCATGAAATGAACGGTGAATGGTTTTGGTGGGGACTTACATCATATAATCAAAGGAT  
 AATGAAAGAATCTCTCTATATAAACAGCTCTACAAGAAAATCTATCATTATATGACCGACACAAGAGGAC  
 TTGATCATTGATCTGGGTTTACTCTCCGACGCCAACCAGATTTTAAAACGATTTTACCCTGGGCGC  
 GTCTTACGTGGATATTGTCGGATTAGATGCGTATTTTCAAGATGCCTACTCGATCAATGGATACGATCAG  
 CTAACAGCGCTTAATAAACCATTTGCTTTTACAGAAGTTGGCCCGCAAACAGCAAACGGCAGCTTCGATT  
 ACAGCCTGTTTCATCAATGCAATAAAACAAAAATATCCTAAAACCATTTACTTCCCTCGCATGGAATGATGA  
 ATGGAGCCAGCAGTAAACAAGGGTGCTTACGCTTTATATCATGACAGCTGGACTCAATAAGGGAGAA  
 ATATGGAATGGCGATTCTTTAACGCCAATCGTTGAATGAA

Figure 11. Sequence of Bs24Man (accession number KY951415).



RMASE24	MFKKHTISLLIIFLLASAVLAKPIEAHTVSPVNPNAQQTTKTMVNWLAHLPNRTENRVLS	60
BEST7613	MFKKHTISLLIIFLLASAVLAKPIEAHTVSPVNPNAQQTTKTMVNWLAHLPNRTENRVLS	60
WL7	MFKKHTISLLIIFLLASAVLAKPIEAHTVSPVNPNAQQTTKTMVNWLAHLPNRTENRVLS	60
GE28	MFKKHTISLLIIFLLASAVLAKPIEAHTVSPVNPNAQQTTKTMVNWLAHLPNRTENRVLS	60
*****		
RMASE24	GAFGGYSHDTFSMAEADRIRSATGQSPAIFYGCDYARGWLETANIEDSIDVSCNGDLMSYW	120
BEST7613	GAFGGYSHDTFSMAEADRIRSATGQSPAIFYGCDYARGWLETANIEDSIDVSCNGDLMSYW	120
WL7	GAFGGYSHDTFSMAEADRIRSATGQSPAIFYGCDYARGWLETANIEDSIDVSCNGDLMSYW	120
GE28	GAFGGYSHDTFSMAEADRIRSATGQSPAIFYGCDYARGWLETANIEDSIDVSCNGDLMSYW	120
*****		
RMASE24	KNGGIPQISLHLANPAFQSGHFKTPITNDQYKKILDSSTVEGKRLNAMLSKIADGLQELE	180
BEST7613	KNGGIPQISLHLANPAFQSGHFKTPITNDQYKKILDSSTVEGKRLNAMLSKIADGLQELE	180
WL7	KNGGIPQISLHLANPAFQSGHFKTPITNDQYKKILDSSTVEGKRLNAMLSKIADGLQELE	180
GE28	KNGGIPQISLHLANPAFQSGHFKTPITNDQYKKILDSSTVEGKRLNAMLSKIADGLQELE	180
*****		
RMASE24	NQGVVPLFRPLHEMNGEWFWWGLTSYNQKDNERISLYKQLYKKIYHYMTDTRGLDHLIIV	240
BEST7613	NQGVVPLFRPLHEMNGEWFWWGLTSYNQKDNERISLYKQLYKKIYHYMTDTRGLDHLIIV	240
WL7	NQGVVPLFRPLHEMNGEWFWWGLTSYNQKDNERISLYKQLYKKIYHYMTDTRGLDHLIIV	240
GE28	NQGVVPLFRPLHEMNGEWFWWGLTSYNQKDNERISLYKQLYKKIYHYMTDTRGLDHLIIV	240
*****		
RMASE24	YSPDANRDFKTDIFYPGASYVDIVGLDAYFQDAYSINGYDQLTALNKPFAFTEVGPQTANG	300
BEST7613	YSPDANRDFKTDIFYPGASYVDIVGLDAYFQDAYSINGYDQLTALNKPFAFTEVGPQTANG	300
WL7	YSPDANRDFKTDIFYPGASYVDIVGLDAYFQDAYSINGYDQLTALNKPFAFTEVGPQTANG	300
GE28	YSPDANRDFKTDIFYPGASYVDIVGLDAYFQDAYSINGYDQLTALNKPFAFTEVGPQTANG	300
*****		
RMASE24	SFDYSLFINAIKQKYPKTIYFLAWNDEWSAVNKGASALYHDSWTLNKGEIWNGLSLTPI	360
BEST7613	SFDYSLFINAIKQKYPKTIYFLAWNDEWSAVNKGASALYHDSWTLNKGEIWNGLSLTPI	360
WL7	SFDYSLFINAIKQKYPKTIYFLAWNDEWSAVNKGASALYHDSWTLNKGEIWNGLSLTPI	360
GE28	SFDYSLFINAIKQKYPKTIYFLAWNDEWSAVNKGASALYHDSWTLNKGEIWNGLSLTPI	360
*****		
RMASE24	VE	362
BEST7613	VE	362
WL7	VE	362
GE28	VE	362
	**	



Figure 12. Amino acid alignment sequence of Bs24Man.

The different residues between Bs24Man and other 3 mannanase are highlighted in yellow.

(Figure 12 continue)

RMASE24 represent amino acid sequence of *Bs24Man*

BEST7613 represent amino acid sequence of exported mannan  
endo-1,4- $\beta$ -mannosidase from *Bacillus subtilis* BEST7613

WL7 represent amino acid sequence of mannan endo-1,4- $\beta$   
mannosidase from *Bacillus subtilis* WL7

GE28 represent amino acid sequence of mannanase from  
*Bacillus subtilis* ge28



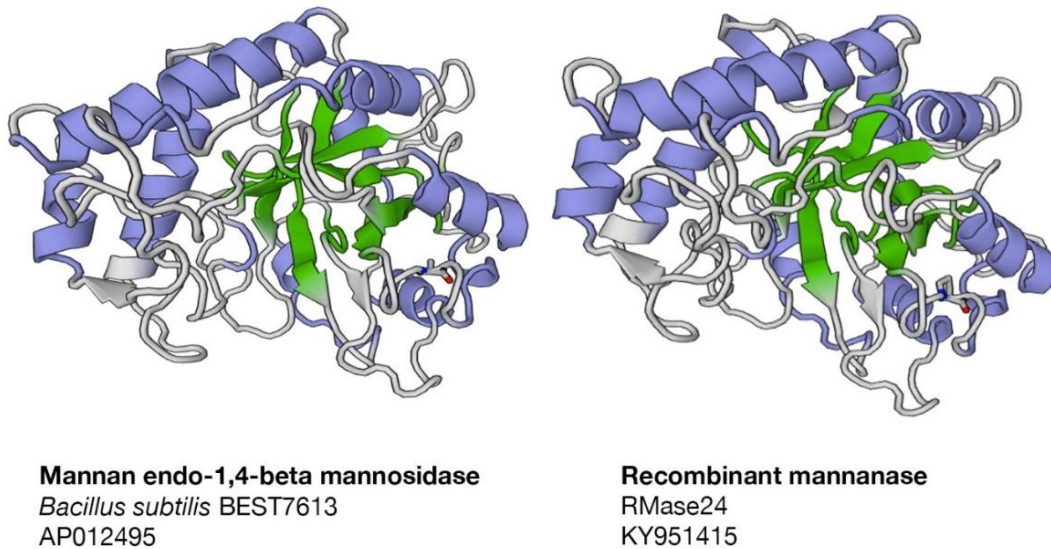
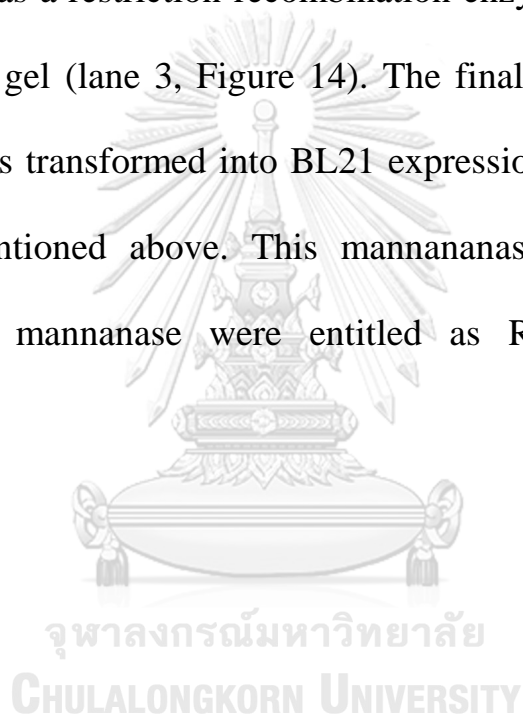


Figure 13. Three-dimensional structure comparison between Bs24Man and exported mannan endo-1, 4- $\beta$ -mannosidase from *Bacillus subtilis* BEST7613.

- (right)** Bs24Man encoded enzyme, as labeled as recombinant mannanase RMase24 (KY951415)
- (left)** exported mannan endo-1,4- $\beta$ -mannosidase from *Bacillus subtilis* BEST7613 (AP012495)

### 3.1.2 Recombination and expression of manannase, RMase24

The PCR product of *Bs24Man* amplification, was recombined to the pGEM-t-easy vector and then transformed to *E.coli* TOP10 using electroporation technique. RM24 collected recombination plasmid was cut and the gene was subcloned into pET21b expression vector using *XhoI* and *NdeI* as a restriction-recombination enzyme and then analyzed on 8% agarose gel (lane 3, Figure 14). The final recombinant plasmid, pvRM24-A, was transformed into BL21 expression host using the same method as mentioned above. This mannanase-containing bacterial strain and its mannanase were entitled as RM24 and RMase24, respectively.



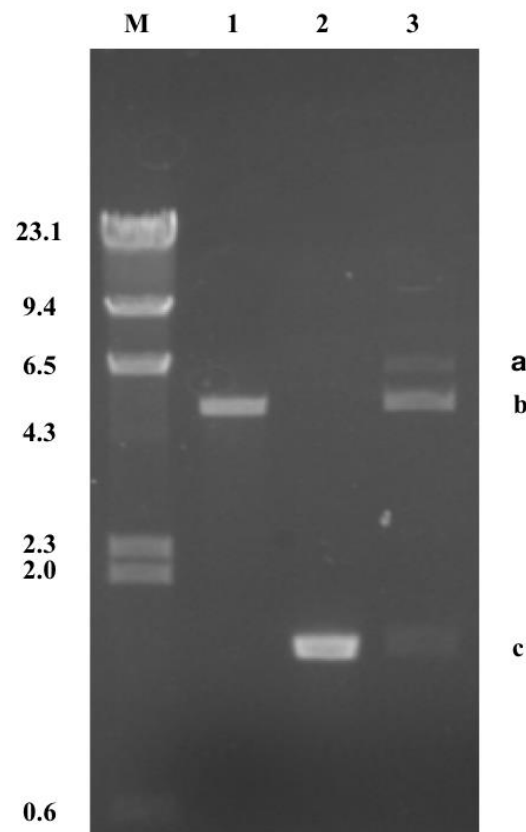


Figure 14. Cloning result of pvRM24-A, analyzed on 0.8% (w/v) agarose gel.

Lane M:     λ/HindIII marker

Lane 1:     pET21b vector

Lane 2:     Mannanase gene insertion

Lane 3:     Double digestion of recombinant plasmid pvRM24-A  
with XhoI and NdeI

((a); uncut recombinant plasmid pvRM24-A,

(b); pET21b,

(c); mannanase gene insertion))

### 3.3 Structural analysis of pretreated galactomannan substrates

Surface structure of sonicated galactomannan substrate (S-Galman) and grounded galactomannan substrate (G-Galman) substrates were imaged by scanning electron microscope represent a different character of fragment's edge and size. Sonication pretreatment gave smaller average fragment size when compared with to non-treatment substrate (Figure 15 A, B). At higher magnification different character of fragment's edge from each type of substrate was observed. S-GalMan had more irregular amorphous shape edges and there was considerable amount of amorphous structure on the surface of the substrate while G-GalMan have less of these characteristics. Interestingly, after the digestion of S-GalMan with RMase24, these small fragments were reduced and the edge and surface of the fragments became smooth. In contrast, digestion of G-GalMan did not change the overall structure observed by SEM much (Figure 15 C-F)

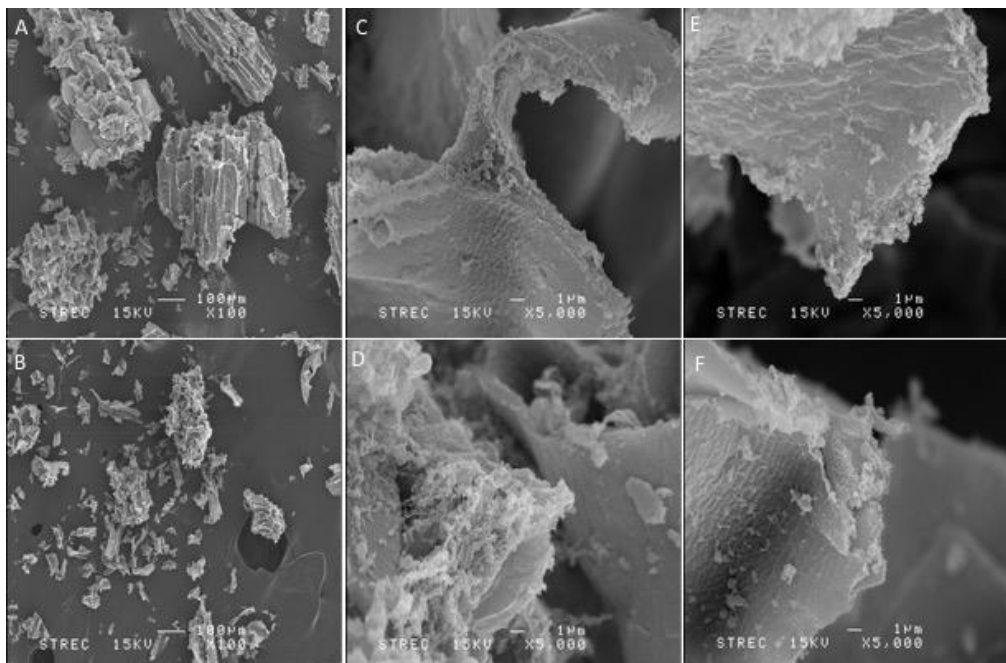


Figure 15. Surface structure of S-GalMan and G-GalMan imaged by scanning electron microscope.

- (A) Represent the average fragment size of G-GalMan at x100 magnification.
- (B) Represent the average fragment size of S-GalMan at x100 magnification.
- (C) Characteristic of the fragment edge and surface of G-GalMan at x5000 magnification.
- (D) Characteristic of the fragment edge and surface of S-GalMan at x5000 magnification.



(Figure 15 continue)

(E)The edge and surface structure of digested G-GalMan at x5000 magnification.

(F)The edge and surface structure of digested S-GalMan at x5000 magnification.



### **3.4 Production and purification of mannan oligosaccharides**

#### **3.4.1 Determination of MOS production yield between a different pretreated galactomannan substrate**

In this study, the results showed that RMase24 can release the higher amount of MOS when compared to the other recent studies (Ghosh et al., 2015; Rungrassamee et al., 2014). Thin layer chromatography shows a spectrum of multiple MOS size ranging from MOS1 to MOS7 and longer. The production of MOS from S-GalMan gave a higher yield of MOS when compared to G-GalMan at every incubation period. Interestingly, S-GalMan took a very short time to perform a digestion since slightly MOS production can be seen at early incubation time. Whereas digestion of G-GalMan was released MOS after 6 hours (Figure 16). Percentage yield of total MOS production from S-GalMan and G-GalMan were 8.25% and 5.09% from its dried substrate, respectively.

Evaluation of RMase24 concentration was also performed with S-GalMan to determine the optimal ratio of enzyme/substrate for the reaction. The results showed that amount of RMase24 used in the digestion was affected the pattern of MOSs produced. The enzyme-substrate ratio at 10 unit per 1 gram of dried substrate showed the highest yield of medium size oligosaccharides which were larger than MOS6

whilst the higher concentration of RMase24 gave a lower intensity of hexamer. (Figure 17).



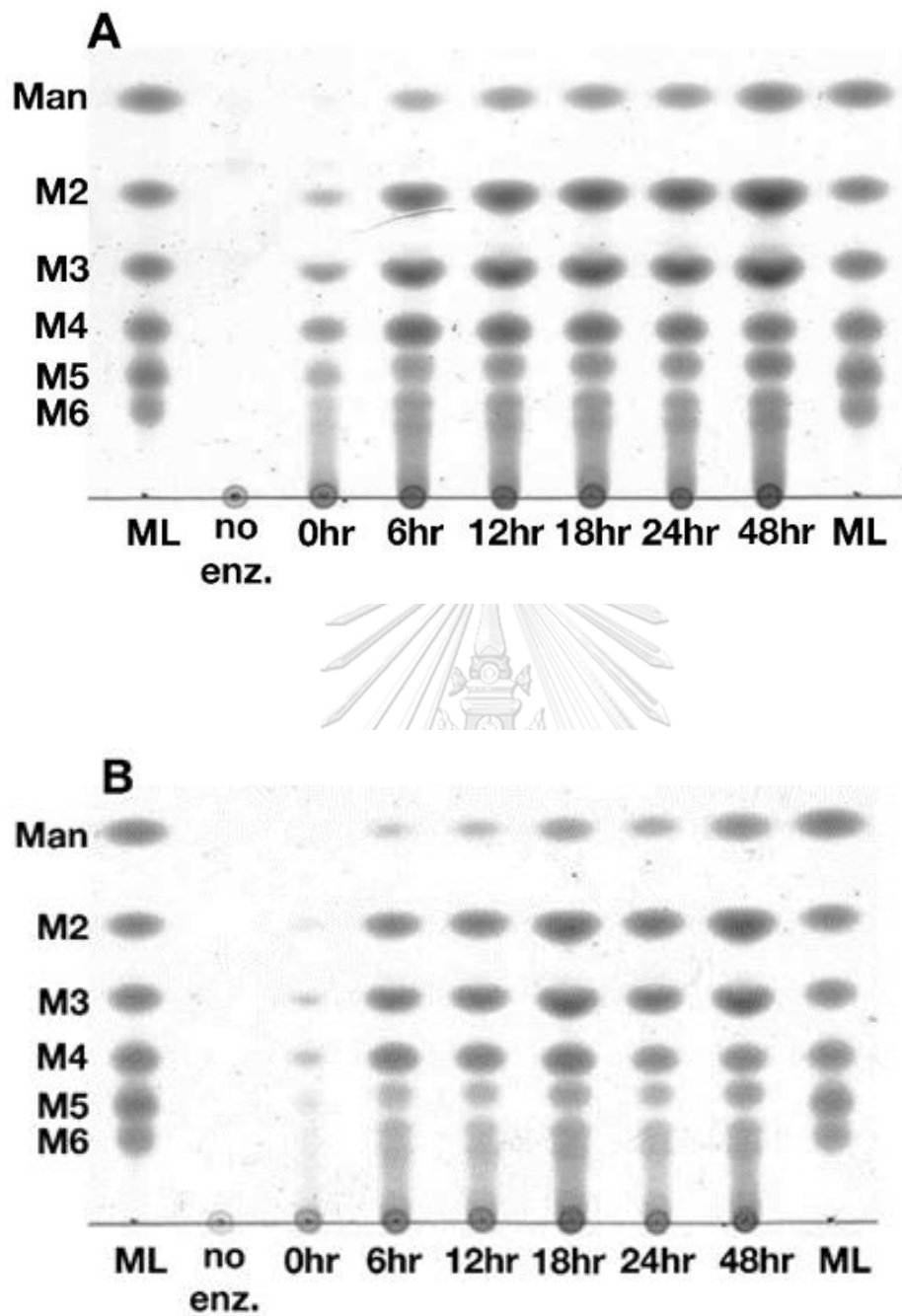


Figure 16. Evaluation of the incubation period at different incubation time, compared between S-GalMan (A) and G-GalMan (B).

(Figure 16 continue)

- ML; Mannooligosaccharides ladder
- M2; standard mannobiose
- M3; standard mannotriose,
- M4; standard mannotetrose
- M5; standard mannopentose
- M6; standard mannohexose
- No enz; a reaction without RMase24
- 0hr - 48 hrs; a reaction collected at 0 hour up to 48 hours  
after incubation.

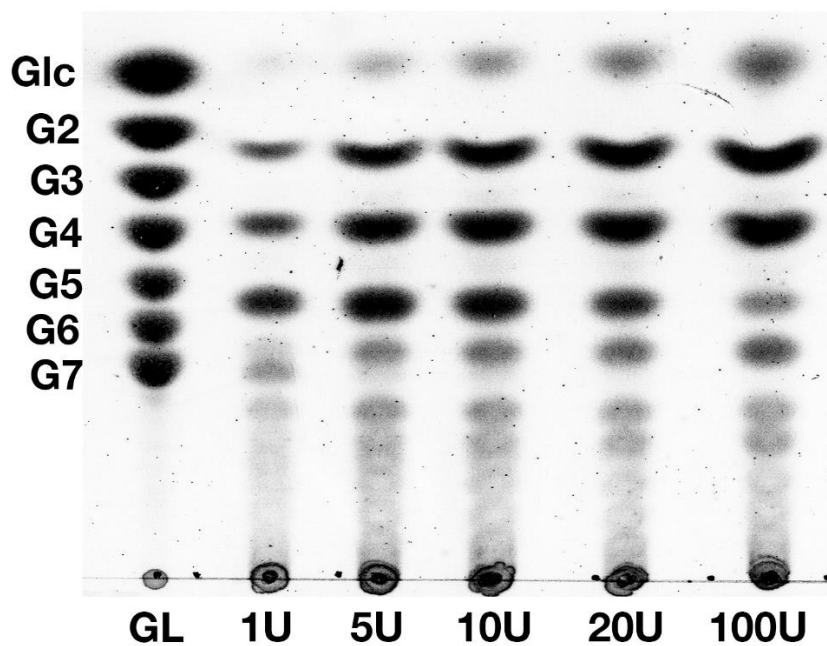


Figure 17. The pattern of MOS production from RMase24 with a different concentration of RMase24.

Glc; Glucose

G2; Glucobiose

G3; Glucotriose

G4; Glucotetrose

G5; Glucopentose

G6; Glucohexose

G7; Glucoheptose

GL; Glucooligosaccharide ladder

1U; S-GalMan digested with 1unit of RMase24

5U; S-GalMan digested with 5unit of RMase24

(Figure 17 continue)

10U; S-GalMan digested with 10unit of RMase24

20U; S-GalMan digested with 20unit of RMase24

100U;S-GalMan digested with 100unit of RMase24

	Total MOS produced (% to dried substrate weight)	MOS5 produced (% to total MOS produced)
S-GalMan	8.25%	27.7%
G-GalMan	5.09%	-

Table 1. Percentage yield of MOS production compared between S-GalMan and G-GalMan.



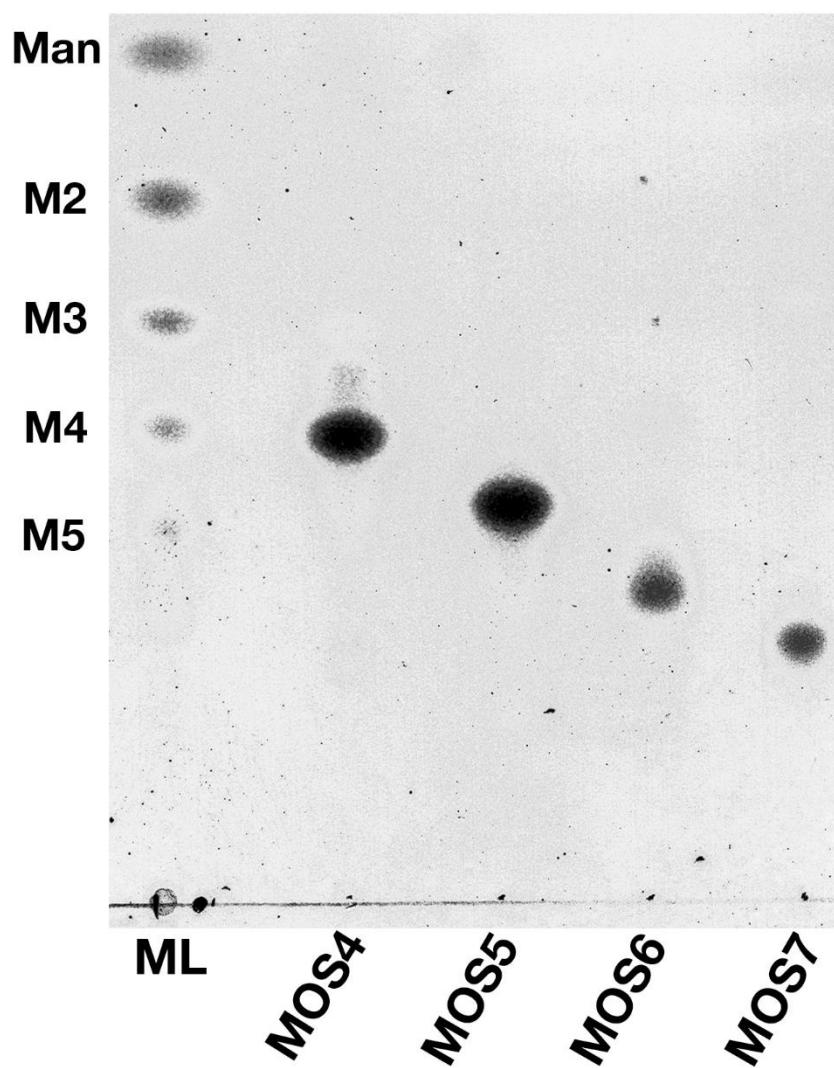
จุฬาลงกรณ์มหาวิทยาลัย  
**CHULALONGKORN UNIVERSITY**



### 3.4.2 Purification and molecular weight determination of MOS

Each MOS was successfully purified through Biogel P2 column. Interestingly, MOS with moderate size such as MOS4, MOS5, and MOS6 did not possess the same mobility as standard mannan oligosaccharide. (Figure 18). Mass spectrometer analysis was performed to confirm their polymeric size by determination of their molecular weight (Figure 19)





CHULALONGKORN UNIVERSITY

Figure 18. A separation of each MOS, from MOS4 to MOS7

demonstrated in thin layer chromatography under butan-1-ol: acetic acid: water, 3:3:2 system.

ML; Mannooligosaccharides ladder

M2; standard mannobiose

M3; standard mannotriose,

M4; standard mannotetrose

(Figure 18 continue)

M5; standard mannopentose

M6; standard mannohexose



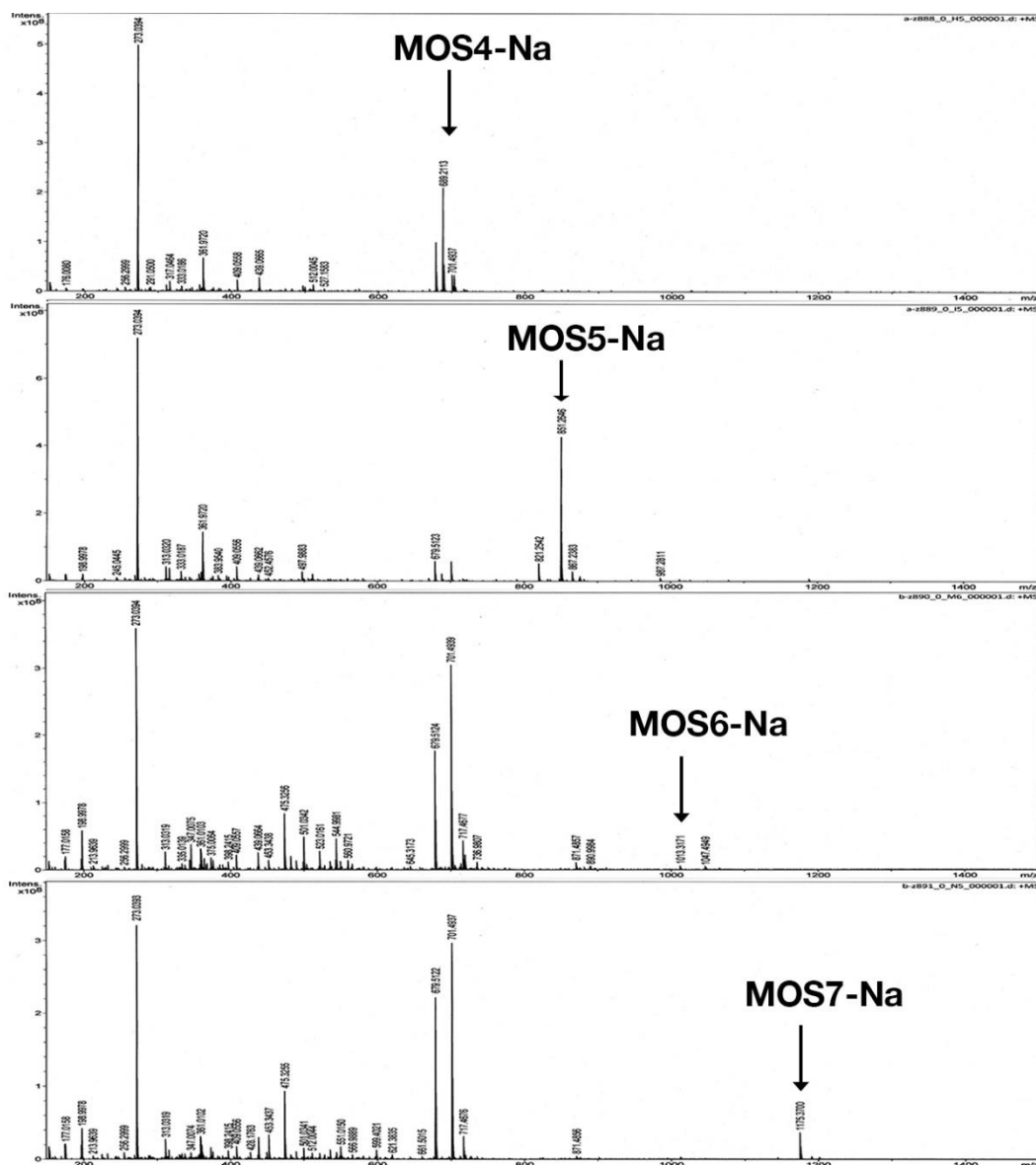


Figure 19. Mass spectrometry analysis of purified MOS.

From top to bottom, High resolution mass spectrometry of purified MOS4, MOS5, MOS6, and MOS7, respectively. The arrow indicated a peak of molecular mass of each MOS with sodium ion following by;

(Figure 19 continue)

MOS4-Na = 679.123m/z

MOS5-Na = 851.2646 m/z

MOS6-Na = 1013.3171 m/z

MOS7-Na = 1175.3700 m/z.



### **3.5 Effect of mannan oligosaccharides on tight junction of epithelial cells**

#### **3.5.1 Screening and dose determination for tight junction-enhancing MOS**

Tight junction integration of T84 experiment was performed with selected MOS candidates and detected using trans-epithelial electrical resistant (TEER) assay. The result showed that MOS5 can significantly enhance the tight junction integration of T84 cultured tissue (one-way ANOVA,  $p < 0.0001$ ), while MOS4, MOS6 and MOS7 had no effects (Figure 20). Furthermore, a determination of MOS5 concentration was also performed and the result showed that a concentration at 20  $\mu\text{M}$  and 10  $\mu\text{M}$  of MOS5 significantly increased the highest TEER (one-way ANOVA,  $p = 0.002$  and  $p < 0.0001$ , respectively), while the concentration below 5  $\mu\text{M}$  showed no different of TEER level compared to vehicle (non-treated control) group. (Figure 21).

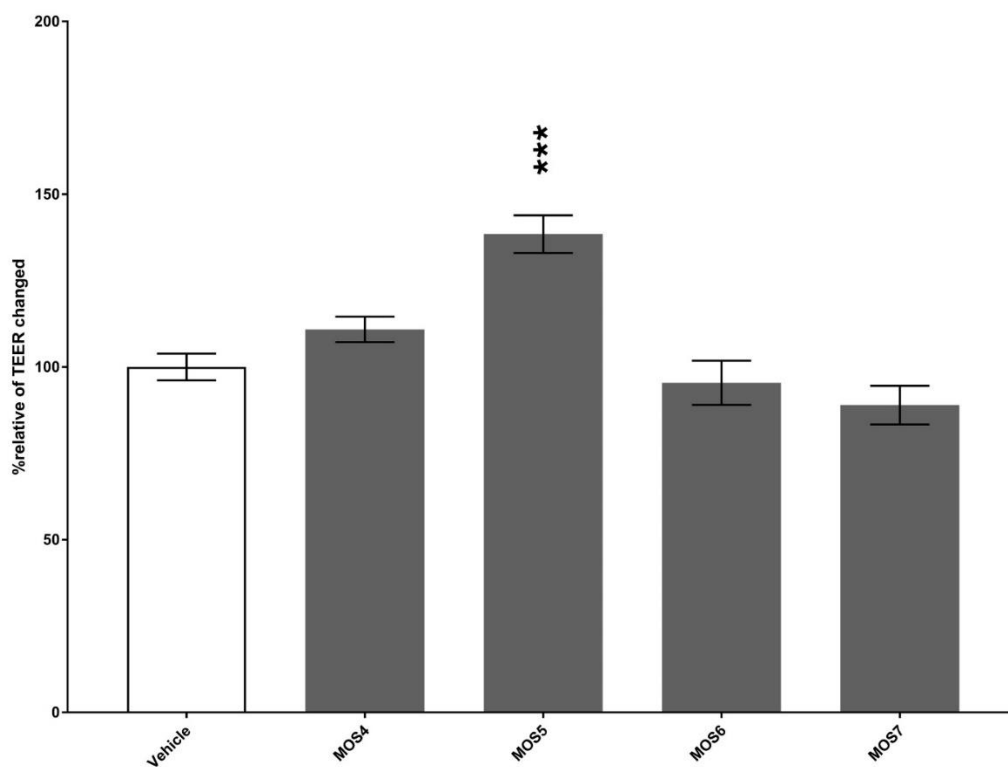


Figure 20. Relative percentage of TEER changed of T84 cells after 24 hours treatment with purified MOS4 to MOS7 compared to control group (DMEM).

(n=3-4, one-way ANOVA,  $p < 0.0001$ ).

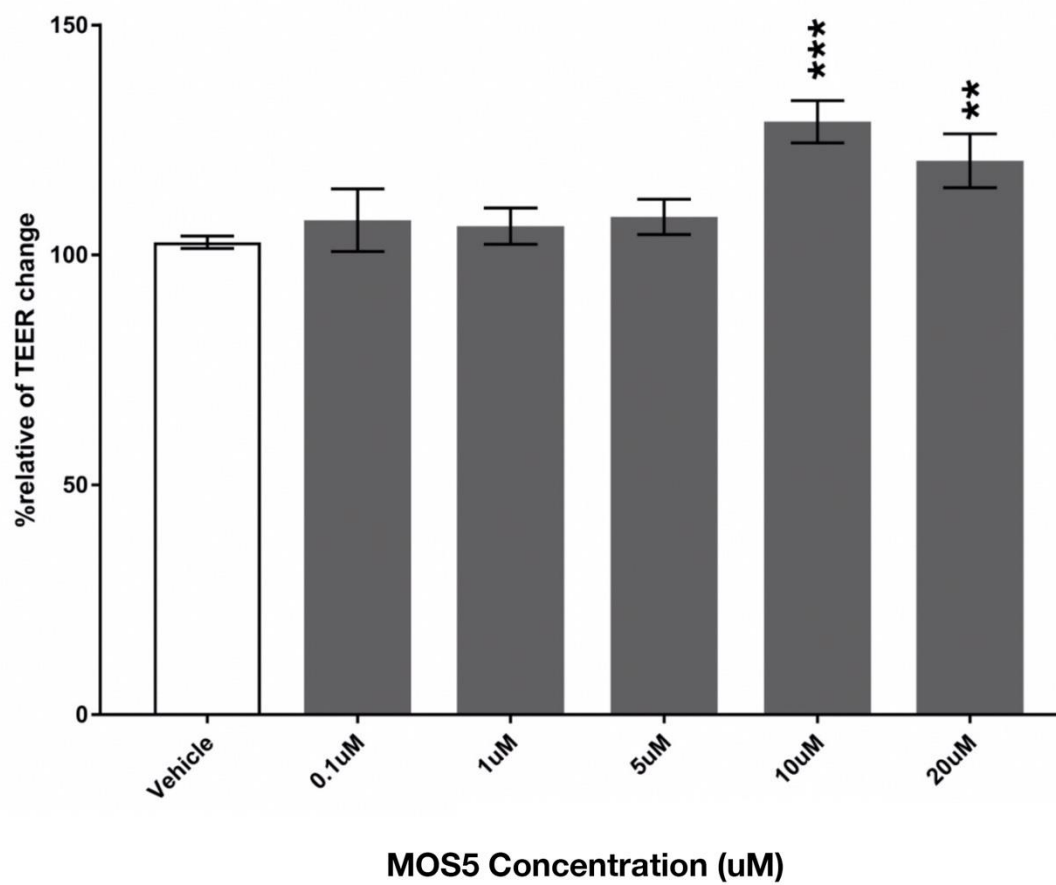


Figure 21. Relative percentage TEER change of T84 cells after a treatment of various concentration of MOS5.

(n=3-4, one-way ANOVA,  $p = 0.002$  and  $p < 0.0001$ , respectively).



### **3.5.2 Determination of MOS5 mechanism of action in tight junction enhancement**

#### **3.5.2.1 Distinguish between tight junction integration and cells proliferation**

The effects of MOS5 over cellular tight junction was distinguished from the cellular proliferation by another experiment that calcium ions was removed from the medium once the cells growth reached 85% of the maximum growth by replacing DMEM with SMEM. After 24 hours of incubation, DMEM medium with Calcium ions and MOS5 was then replaced SMEM and TEER was monitored every 15 minutes for 12 hours. The results showed that MOS5 can help T84 reassembled their tight junction significantly faster and higher than vehicle control group (n=4, two-way ANOVA,  $p < 0.0001$ ) (Figure 22).

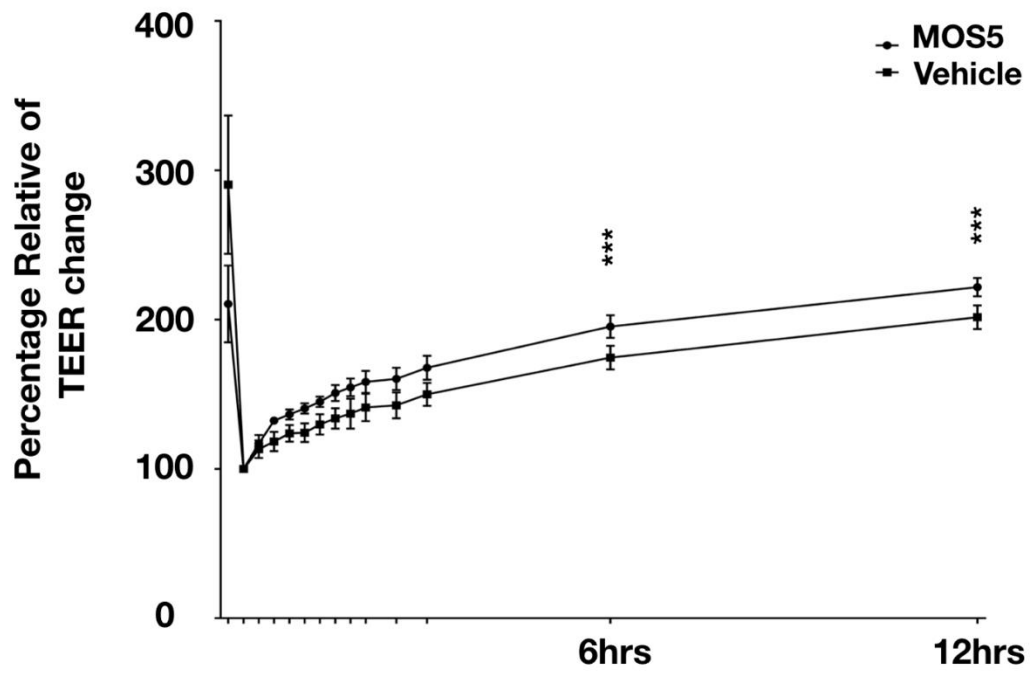


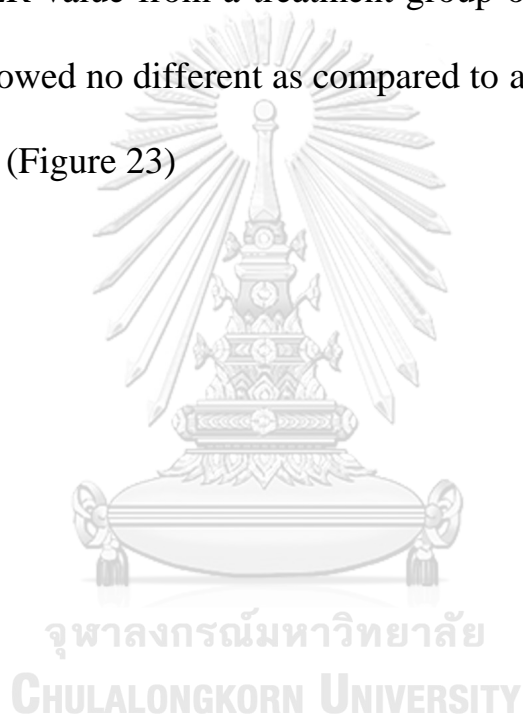
Figure 22. Determination of tight junction reassembly of M5 compared to control.

(n=4, two-way ANOVA,  $p < 0.0001$ ).

### 3.5.2.2 An activation of MOS5 through AMPK pathway

#### 3.5.2.2.1 TEER-Calcium switch analysis

TEER results under a challenging of AMPK inhibitor (Compound C) showed a significantly different of TEER recovering between GM4 treatment and vehicles (non-treated control) groups (two-way ANOVA,  $p < 0.0001$ ). TEER value from a treatment group of MOS5 together with compound C showed no different as compared to a group with compound C treated alone. (Figure 23)



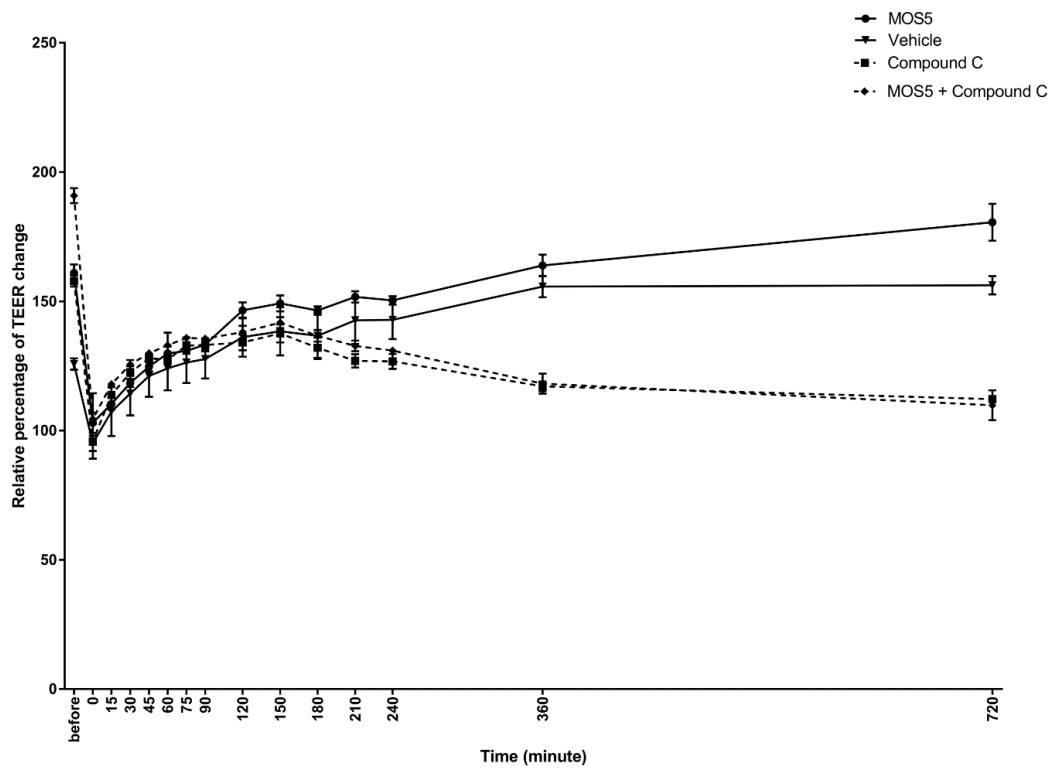


Figure 23. Determination of AMPK activation of MOS5 through a challenging of Compound C.

(n=4, two-way ANOVA,  $p < 0.0001$ ).

### 3.5.2.2.2 Western blot analysis

Western blot analysis of pAMPK/ AMPK- $\alpha$  also shown a significantly elevated level of pAMPK over AMPK- $\alpha$  intensities at 60 minutes after a treatment of MOS5 when compared to vehicle (non-treated control) group. (n=3, one-way ANOVA, p = 0.0014) (Figure 24, 25).



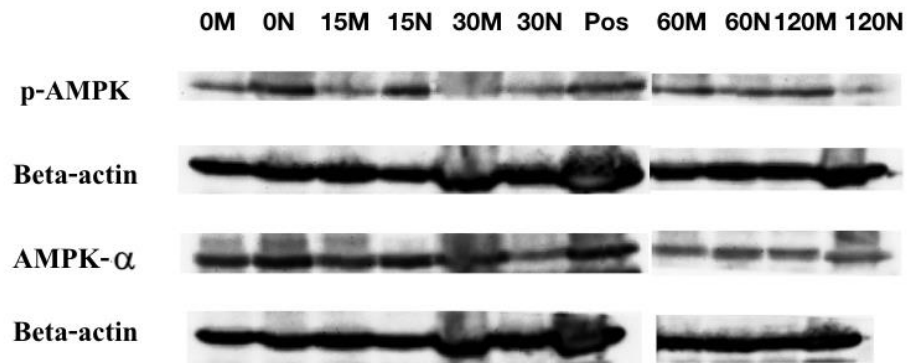


Figure 24. Western blot analysis of p-AMPK, AMPK- $\alpha$ , and  $\beta$ -actin protein collected at various time point of MOS5 treated group and vehicle (non-treated) group.

0M; MOS5 treated collected at 0 minute

15M; MOS5 treated collected at 15 minutes

30M; MOS5 treated collected at 30 minutes

60M; MOS5 treated collected at 60 minutes

120M; MOS5 treated collected at 120 minutes

0N; Vehicle (non-treated) group collected at 0 minute

15N; Vehicle (non-treated) group collected at 15 minutes

30N; Vehicle (non-treated) group collected at 30 minutes

60N; Vehicle (non-treated) group collected at 60 minutes

120N; Vehicle (non-treated) group collected at 120 minutes

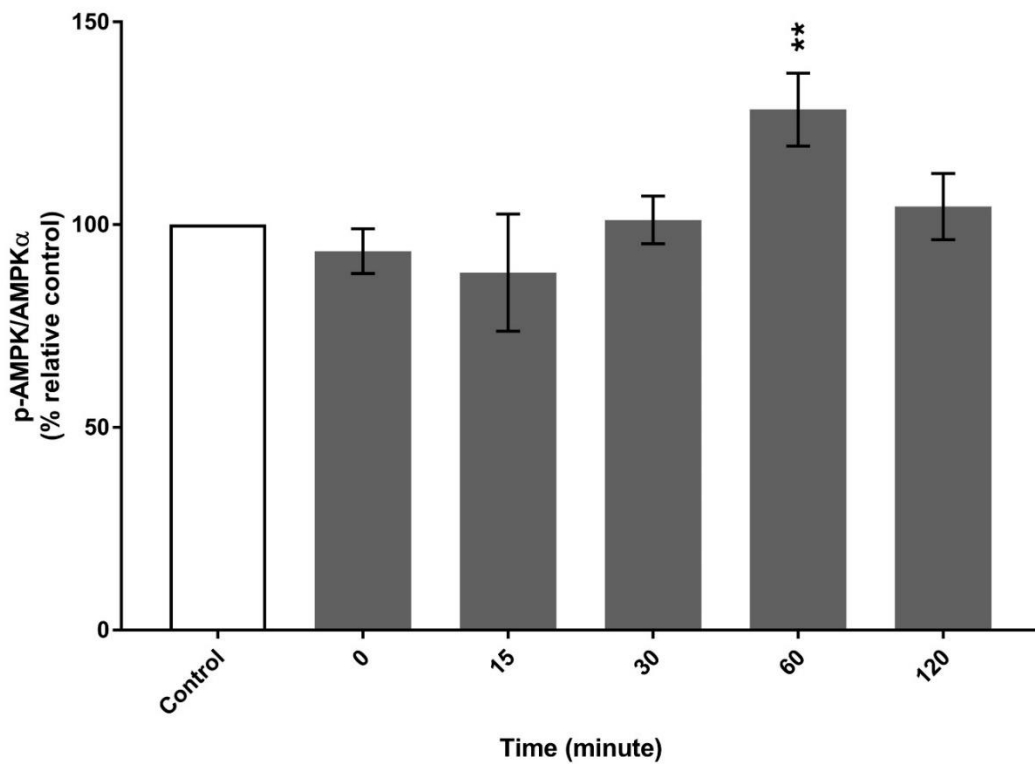


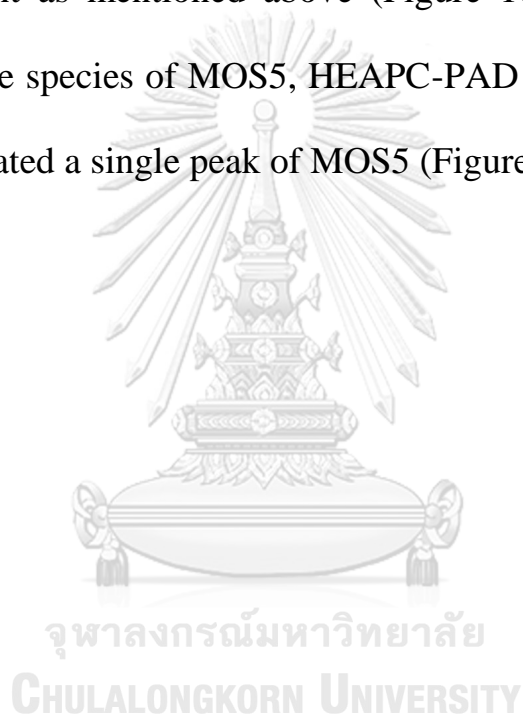
Figure 25. Relative percentage of expression level of p-AMPK over AMPK- $\alpha$ .

(n=3, one-way ANOVA, p = 0.0014).

### **3.6 Characterization of bioactive MOS5**

#### **3.6.1 Determination of MOS5 structure via enzymatic hydrolysis assay**

Though the molecular weight of the purified MOS5 is same as the standard mannan pentasaccharide, but the mobility on TLC are yet slightly different as mentioned above (Figure 16). To determine the structure and the species of MOS5, HEAPC-PAD was performed and its result demonstrated a single peak of MOS5 (Figure 24).





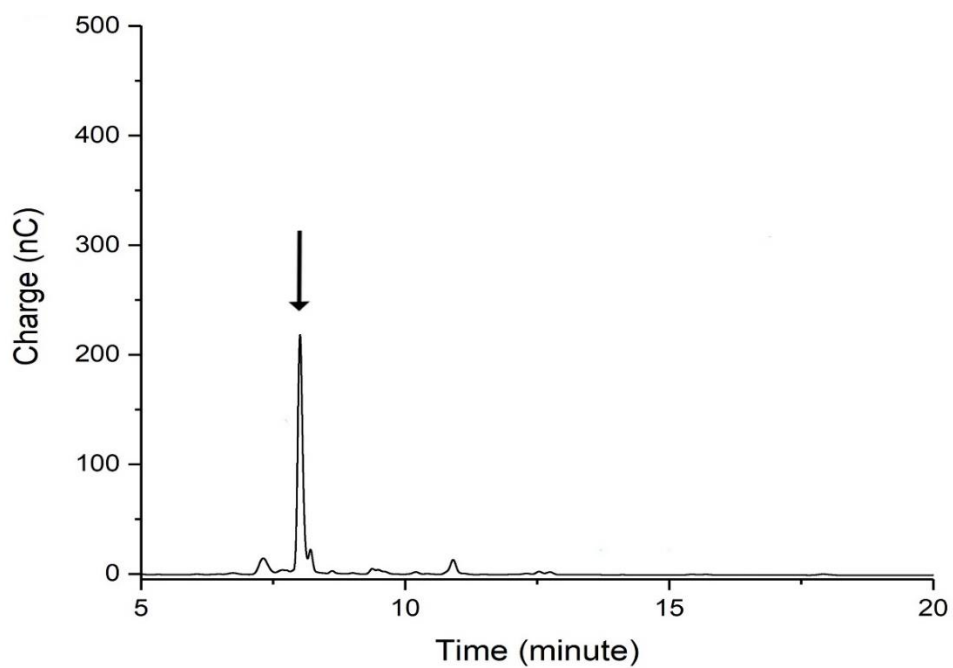
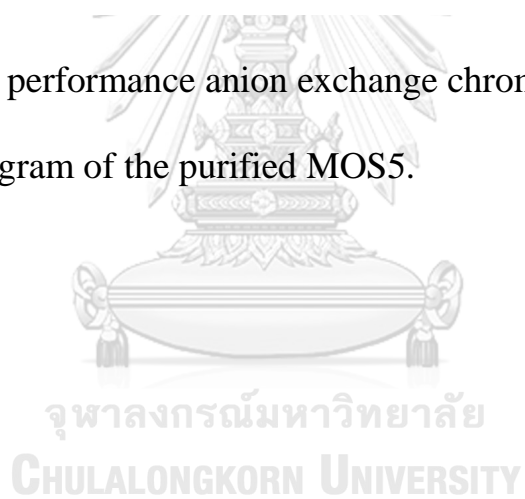


Figure 26. High performance anion exchange chromatography (HPAEC-PAD) chromatogram of the purified MOS5.



### 3.6.1.1 Hydrolysis of MOS5 with $\alpha$ -galactosidase from *A. fulica* (Amano)

Since  $\alpha$ -galactosidase from *A. fulica* (AMAN-AfGLA) obtained from Amano corporation was a commercial enzyme with mixed activities between galactosidase and mannosidase. Separation of each activity was performed. AMAN-AfGLA had been purified through ammonium sulfate precipitation technique. The purified enzyme was obtained as a precipitated at 30, 70, and 90% w/v of ammonium sulfate. The collected precipitated enzyme labeled as P-AMAN-AfGLA. P-AMAN-AfGLA was also tested with 10 mM mannobiose and 10 mM melibiose to determine its  $\alpha$ -galactosidase and  $\beta$ -mannosidase activities. The results showed that P-AMAN-AfGLA can digested melibiose to mannose and galactose, also digest mannobiose to mannose (supplementary data). P-AMAN-CAfGLA had been purified through Sephadex G150 gel filtration column chromatography and 5 mL was collected in each fraction.

The result from an incomplete digestion of the purified MOS5 with a fraction of purified  $\alpha$ -galactosidase from *A. fulica* (Amano, Japan) that possessed  $\alpha$ -galactosidase activity showed a monosaccharide band which have different retention distance (Rf) than mannose (g), and a band

with the same Rf as mannotetrose (m-4). Interestingly, once the concentration of  $\alpha$ -galactosidase is increased, the products revealed other oligosaccharides. There were a disaccharide band with the same Rf as mannobiose (m-2) and a trisaccharide band (m-3) with a slightly different Rf than mannotriose. (Figure 27)



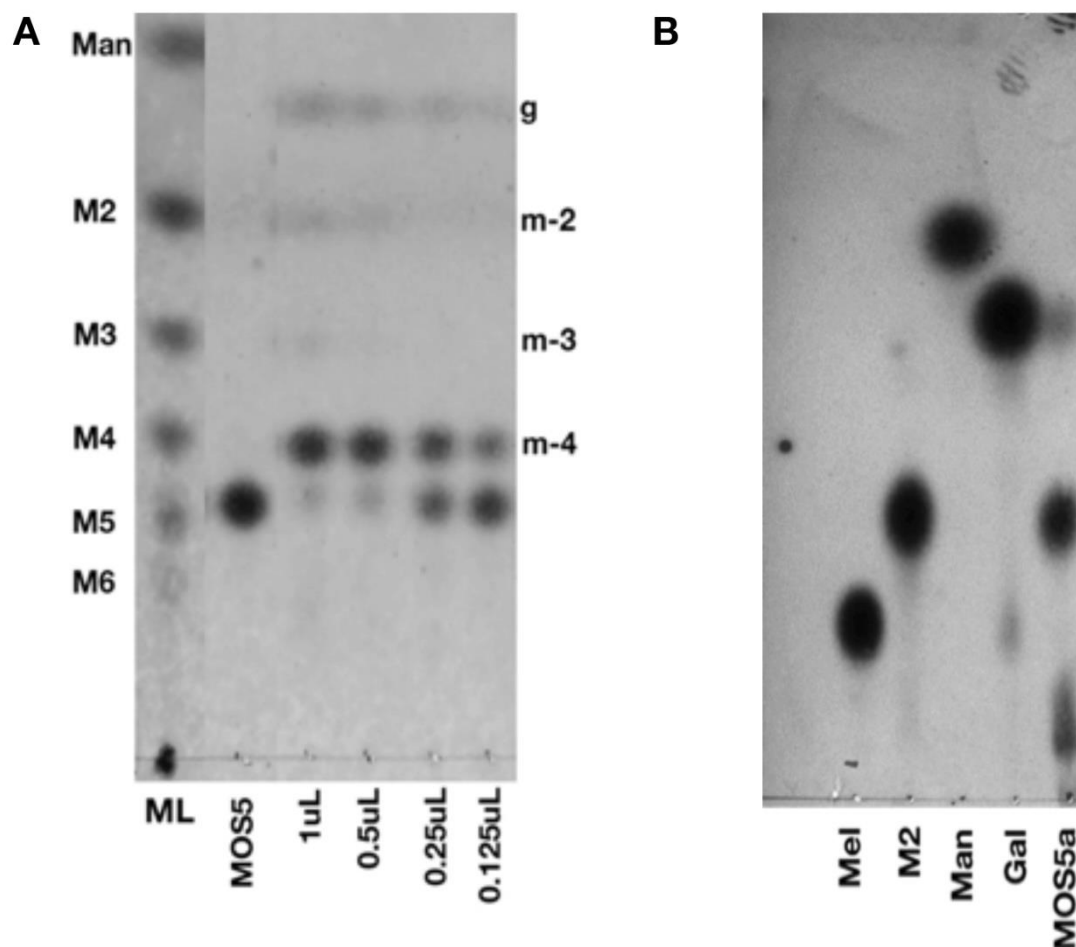


Figure 27. Thin layer chromatography of digestion products of MOS5 with a fraction of purified  $\alpha$ -galactosidase from *A. fulica* (Amano, Japan) in butyl acetate system (A) and acetonitrile system (B).

The lanes were cropped from the same TLC plate.

ML; Mannooligosaccharides ladder

M2; standard mannobiose

M3; standard mannotriose,

M4; standard mannotetrose

(Figure 27 continue)

M5; standard mannopentose

M6; standard mannohexose

g; a monosaccharide band

m-2; a disaccharide band

m-3; a trisaccharide band

m-4; a tetrasaccharide band

1  $\mu$ L -0.125  $\mu$ L; 1  $\mu$ L of 1  $\mu$ M MOS5 digested with 1  $\mu$ L to

0.125  $\mu$ L of 20mg/mL of fraction of purified  $\alpha$ -galactosidase, respectively.

Mel; melibiose

M2; mannobiose

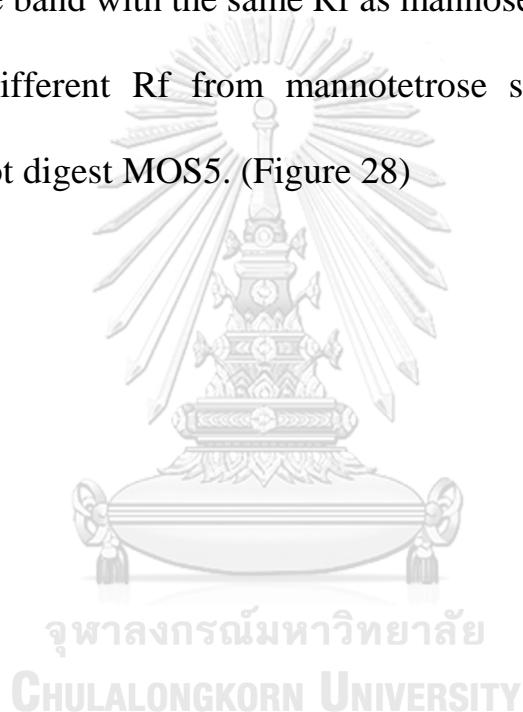
Man; mannose standard

Gal; galactose standard

MOS5a; digested MOS5 with  $\alpha$ -galactosidase

### 3.6.1.2 Hydrolysis of MOS5 with *exo*- $\beta$ -D-mannosidase (*A. fulica*) (Seigaku) and purified $\alpha$ -galactosidase (*A. fulica*) (Amano)

The result from a digestion of MOS5 with *exo*- $\beta$ -D-mannosidase (*A. fulica*) (Seikagaku corporation, Japan) (AfMAN) revealed a monosaccharide band with the same Rf as mannose, and a tetrasaccharide band with a different Rf from mannotetrose standard. Interestingly, RMase24 cannot digest MOS5. (Figure 28)



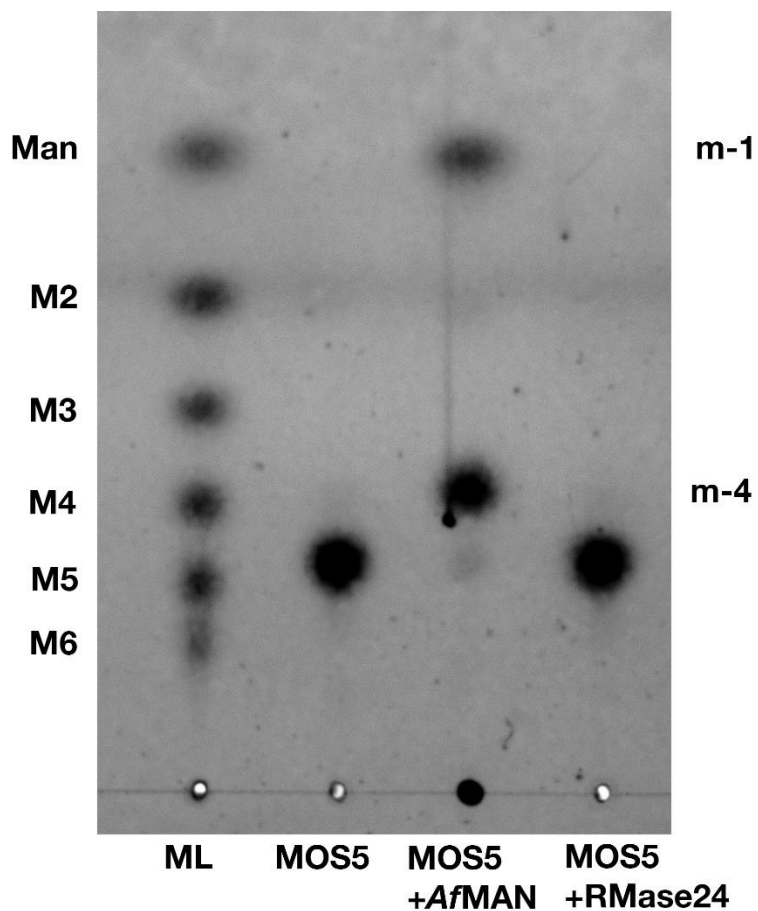


Figure 28. A digestion of MOS5 with AfMAN and RMase24.

ML; Mannooligosaccharides ladder

MOS5+ AfMAN; MOS5 digested with AfMAN

MOS5+ RMase24; MOS5 digested with RMase24

M2; standard mannobiose

M3; standard mannotriose,

M4; standard mannotetrose

M5; standard mannopentose

M6; standard mannohexose

(Figure 28 continue)

- m; a monosaccharide band with the same Rf as mannose
- m-4; a tetrasaccharide band with a slightly different Rf from  
mannotetrose





Fraction number 35 (F35) of separated P-AMAN-AfGLA was labeled as P-AMAN-AfGLAF35, found to possess endo- $\beta$ -mannosidase as shown in figure R24. A digestion of MOS5 with a lower amount of PAfGLAF35 than 2  $\mu$ L per 1  $\mu$ L of 1  $\mu$ M MOS5 were produced oligosaccharides larger than MOS5. A concentration of P-AMAN-AfGLAF35 used in a digestion for NMR analysis was at excess to avoid a transferase by-product (Figure 29).



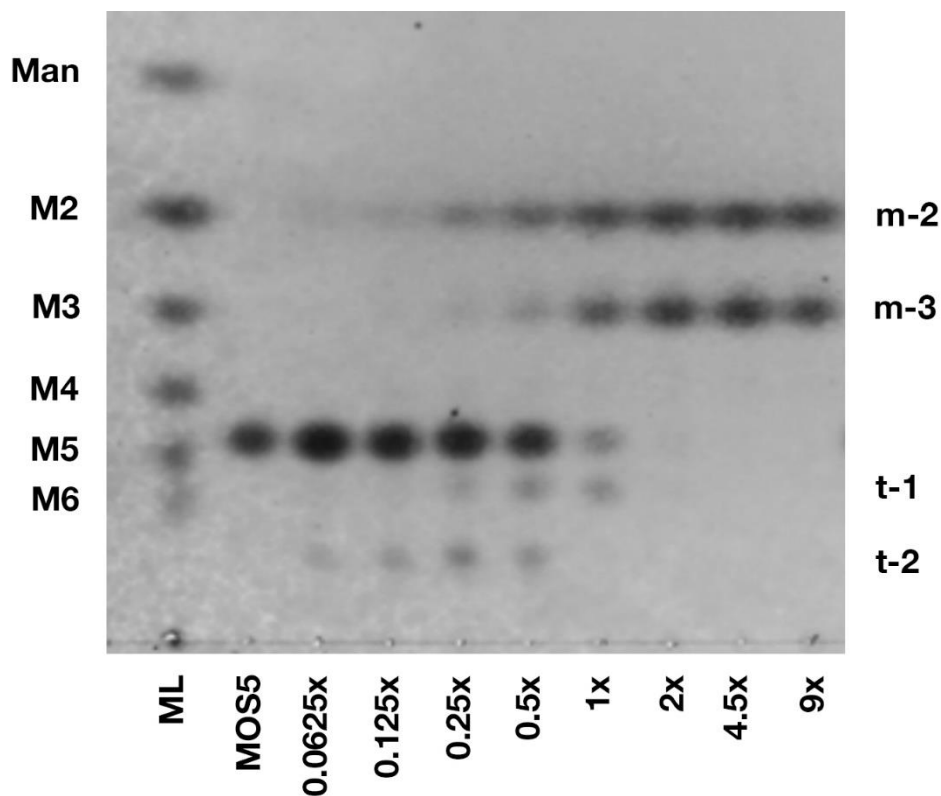


Figure 29. Thin layer chromatography analysis of a digestion of MOS5 with various amount of P-AMAN-AfGLA-f35.

Man; Standard Mannose

M2; Standard Mannobiose

M3; Standard Mannotriose

M4; Standard Mannotetrose

M5; Standard Mannopentose

M6; Standard Mannohexose

m-2; A disaccharide band

m-3; A trisaccharide band

t-1; A transferase product 1

(Figure 29 continue)

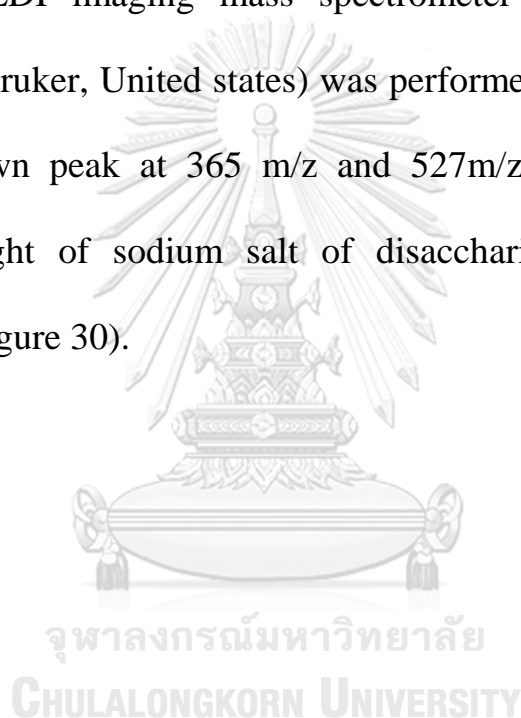
t-2; A transferase product 2

0.0625x – 9x; A digestion reaction between 1  $\mu\text{L}$  of 1  $\mu\text{M}$  MOS5 with 0.0625  $\mu\text{L}$  to 9  $\mu\text{L}$  of pAfGLAF35, amount ranging as labeled respectively.



### 3.6.2 Mass spectrometry analysis

Digestion products of MOS5 with PA/GLAF35, m-2 and m-3, were collected and purified through Biogel P2 size exclusion chromatography before submitted to Mass spectrometry and NMR analysis to confirm the structure. MALDI imaging mass spectrometer (Solaris X, FT mass spectrometry, Bruker, United states) was performed and the result of M2 and GM2 shown peak at 365 m/z and 527m/z, which indicated the molecular weight of sodium salt of disaccharide and trisaccharide, respectively (Figure 30).



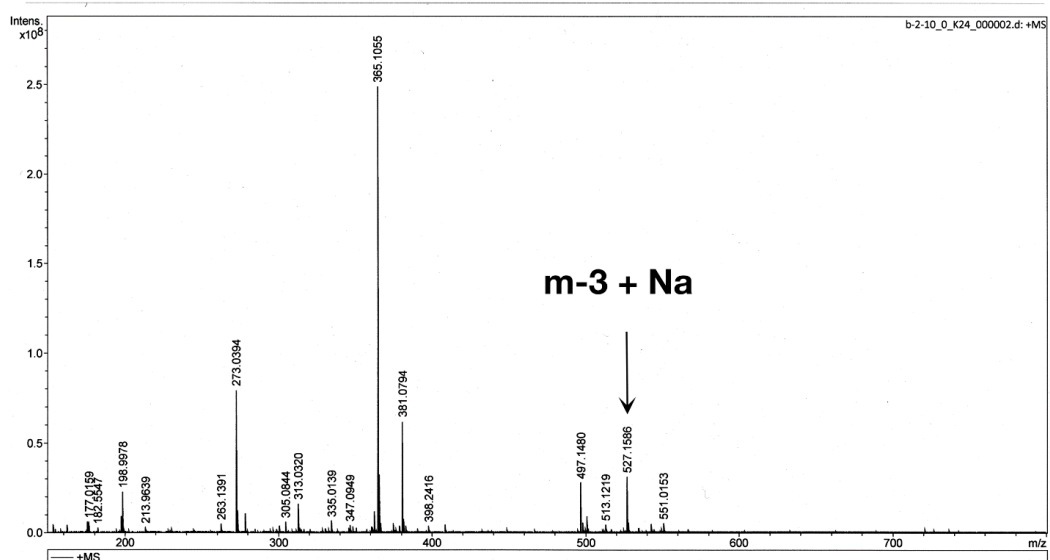
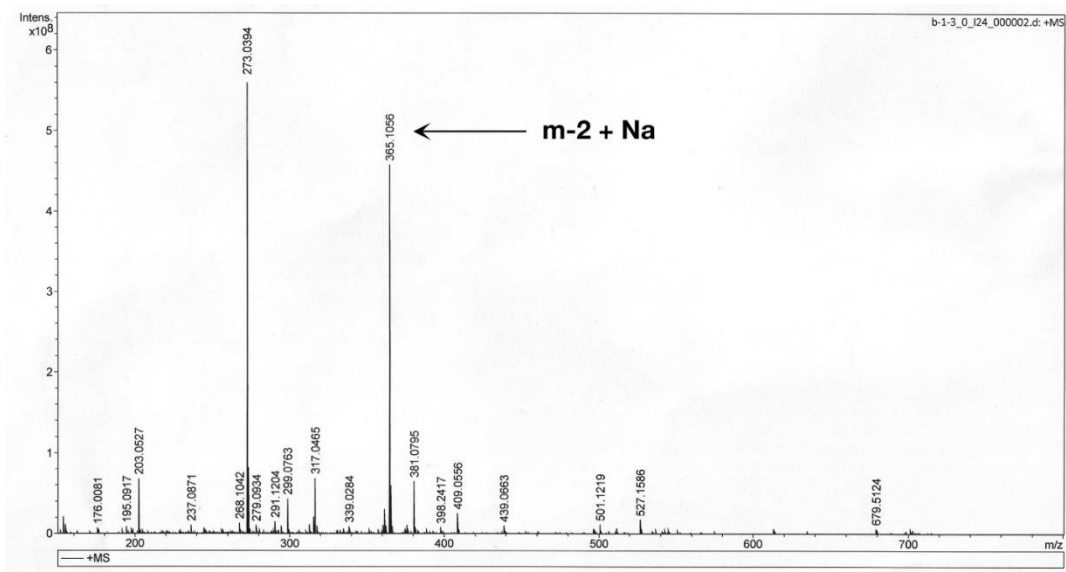


Figure 30. MALDI imaging mass spectrometer analysis of m-2 and m-3 (Upper panel and lower panel, respectively.)

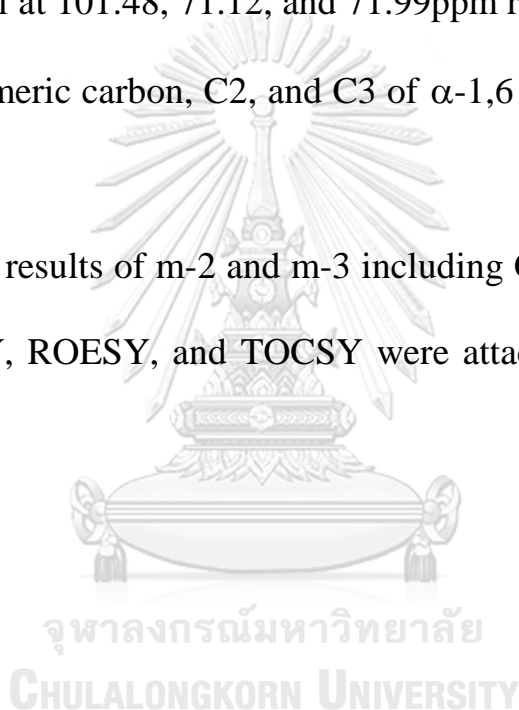
### 3.6.3 NMR analysis

FT-NMR was performed and the analytic results were obtained from Osaka City University.  $^1\text{H}$  and  $^{13}\text{C}$  NMR spectra of m-2 and m-3 were analyzed at 600MHz and 150 MHz in  $\text{D}_2\text{O}$ , respectively. The structural result of m-2 is shown in figureR27. The anomeric proton of mannose was identified with chemical shift of protons following by; C1 on  $\beta$ -1,4 was identified at  $\delta$  5.169 ppm. C2 approximately at  $\delta$  3.98 to 4.06 ppm, and C4 approximately at  $\delta$  3.56 to 3.61 ppm. Moreover, a long-range CH proton chemical shift also shown at  $\delta$  4.731 ppm and  $\delta$  3.96 ppm which represented proton of C1 and C4 at  $\beta$ -1,4-mannosidic linkage, respectively. This had been confirmed with results from  $^{13}\text{C}$  NMR which revealed a chemical shift of carbon at following; anomeric C1 at  $\delta$  96.53ppm, C2 at  $\delta$  72.90 and 73.23 ppm, and non-linkage C4 at  $\delta$  69.41ppm (Figure 31-33)

Whereas  $^1\text{H}$  and  $^{13}\text{C}$  NMR spectra of m-3 represent the similar chemical shift signals as m-2, other different signals had been detected.  $^1\text{H}$  NMR spectra of m-3 revealed a signal of C1 on  $\beta$ -1,4 at  $\delta$  5.217 ppm. C2 approximately at  $\delta$  4.04 to 4.13pp, and C4 approximately at  $\delta$  3.61 ppm, but there were others proton chemical shift at  $\delta$  3.88 ppm,  $\delta$  4.04 ppm and 5.055 ppm which were identified as a proton chemical shift of

C2, C4, and anomeric proton of C1 of  $\alpha$ -1,6 linkage of galactose, respectively. The result shown on  $^{13}\text{C}$  NMR went along with the same trend to  $^1\text{H}$  NMR as it shown a similar pattern of carbon chemical shift of mannose at  $\delta$  96.57ppm on anomeric C1,  $\delta$  72.13 and 73.35 ppm on C2, and non-linkage C4 at  $\delta$  69.47ppm.  $^{13}\text{C}$  NMR result of m-3 also shown additional signal at 101.48, 71.12, and 71.99ppm representing a chemical shift of C1 anomeric carbon, C2, and C3 of  $\alpha$ -1,6 galactose, respectively (Figure 34-36).

2D NMR results of m-2 and m-3 including COSY, DEPT, HMBC, HSQC, NOESY, ROESY, and TOCSY were attached in supplementary data.



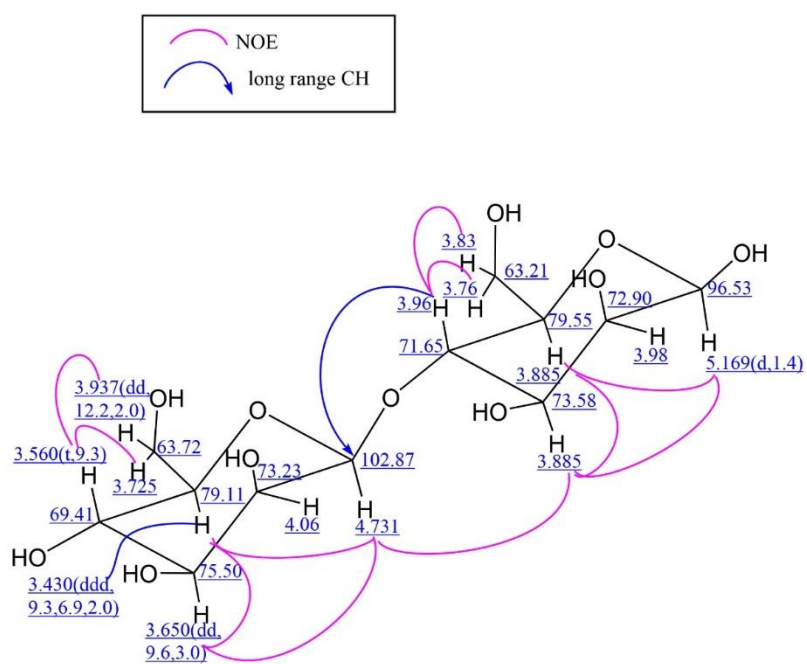


Figure 31. NMR structural analysis of m-2.







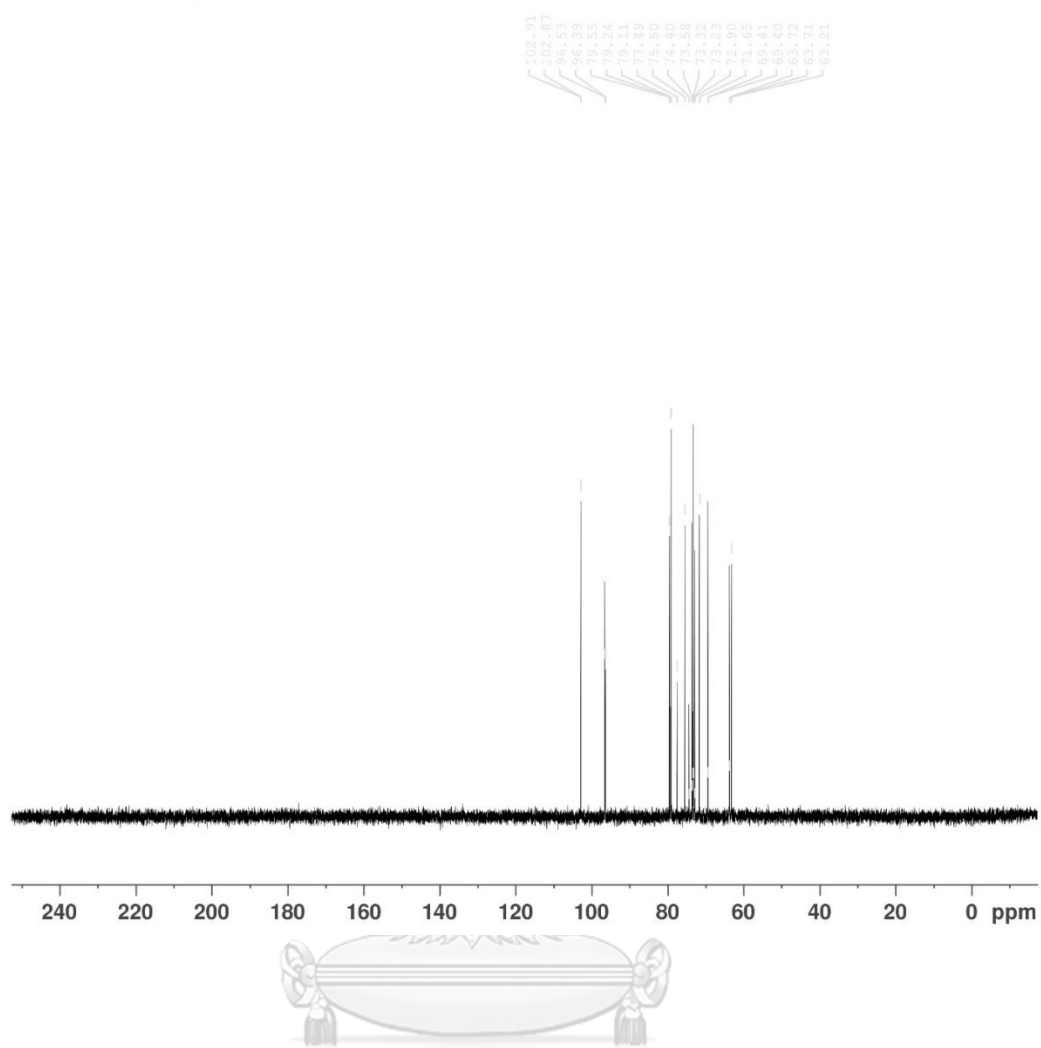


Figure 33.  $^{13}\text{C}$  NMR spectra of m-2, analyzed at 150MHz.

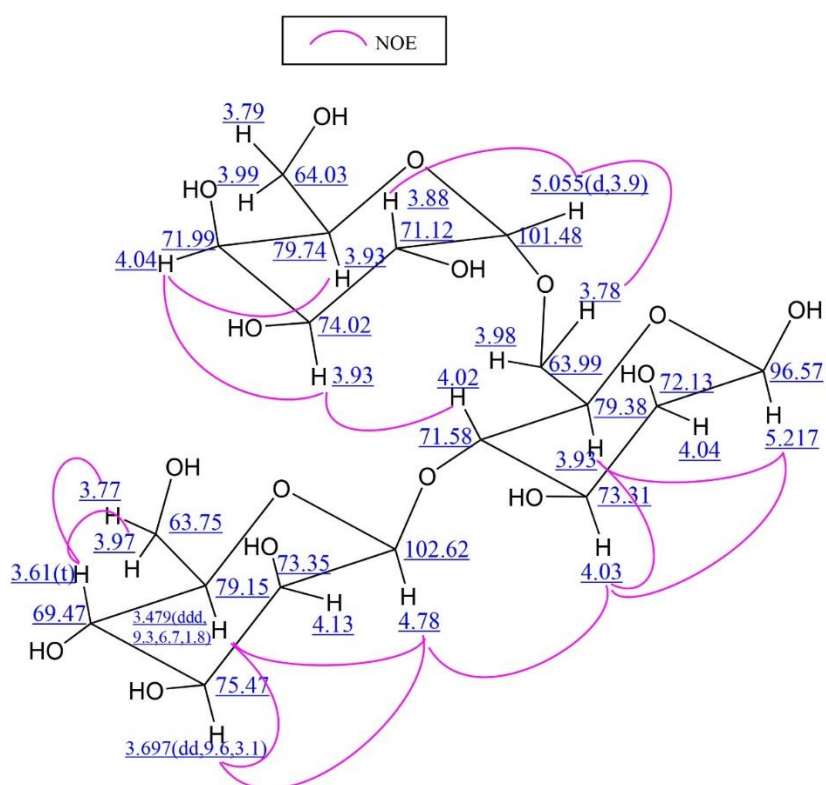
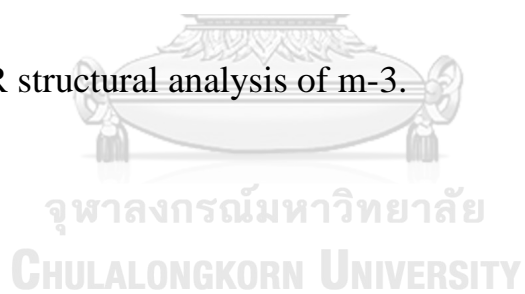


Figure 34. NMR structural analysis of m-3.



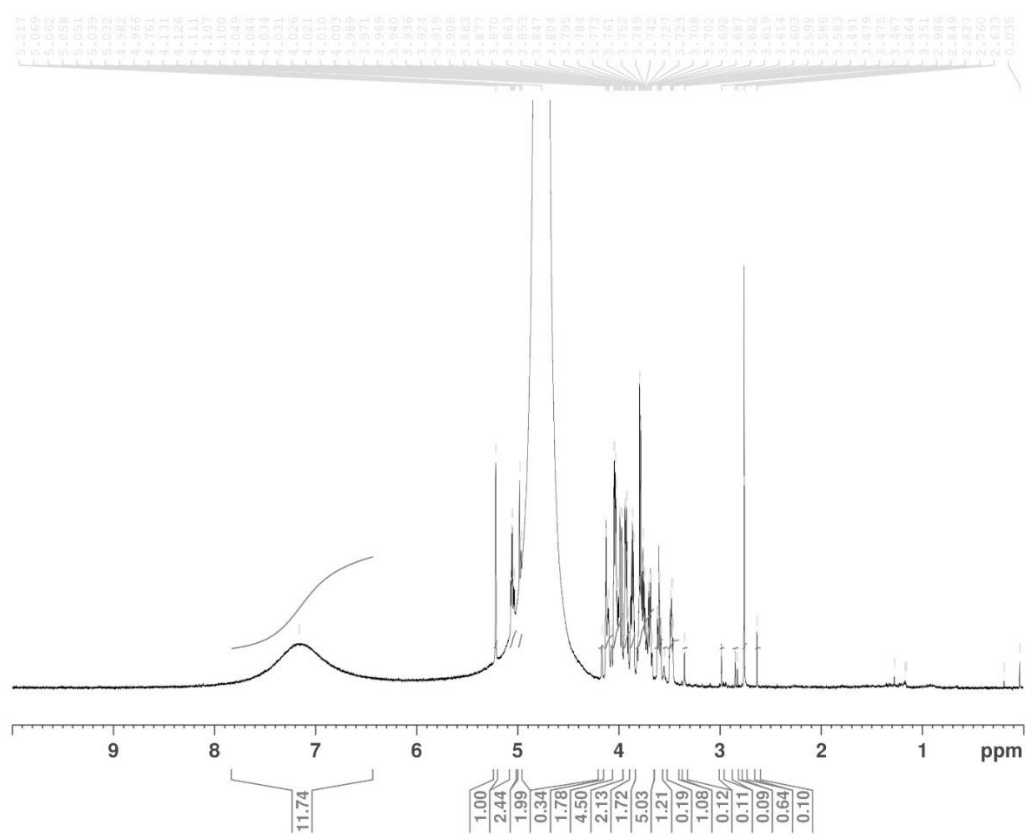


Figure 35.  $^1\text{H}$  NMR spectra of m-3, analyzed at 600MHz.

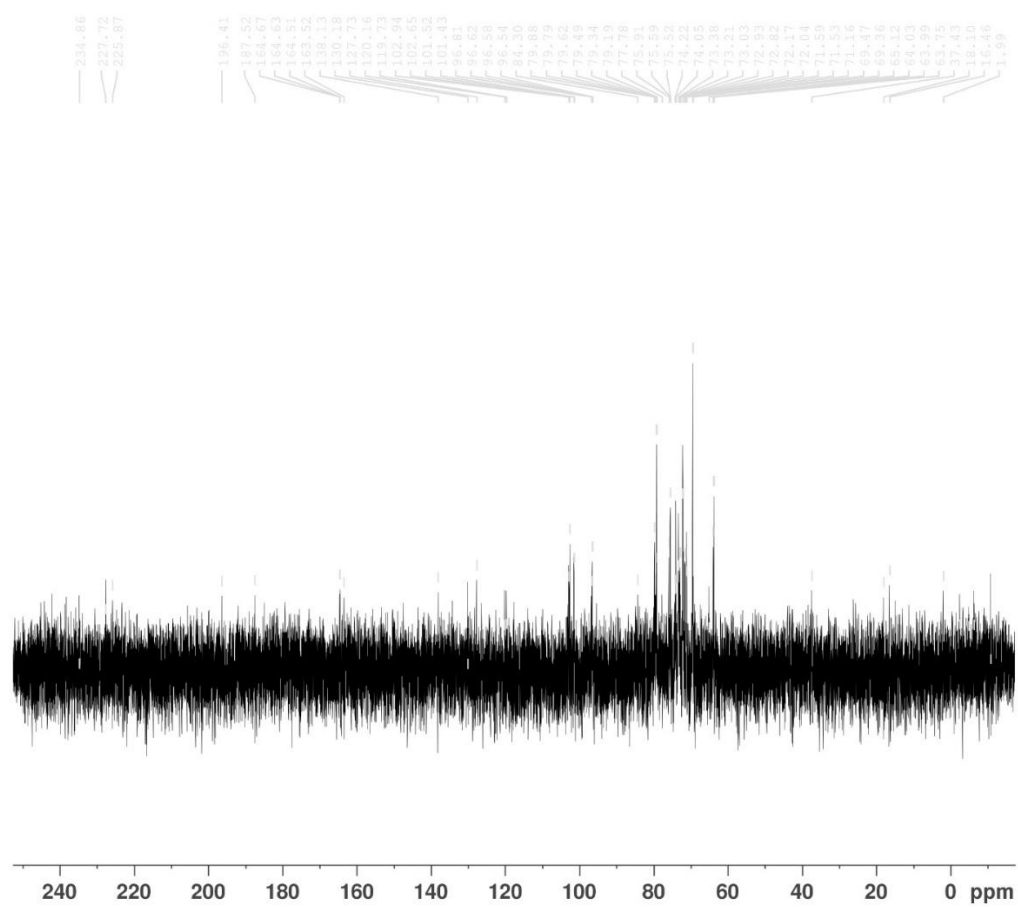


Figure 36.  $^{13}\text{C}$  NMR spectra of m-2, analyzed at 150MHz.

## CHAPTER IV

### DISCUSSION

#### **4.1 Characterization of RMase24 and effects of Galactomannan pretreatment on MOS production yield**

In this study, the recombinant mannanase was successfully engineered and purified and entitled as RMase24. The stability of the purified enzyme is steady and can be used in a wide range of temperature and work properly in a slightly basic pH between 6.5 -8. Interestingly, the production of MOS can be performed effectively with a crude enzyme, RMase24. The results showed that the substrate pretreatment can affect to the oligosaccharides product pattern. The additional sonication over the G-GalMan also affected the production yield of total MOS which is about 1.6 fold increased (8.25% on S-GalMan, and 5.09% on G-GalMan) Moreover, sonication also changed the production pattern of MOS to yield more moderate MOS than those without sonication as the result was shown in TLC in figure R11 A and B. These results may because of S-GalMan had a higher surface area since it had more irregular and cracked-like surface. This might led S-GalMan had a higher binding ability to enzyme and be

digested more. Moreover, the higher concentration of RMase24 also result in a lower yield of some MOS. This can be hypothesized that the higher concentration of RMase24 may lead to the higher amount of free enzyme in a solution that can bind to some large MOS that had been previously produced in the early time of the reaction. This suggestion was obtained from the higher amount of some small oligosaccharides produced and the loss of some moderate oligosaccharides as the results showed above.

#### **4.2 Effect of a MOS on tight junction and its possible mechanism of action**

T84 were treated with different size of purified MOS and changes tight junction integration was observed. The result showed that 10  $\mu\text{M}$  of MOS5 had a significant effect on tight junction enhancement. This result in tight junction integration was excluded from cells proliferation as the result obtained from a TEER experiment on cellular tight junction disintegration. In that experiment, cells were grown until 80% saturated on the cultured plates before the tight junction were disrupted. The rate of electrical resistance recover was

significantly restored after a treatment of MOS5 which indicated that MOS5 possessed an ability to enhance the tight junction of epithelial cells, *in vitro*.

To identify the possible mechanism pathway of tight junction activation of MOS5, dorsomorphine (Compound C) an AMPK inhibitor was used to investigate MOS5 function in tight junction integration activation through AMPK. The result showed that even MOS5 treatment had increased cells electrical resistance, a treatment of dorsomorphin together with MOS5 inhibit the tight junction reassembling of the cells since there was a very low electrical resistance recovered after a broke down as almost the same as a negative control which was treated with dorsomorphin only. This suggests that MOS5 might activate cells tight junction assembling through an activation of AMPK pathway. To confirm this hypothesis, a western blot analysis on a phosphorylation of AMPK protein was performed. The expression ration of p-AMPK over AMPK- $\alpha$  which were neutralized with their own  $\beta$ -actin expression level was determined and the result showed that after 60 minutes MOS5 treatment, phosphorylation level of cells was significantly increased. Interestingly, phosphorylation level of cells was decreased once we



measured after 120 minutes after a treatment. This result might be from that MOS5 could activate phosphorylation of AMPK as a single time signaling transduction or might induce through some other upstream signaling pathways since it had the time onset delayed after a treatment.

Although other studies were found that animals fed with MOS supplements were possessed a better body composition and villi length increased, it can be concluded that a better body composition and villi length of treated animals were because of MOS5 within the crude MOS in the supplement may reacted directly and enhanced the tight junction integration of their epithelial cells. This suggestion was strongly supported by the study of Ghosh, et al. (2015) who reported that MOS was highly resistant to gastric juice and intestinal juice which indicated that MOS5 might also survived through animal digestive tract till it reached intestinal epithelial cells and exhibit its ability (Ghosh et al., 2015). Hence, effect of MOS through innate immune activation still require further investigation.

### 4.3 Structural analysis of MOS5

A production of MOS from a heteropolymer substrate like galactomannan might result in several types of oligosaccharides and also multiple isoforms. Structural determination was really important to reveal the identity of MOS that possessed a biological activity. Since NMR analysis of a large oligosaccharide was inaccurate and difficult to analyze, a multiple enzymatic hydrolysis of MOS5 had been performed to gather results as pieces of puzzle and constructed them together to identify a true structure of MOS5.

HPAEC-PAD analysis of MOS5 had been performed to identify the singularity of MOS5 species. The results showed that bioactive MOS5 had a single isoform with over 95% purity. This indicated that MOS5 produced from a hydrolysis of pretreated galactomannan from copra meal with RMase24 had only 1 isoform. This can be suggested that RMase24 may have some specific activity that can produce only one type of MOS5.

In the first step of investigation, a digestion of MOS5 with  $\alpha$ -galactosidase was planned to investigate if there was any galactose branch attached to the mannose backbone. In this study, a commercial enzyme of  $\alpha$ -galactosidase (*A. fulica*), labeled as AMAN-AfGLA, was kindly given from Amano corporation Japan. A digestion

AMAN-AfGLA with MOS5 revealed a band of galactose and a band of disaccharide, trisaccharide, and a band of tetrasaccharide which have the same R<sub>f</sub> in TLC as mannotetrose (Figure 27). This can be suggested into 2 hypotheses; 1) a band of galactose and a band of tetrasaccharide indicated that MOS5 contained a mannose tetrasaccharide backbone with a branch of galactose unit with  $\alpha$ -1, 6-galactosic linkage. 2) AMAN-AfGLA was not a purified enzyme and might contain mannanase since there were a band of disaccharide and trisaccharide presented in a reaction product.

MOS5 was digested with exo-mannosidase (*A. fulica*) (Seigaku) and produced monosaccharide and tetrasaccharide as shown in Figure 28. Interestingly, a tetrasaccharide band shown a different R<sub>f</sub> from mannotetrose standard. This can be suggested that tetrasaccharide product might contain galactose unit that can block a further digestion of exo-mannosidase. This suggestion was strongly supported with a study from McCleary, et al (1974) that exo-mannosidase can hydrolyze mannose from galactomannan substrate but a galactose branch contents was a limitation of this enzyme [51].

Hence, results obtained from a digestion of MOS5 with  $\alpha$ -galactosidase and exo-mannosidase showed that MOS5 might be a galactomannan polymer composed of mannose tetrasaccharide with a

galactose branch attached at second or third mannose backbone from non-reducing end, a further digestion between MOS5 and endomannannase was performed to prepare a substrate for NMR analysis. Since MOS5 was a pentasaccharide and it was too large to perform an accurately NMR analysis, a digestion of MOS5 into smaller oligosaccharides before submitted to NMR analysis was important to obtain a correct information about MOS5 structure.

AMAN-AfGLA was also purified through Sephadex G150 column chromatography to distinguish the enzymatic activities. Fractions collected were used to digest melibiose (D-Gal- $\alpha$  (1 $\rightarrow$ 6)-D-Glc) and mannobiose (D-Man- $\beta$ (1 $\rightarrow$ 4)-D-Man) to reveal their  $\beta$ -mannosidase and  $\alpha$ -galactosidase activities. A fraction contained  $\beta$ -mannosidase activity (P-AMAN-AfGLA-f35) was obtained and performed another digestion with MOS5. The result shown a different product pattern along a various amount of P-AMAN-AfGLA-f35. An excess amount of P-AMAN-AfGLA-f35 was used to perform a digestion with MOS5 to prevent a transferase by-product that produced at low amount of enzyme usage. TLC analysis shown 2 bands consist of a band of disaccharide (m-2) and a band of trisaccharide (m-3). These two products were purified through Biogel P2 column chromatography

which ensured that there was no P-AMAN-AfGLA-f35 contaminated that might modified those purified products. Mass spectrometry was then performed to identify the molecular mass of m-2 and m-3 and the results shown that m-2 and m-3 were truly disaccharide and trisaccharide, respectively.

NMR was performed and analyzed at Osaka City University and the results obtained was revealed that m-2 was D-Man- $\beta$ (1 $\rightarrow$ 4)-D-Man, while m-3 was D-Man- $\beta$ (1 $\rightarrow$ 4)-D-Man with D-Gal- $\alpha$ (1 $\rightarrow$ 6)-D-Man on its reducing end. This result went to the same direction with previous TLC result since m-2 had the same Rf with mannobiose while m-3 had slightly different Rf with mannotriose (Figure30), and MOS5 also had a different Rf than mannopentose, indicated that m-3 and also MOS5 were a heteropolymer composed of galactose and mannose rather than a mannose homopolymer.

A previous TLC result showed in figure 26 also supported that a position of galactose located near non-reducing end of MOS might inhibit a digestion of exo-  $\beta$  -mannosidase. The hypothesis was that galactose might locate on second or third mannose unit from a non-reducing end of MOS5. This indicated that m-3 would be located on the non-reducing end and m-2 was the part that been at the reducing

end of MOS5. In conclusion with NMR data, MOS5 is  $\beta$ -(1-4)-mannotetros with  $\alpha$ -Gal-(1-6) attached on the second mannose unit from non-reducing end and a digestion of exo- $\beta$ -1,4-mannosidase was cleaved the first mannose from non-reducing end of MOS5 and left tetrasaccharide which was  $\alpha$ -Gal-(1-6)- $\beta$ -(1-4)-mannotriose.

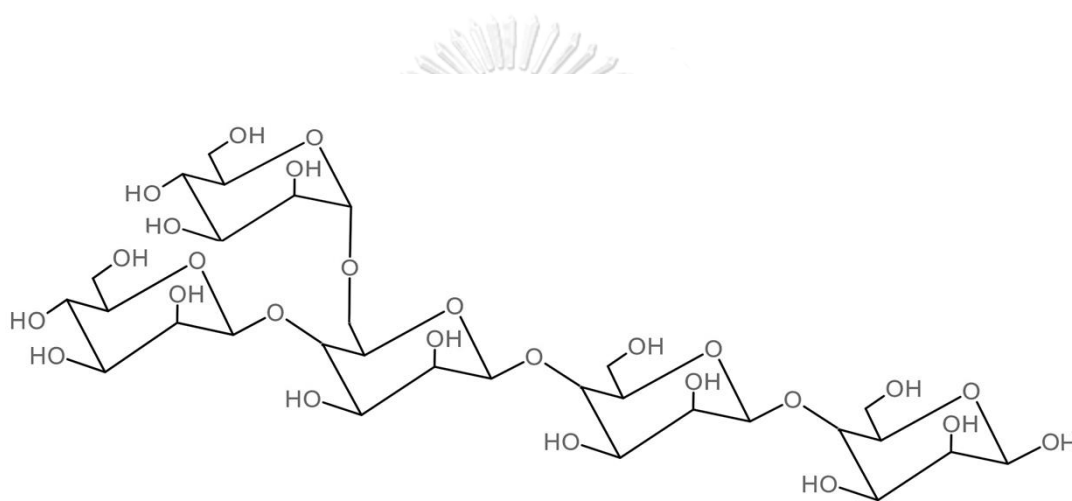


Figure 37. Structure of MOS5

## CHAPTER V

### CONCLUSION

Mannan oligosaccharide (MOS) supplement for livestock possesses an ability to improve their life quality by increasing the density and length of their villi. In this work, MOS was made by a hydrolysis of pretreated galactomannan from copra meal. A sonication was a better method to produce MOS when compared to normal grinding method since the surface of sonicated copra meal was rougher, resulting in a higher surface area, this made it more compatible to digest with recombinant mannannase, RMase24, and yielded a high amount of MOS. Interestingly, different RMase24 concentration used in a reaction yielded a different MOS production ratio.

Moreover, MOS produced from RMase24 yielded more moderate size oligosaccharides when compared to other study (Ghosh et al., 2015; Rungrassamee et al., 2014). This might result in a higher biological activity of crude product. To prove this hypothesis, MOS crude was separated through size exclusion chromatography. MOS4 to MOS7 were collected and tested their ability to increase tight junction integration of epithelial cells using T84 as a model. The result shown that MOS5 was significantly increased tight junction integration of epithelial cells when

compared with negative control. Moreover, MOS5 cannot activated tight junction integration with a presence of adenosine monophosphate kinase (AMPK) inhibitor, dorsomorphine. This result could be suggested that MOS5 might activated tight junction integration of epithelial cells through activation of AMPK pathway. This hypothesis had been proven by a result from western blot analysis of phosphorylated AMPK (pAMPK) protein which shown that MOS5 treatment could elevated level of pAMPK in epithelial cells when compared to negative control.

Since MOS made from galactomannan was a heteropolymer composed of mannose and galactose, MOS5 possessed a different mobility compared to mannopentose standard in ethyl acetate solvent system of thin layer chromatography. The structure of bioactive MOS5 was determined by enzyme hydrolysis together with mass spectrometry and nuclear magnetic resonance technique. Results obtained from a digestion of MOS5 with *exo*- $\beta$ -mannosidase (Seigaku),  $\alpha$ -galactosidase (Amano), and purified  $\alpha$ -galactosidase (from Amano) showed that MOS5 was a heteropolymer composed of mannotetrose with  $\beta$ -1,4-glycosidic linkage and a galactose attached at a second mannose unit from non-reducing end with  $\alpha$ -1,6-glycosidic linkage.



## APPENDICES

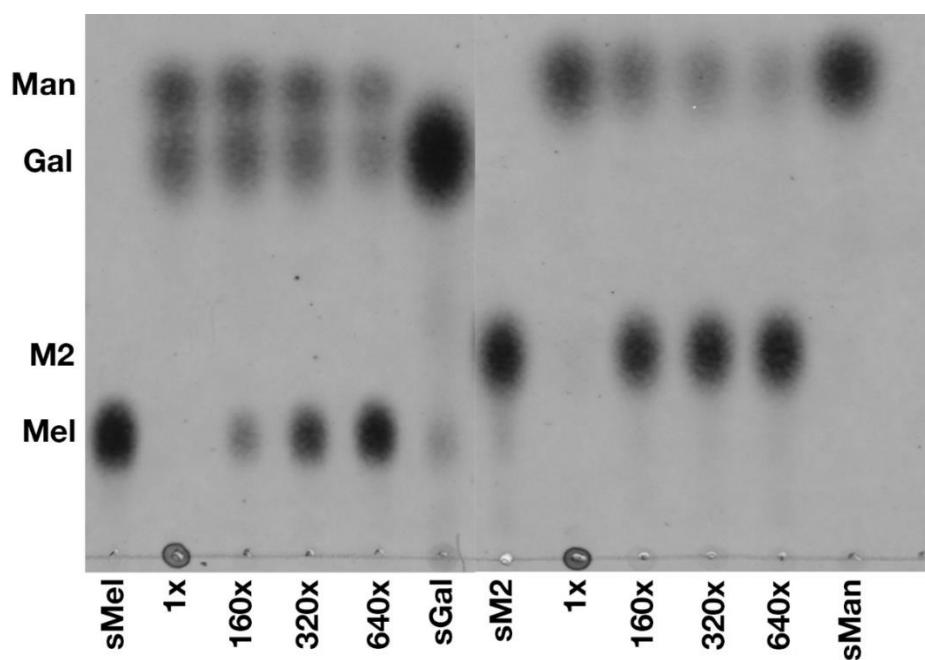


Figure S1.  $\alpha$ -galactosidase and  $\beta$ -mannosidase activities of P-AMAN-AfGLA.

The lanes were cropped from the same TLC plate.

Man; Mannose

Gal; Galactose

M2; Mannobiose

Mel; Melibiose

sMel; Standard melibiose (10mg/mL)

sM2; Standard mannobiose (10mg/mL)

(Figure s1 continue)

sGal; Standard Galactose (20mg/mL)

sMan; Standard Mannose (10mg/mL)

1x; non-diluted P-AMAN-AfGLA

160x; 1  $\mu$ L of P-AMAN-AfGLA in 160  $\mu$ L of diluted solution

320x; 1  $\mu$ L of P-AMAN-AfGLA in 320  $\mu$ L of diluted solution

640x; 1  $\mu$ L of P-AMAN-AfGLA in 640  $\mu$ L of diluted solution



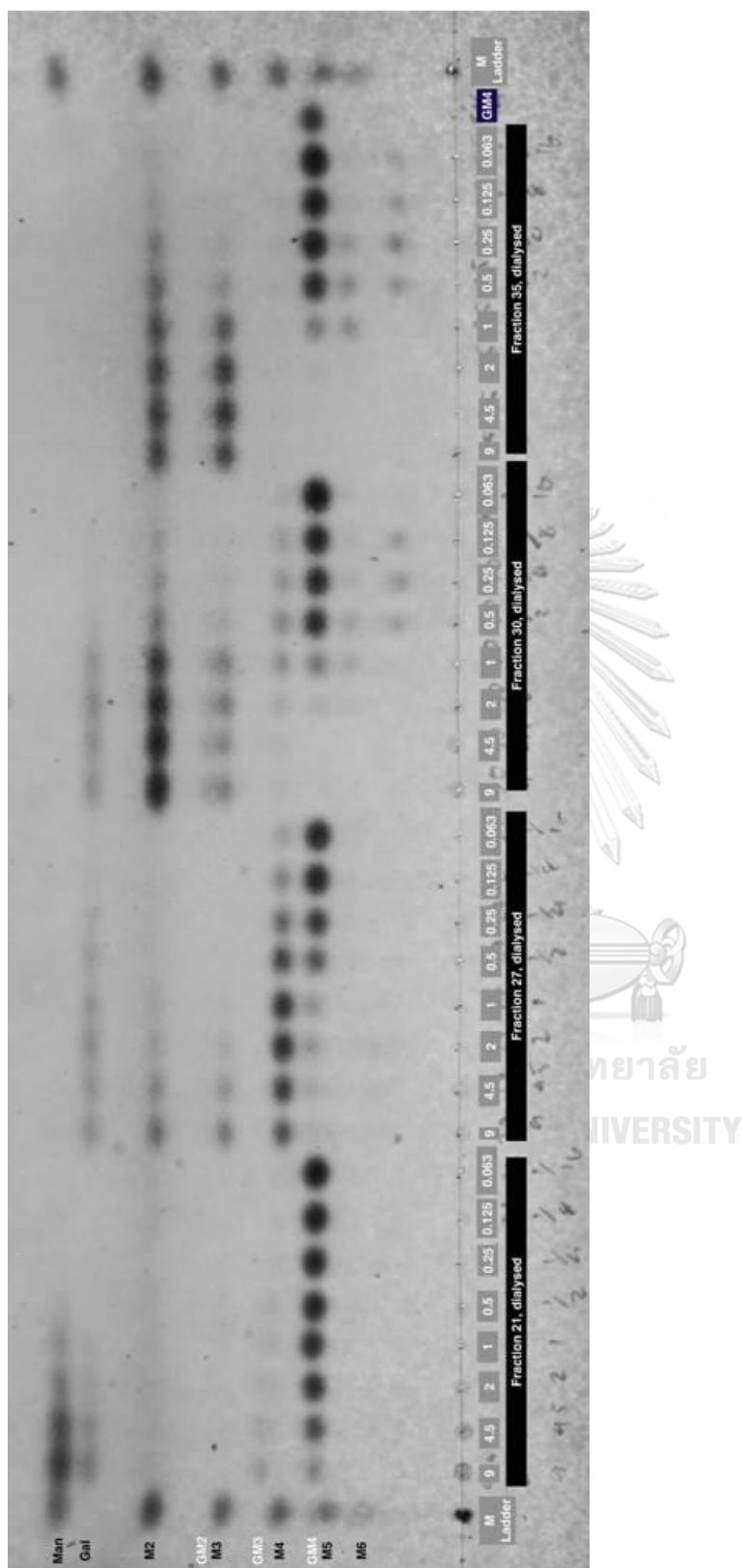


Figure S2. Digestion of MOS5 with fractions of P-AMAN-A/GLA.

M2\_cosy\_D20-temp25

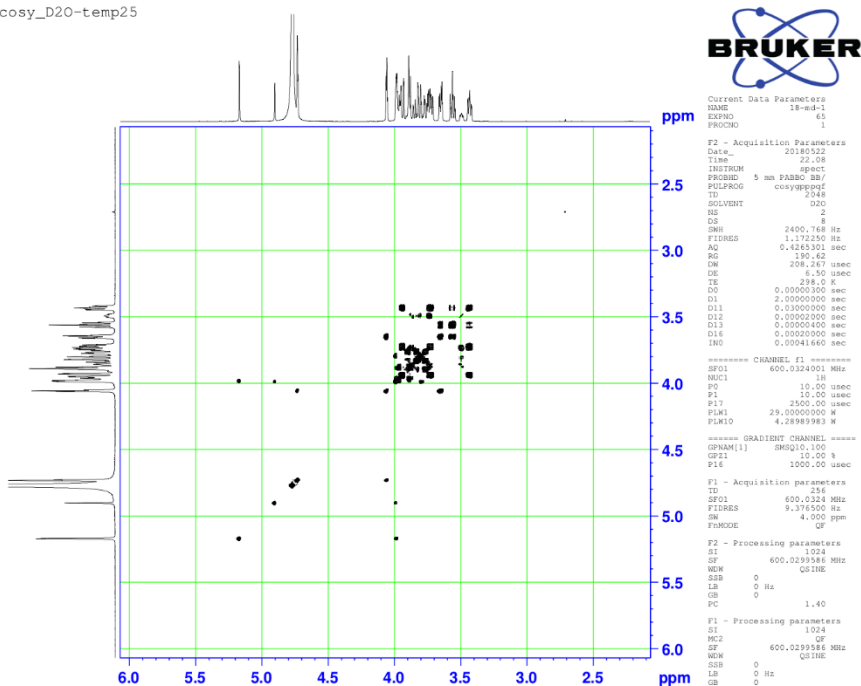


Figure S3. NMR COSY of m-2

M2\_dept135\_D20-temp25

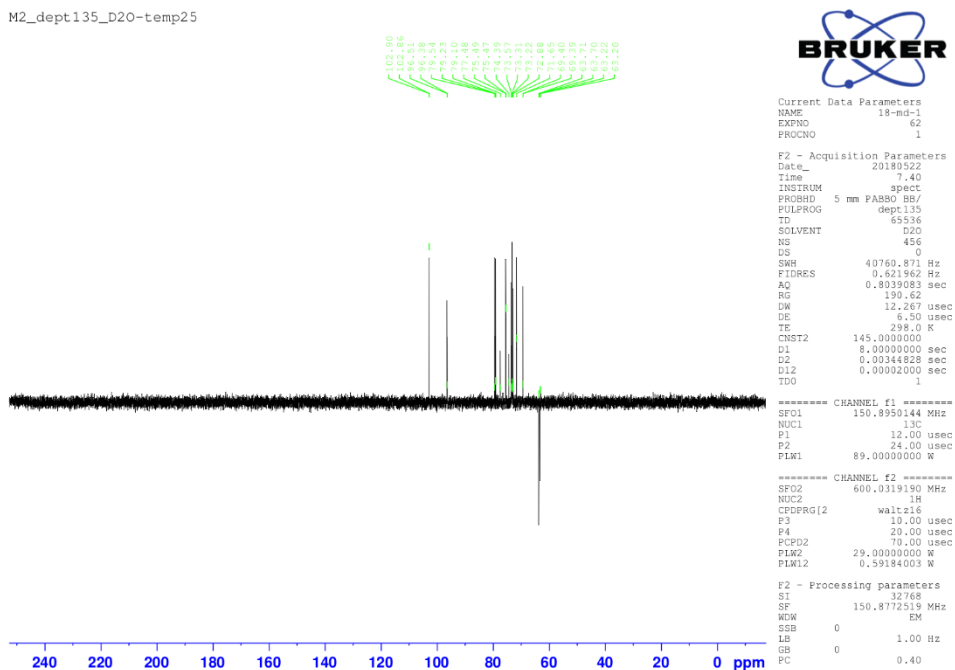


Figure S4. NMR DEPT of m-2.

M2\_hmbc\_D20-temp25

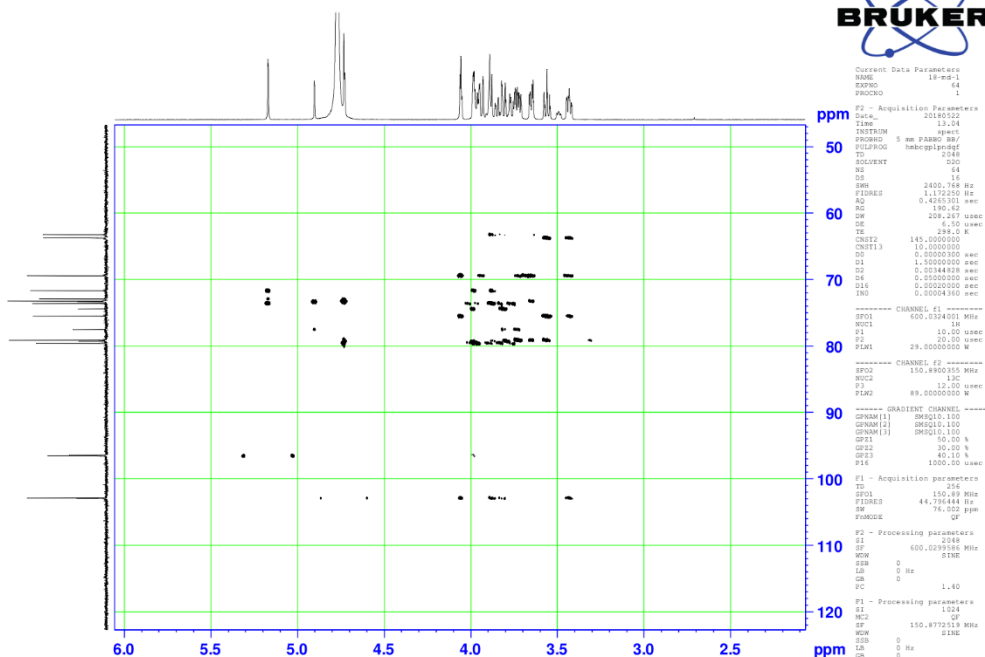


Figure S5. NMR HMBC of m-2.

M2\_hsqc\_D20-temp25

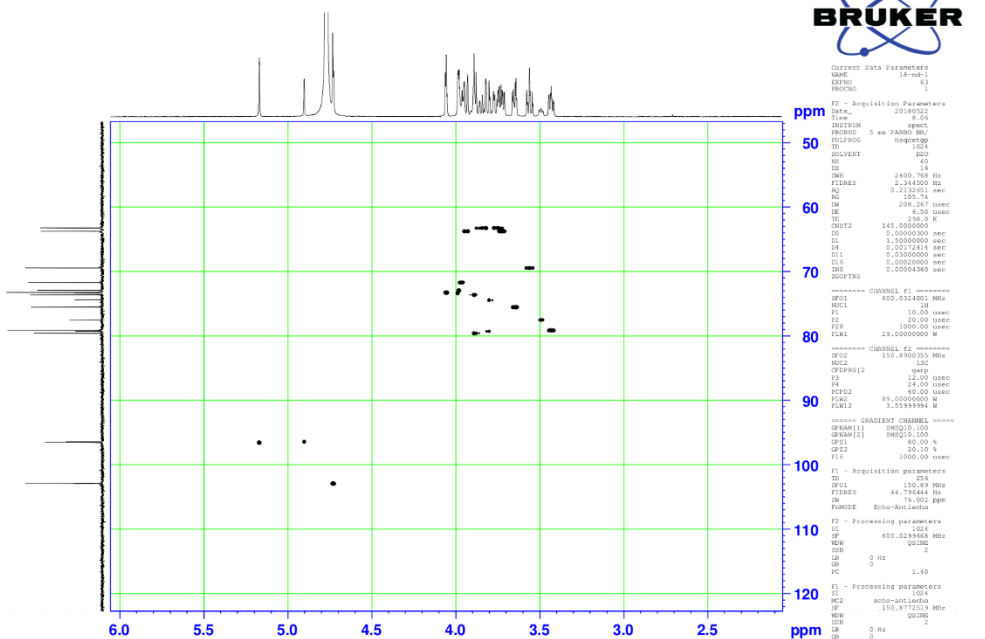


Figure S6. NMR HSQC of m-2.

M2\_noesy\_D20-temp25

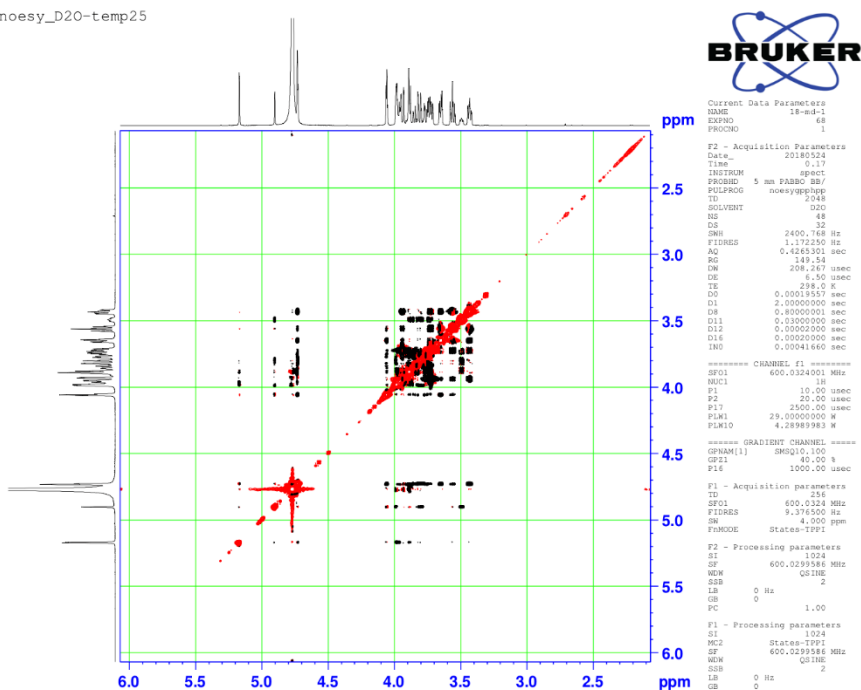


Figure S7. NMR NOESY of m-2.

M2\_roesy\_D20-temp25

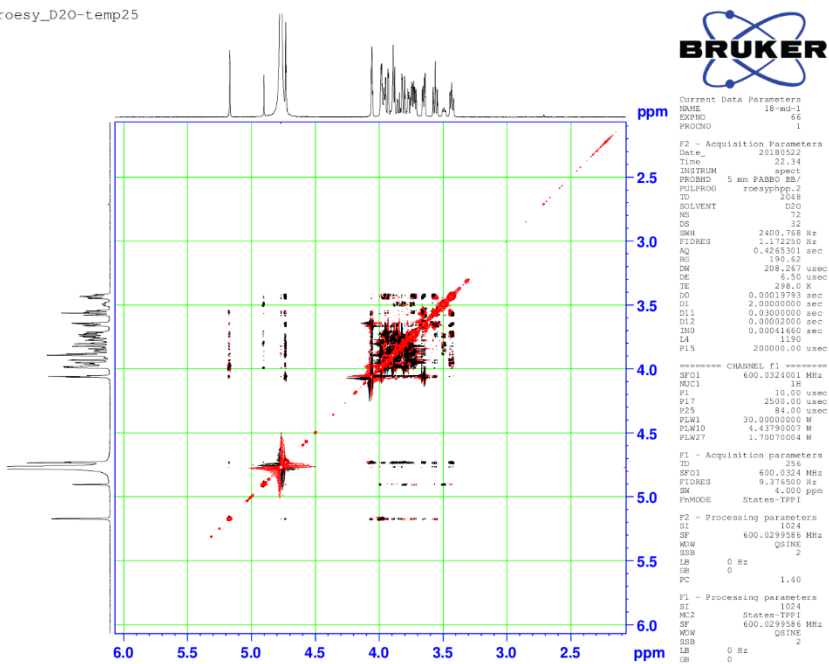


Figure S8. NMR ROESY of m-2.

M2\_tocsy\_D20-temp25

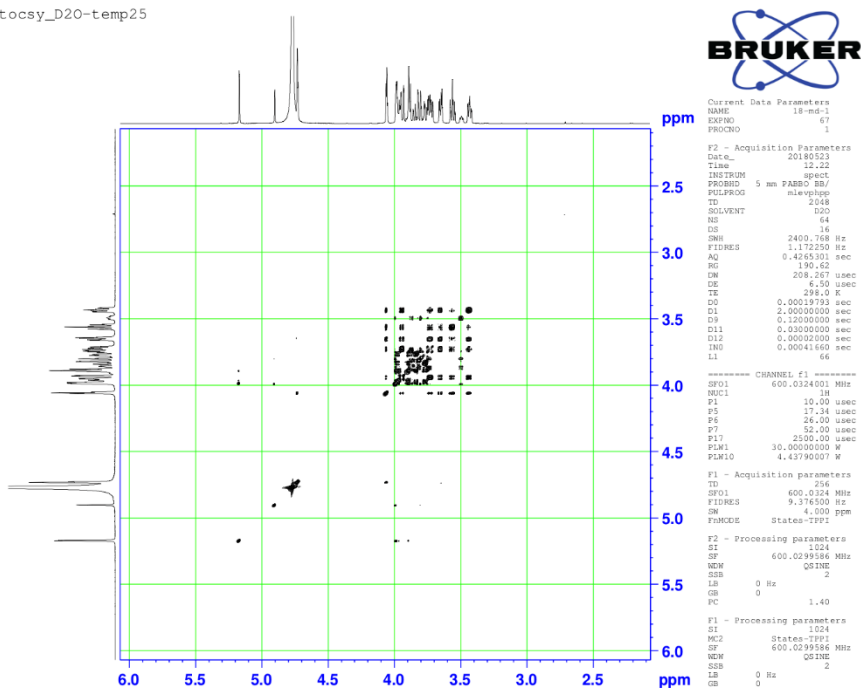


Figure S9. NMR TOCSY of m-2.



M2G\_cosy\_D20-temp25

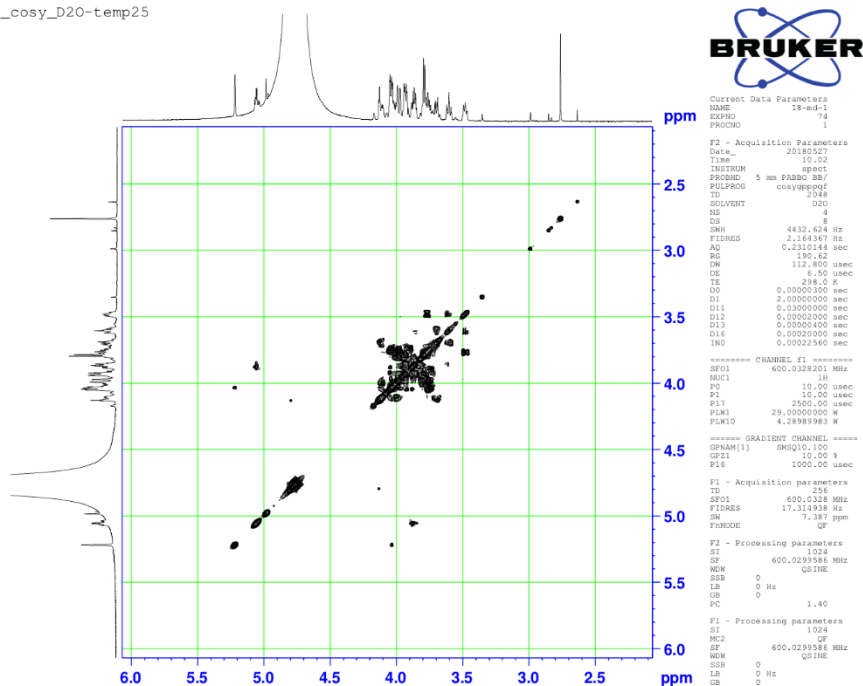


Figure S10. NMR COSY of m-3.

M2G\_dept135\_D20-temp25

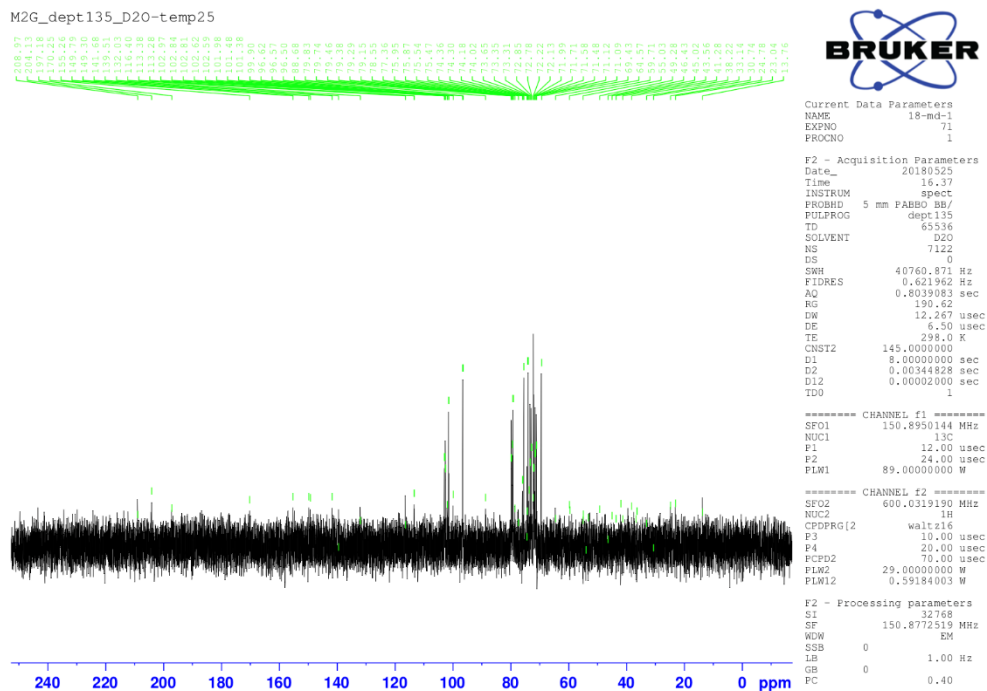


Figure S11. NMR DEPT of m-3.



M2G\_hmbc\_D20-temp25

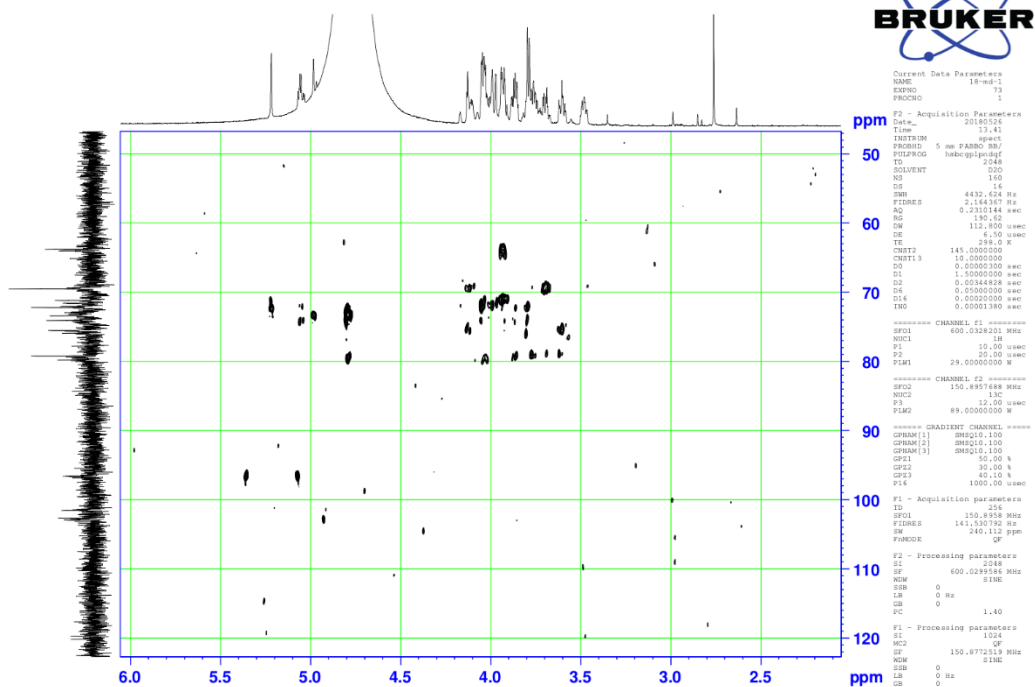


Figure S12. NMR HMBC of m-3.

M2G\_hsqc\_D20-temp25

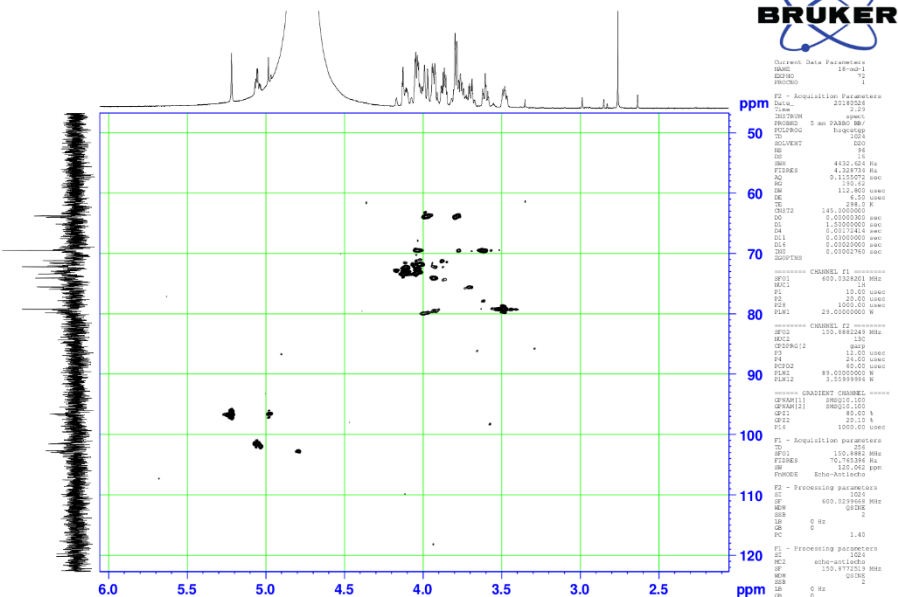


Figure S13. NMR HSQC of m-3.

M2G\_noesy\_D20-temp25

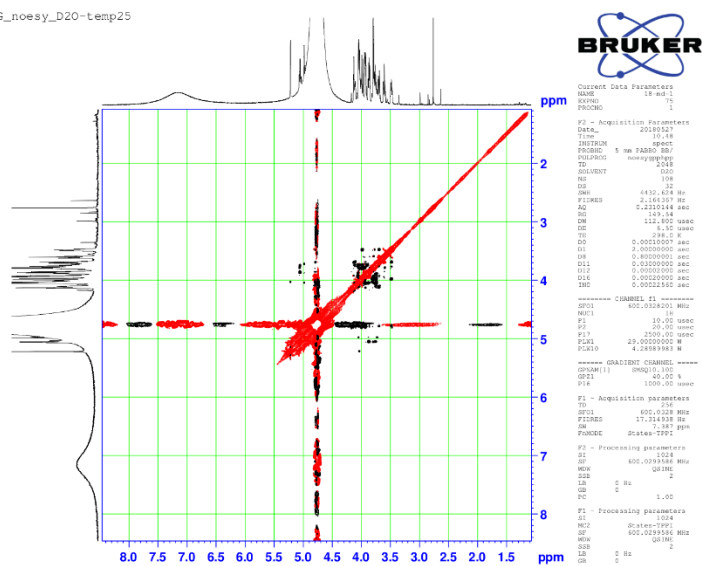


Figure S14. NMR NOESY of m-3.

M2G\_roesy\_D20-temp25

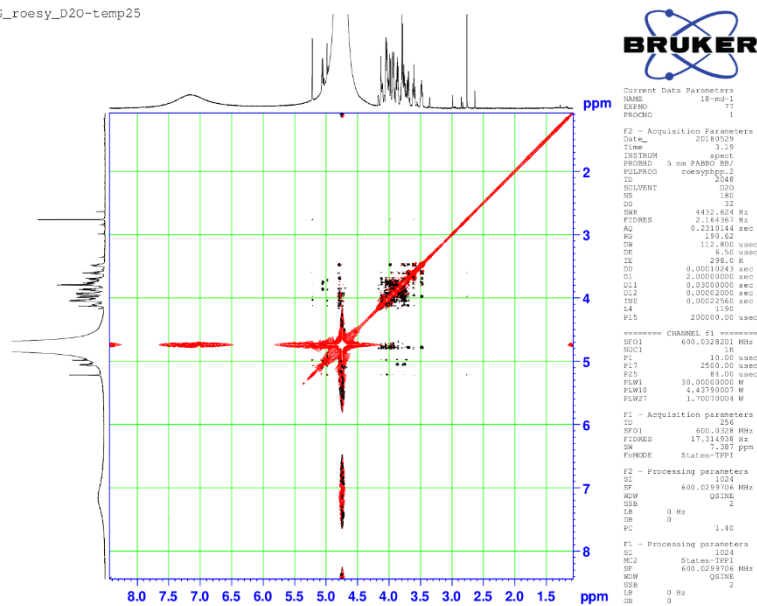


Figure S15. NMR ROESY of m-3.

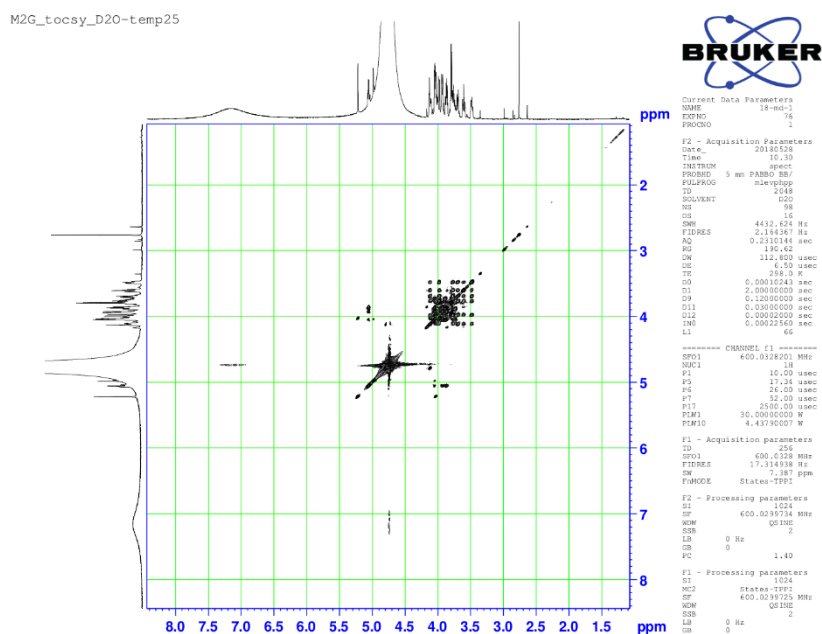


Figure S16. NMR TOCSY of m-3.



Enzymatic activity	Activity (U/mL)	Specific activity(u/mg)	Total Activity (U)
$\alpha$ - galactosidase	973.3	167.8	4866.5
$\beta$ -mannanase	28.8	4.974	144
A280 = 5.8 (mg/mL)			

Table S1.  $\alpha$ -galactosidase and  $\beta$ -mannosidase activities of P-AMAN-AfGLA

## VITA

**NAME** Chatchai Nopvichai

**DATE OF BIRTH** 03 May 1986

**PLACE OF BIRTH** Bangkok, Thailand

**INSTITUTIONS ATTENDED** 2004-2007, Department of Botany and Genetic, Faculty of Science, Chulalongkorn University.

2008-2011, Department of Pathology, Faculty of Medicine, Chulalongkorn University.

**HOME ADDRESS** 90/13 Ladprao23 Ladprao Chandrakaseum Jatujak Bangkok 10900

**PUBLICATION**

1. Nopvichai, C. et al. PCR detection of Mycobacterium tuberculosis in necrotising non-granulomatous lymphadenitis using formalin-fixed paraffin-embedded tissue: a study in Thai patients. J Clin Pathol. 9, 812-5. (2009)
2. Nopavichai, C. Change in LINE-1 methylation in cancers during metastasis. Asian Biomed. 6, 307-12. (2012)